COMPUTER-AIDED DESIGN OPTIMISATION OF WIND TURBINE AIRFOIL FOR LOW WIND SPEED APPLICATIONS

By

SAMUEL ADU-GYAMFI

A Thesis submitted to the School of Graduate Studies, Kwame Nkrumah University of Science and Technology in partial fulfilment of the requirements for the degree of

MASTER OF SCIENCE

IN

MECHANICAL ENGINEERING

Department of Mechanical Engineering

College of Engineering

JANUARY, 2013

DECLARATION

I hereby declare that this submission is my own work towards the MSc and that, to the best of my knowledge, it contains no material previously published by another person nor material which has been accepted for the award of any other degree of the University, except where due acknowledgement has been made in the text.

Samuel Adu-Gyamfi (PG 2677408)	....	....
Student Name & ID	Signature	Date

Certified by:

Dr. Joshua Ampofo	....	....
(Supervisor)	Signature	Date

Certified by:

Dr. S. M. Sackey	....	....
Head of Department	Signature	Date

ABSTRACT

Low wind speed conditions in various parts of Ghana calls for a wind turbine blade capable of giving maximum circulation to produce a high lift which will turn turbines. In this thesis, a wind speed of at least 3 m/s is used as a benchmark in optimizing the design of a blade airfoil to give optimal performance during low wind speed conditions.

Blade-element momentum theory which is the current mainstay of aerodynamic design for horizontal-axis wind turbine blade was used in the optimization process. A couple of design processes were considered to arrive at successful wind turbine design.

Ten high-lift-coefficient airfoils, which could give high lift leading to high moment at low wind speed conditions, were selected and their aerodynamics parameters iterated and tested for optimum performance under low wind speed conditions. The iteration of these aerodynamics parameters were computed and analysed using a programmed spreadsheet for all the ten profiles. For each section of the blade, the airfoil that gave the highest power coefficient was used. The sections were then lofted to form a seamless blade.

The resulting low wind speed blade airfoil design offers substantial improvements on the reference designs. The application of optimization methods successfully aided the creation of a wind turbine blade with consistent peak performance over a range of design points.

TABLE OF CONTENT

LIST OF TABLES

LIST OF FIGURES

NOMENCLATURE

Symbol	Unit
a	Axial induction factor
a^{1}	Angular induction factor
B	Number of blades
c	Airfoil chord length
C_L	Lift coefficient
C_D	Drag coefficient
C_P	Power coefficient
D	Drag force
F_x	Axial force
F_Θ	Tangential force
L	Lift force, angular moment
$\dot{m}$	Mass flow
N	Number of blade elements
p	Pressure
P	Power
Q	Tip loss correction factor

r	radius and radial direction
R	Blade tip radius
T	Torque
V	Absolute velocity
W	Relative velocity
x	Axial coordinate
β	Relative Wind Angle
λ	Tip speed ratio
λ_r	Local Tip speed ratio
η	Mechanical/electrical efficiency
ρ	Density
σ^l	Local Solidity
θ	Tangential coordinate
Ω	Blade rotational speed
ω	Wake rotational speed
γ	Twist Angle

ACKNOWLEDGEMENT

To the Lord Jesus Christ who is above all the most faithful and most gracious. I am grateful to the Kwame Nkrumah University of Science and Technology for my fantastic research experience and especially to Dr. Joshua Ampofo who has been a fantastic guide. Thank you so much for your patience, encouragement and support.

Thank you to Eric Akowuah and all colleagues' whose moral support during the entire thesis was very inspirational.

Many thanks to my family for their prayers and support.

CHAPTER ONE

Introduction

1.1 Background

The significant rise in the cost of petroleum oil has increased the search for viable alternative technologies for power generation. One option under consideration is wind power which utilizes the turning effect of a turbine to generate energy. A wind turbine operates by using the wind's energy to spin a shaft that drives an electricity-producing generator.

One critical aspect of the wind turbine that has not been evaluated until recently is the blade itself. Interest in using wind turbines at low wind speed is growing, so technical improvement to the operating angles of the blade is needed so as to boost its performance. The operation of wind turbines at low wind speeds must be upgraded. [1]

The main approach to improving the performance of the blade at low wind speeds is to increase its angle of attack, the angle that the blade makes into the incident wind. A recurring problem is that increasing the angle eventually forces the blade to stall. Stalling, which is determined by wind speed and direction, is difficult to predict. This has resulted blade manufacturers with limited operating angles to ensure that stalling is minimized and unfortunately, leads to inferior blade performance [1].

The correct choice of wind turbine blade profile and blade design procedures taking into consideration the rotor diameter, tip speed ratio, number of blades, twist angles etc. will lead to good lift and drag coefficients for a good rotor performance. It has been noticed that the blade manufacturers put some fins on certain length of the blade to create a thin layer of turbulence and curiously make the blade stall at a steeper angle. This technology has been used on aircraft for a long time. If a technology could be developed to boost the operating angle of the blade, the prospect exists for improved wind turbine performance [2].

This study confirms that the low wind energy at onshore can play a major role in achieving Ghana's renewable energy. This is achieved by optimizing and improving the available wind turbine blade profiles to maximize energy capture and power output.

1.2 Scope of Study

Blade-element momentum theory (BEM) also known as strip theory is used for the optimization of design, analysis, modification and optimization of the horizontal-axis wind turbines blade in this thesis. The thesis develops systematic procedures for analyzing the airfoil of the three bladed-wind turbine at low speed wind speed of at least 3 m/s.

The optimum wind turbine profiles for horizontal axis wind turbine are analysed and their optimized aerodynamics properties and sections stored and used in the designed of the new low wind speed airfoil blade.

The main work is limited to aerodynamics design of the blade without due consideration of the structural and electrical requirements.

Moreover, Club Cycom, a computer user-interface program for turbine blade design would be used in the design of blade airfoils.

1.3 Justification

The quest for renewable energies that preserves the environment is an issue of major importance in Ghana and the world at large. Wind energy is one typical example among many others. A wind turbine with carefully designed blade will utilize wind energy for the production of electricity which will subsequently reduce the energy problem in the country.

In the process of generating electricity from wind, a slowly turning wind turbine connected through a gear box to a fast-turning electric generator efficiently converts the kinetic energy of wind to electrical energy as shown in Figure 1.1. Almost all wind turbines producing electricity consist of rotor blades which rotate around a horizontal hub. The hub is connected to a gearbox and generator, which are located inside the nacelle. The nacelle is the large part at the top of the tower where all the electrical components are located [3].

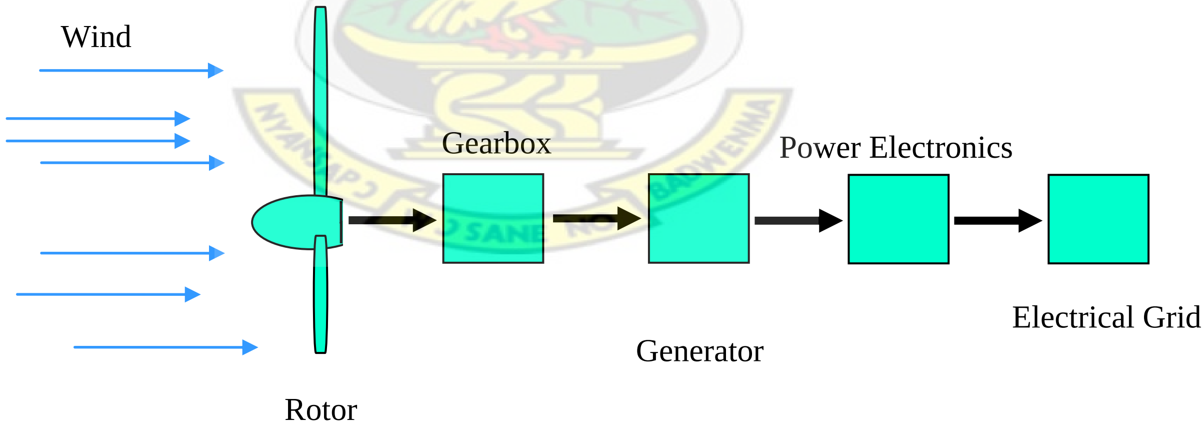

Figure 1.1 Model of a Wind Turbine

The aerodynamic characteristics of wind turbines are closely related to the geometry of their blades. The innovation and the technological development of wind turbine blades can be centered on two tendencies in areas of low wind speed. The first is to improve the shape of the existing blade, in order to achieve an optimal circulation. The second is to design new shapes of blades in order to get some more ambitious aerodynamic characteristics. The blade profile is the critical aspect of the system design which affects the maximum energy capture of the turbine, its optimal rotational speed, its self-starting ability, and its susceptibility to stalling in turbulent wind. In horizontal axis wind turbine, NACA profiles standards of the National Advisory Committee for Aerodynamics are normally used [4].

This thesis presents a three bladed rotor optimization analysis on existing blade profiles using the Blade Element Momentum theory. The accuracy of the results is validated with international data to see how the optimized blade would perform in areas of low wind speed in the country.

1.4 Aims

To use a computer to optimize a wind turbine blade airfoil for low wind speed applications

1.5 Objectives

The aim can be achieved through the realization of the following objectives:

- To study and analyze existing horizontal axis wind turbine blade airfoils.

- To use BEM theory to conduct an analytical design for a horizontal axis wind turbine blade airfoil.
- To use a computer software to aid in the design optimization of the blade airfoil.

1.6 Methodology

The problems to be discussed in this thesis cover a wide range of technical issues. In order to come out with appropriate airfoil for horizontal axis wind turbine blade at a certain wind condition, we need to have knowledge on the aerodynamic forces and parameters. This report commences with examination of wind turbine blade airfoil which can give satisfactory lift, low drag and maximum circulation at low wind speed of at least 3.0 m/s.

The Blade Element Momentum theory is used to determine the optimum airfoil sections for the wind turbine blade. The blade is divided into N number of elements. The elemental power coefficients, chord length, blade twist angle, torque and power distributions along the span of the blade are iterated repeatedly in a spreadsheet for optimum parameters for the blade. The optimum parameters are then used in a computer software application to come out with the optimum section of the airfoil.

Finally, optimum sections of the existing blade airfoils are brought together to come with an optimized one which can work well in low wind speed conditions. The optimized blade is finally validated with standard data.

1.7 Facilities Available

The facilities available for the thesis include the following;

- Internet facilities at both the Mechanical Engineering Department and the Postgraduate office in the University, wind turbines designed by students of KNUST and Energy center at KNUST.

- Wind data from KNUST, the Energy Commission and Metrological Service Department of Ghana would be examined and validated for blade analysis.

- There is access to Computer laboratory for computer software and literature for the thesis. The accuracy and the validity of the results are tested using recognized wind turbine companies to see how the optimized blade profile can stand the low wind speed experienced in almost all low wind speed areas in Ghana.

CHAPTER TWO

Literature Review

2.1 Background

The sole dependence on hydroelectric and thermal powers in Ghana has been increasingly mounting pressure on its infrastructure. Blackouts are routine almost every week within many areas in the country. This is frustrating homes, businesses and people who use hydroelectric power in many ways of their lives. Companies are devising alternative means such as power generators, solar panels and other forms of power to compensate for the shortfall of hydroelectric power in the country. The exploitation of renewable energy sources can help meet many of environmental and energy policy goals, including obligation to reduce greenhouse effect.

Increasing world population and increasingly reducing oil reserves and resulting requirement for clean, reliable, renewable energy systems intensifies the requirement for wind energy in long term. As a proven source of clean, affordable energy, wind resources clearly have a vital role to play in realizing these goals. For that to be in reality, wind turbines are used to transform the wind energy into electrical and mechanical energy. In order to economically gain from a wind turbine in terms of maximum performance, data based on blade cross-section characteristics must be investigated and used. The innovation and the technological development of wind turbine blade is of major importance [5].

Wind turbines operating at low wind speed are unable to turn the blade to optimize its efficiency in generating electric power. This has lead to a lot of test on wind turbines to increase its power performance. One of such test was performed by Wind Energy Institute of Canada. They conducted a test on Whale Power tubercle blade power performance characteristic. These blades contain tubercles along most of the leading edge of the blade, much in the same way that humpback whales have tubercles on their flippers [1].

2.2 Blade Profiles

Horizontal axis wind turbine blades use airfoils to develop mechanical energy. It is through the rotor that the energy of the wind is transformed into mechanical energy that turns the main shaft of the wind turbine**.** The cross-sections of horizontal axis wind turbine blades have the shape of airfoils. The width and length of the blade are functions of the desired aerodynamic parameter, the maximum desired rotor power, the assumed airfoil parameters and strength calculations [6]. Hence designing Horizontal axis wind turbine blade depends on knowledge of the properties of airfoils. The most significant flow factor influencing the behaviour of airfoils is that of viscosity which is characterized by the *Reynolds number*. Airfoils in use on modern wind turbines range in representative chord size from about 0.3 m on a small-scale turbine to over 2 meters on a megawatt-scale rotor. For horizontal axis wind turbines, the Reynolds number ranges from about 0.5 million to 10 million. This implies that turbine airfoils generally operate beyond sensitive. It should be noted that there are significant differences in airfoil behaviour at different Reynolds numbers. For that reason it must be made sure that appropriate Reynolds number data are available for the blade design [6, 7].

There are evidently many engineering requirements into the selection of a wind turbine airfoil. These include primary requirements related to aerodynamic performance, structural, strength and stiffness, manufacturability and maintainability.

Two very important elements of a successful wind turbine are the blade and the power control system. In designing the blade, the most essential thing is to choose a good profile. Before designing the blade, a number of compromises including good lift and stall characteristics are taken into consideration. In selecting a profile for a wind turbine blade for a low wind speed ranging between 1.5 m/s and 4 m/s, one must check several important criteria: it should have a high coefficient of lift while maintaining a low coefficient of drag. Consequently, the lift/drag coefficient C_L/C_D should have a high value [8].

2.2.1 The Aerodynamic Profiles

The shape of the aerodynamic profile is decisive for blade performance. Even minor alterations in the shape of the profile can greatly alter the power curve and noise level. Therefore a blade designer does not merely sit down and outline the shape when designing a new blade. The aerodynamics of wind turbine blades has been largely based on models and calculations from the aeronautical industry. The shape must be chosen with great care on the basis of past experience. For this reason blade profiles were previously chosen from a widely used catalogue of airfoil profiles developed in wind tunnel research by NACA around the time of the Second World War [9]. The shape of the NACA airfoil is described using a series of digits following the word "NACA". The parameters in the numerical code can be entered into equations to precisely generate the cross-section of the airfoil and calculate its properties. At the start of a blade thesis, the specifications for the wind turbine are clearly stated so that the designer can use these specifications to perform initial calculations of the geometry and structure [10].

Figure 2.1 shows a wind turbine profile showing all the relevant parts. The mean camber line is the locus of points halfway between the upper and lower surfaces as measured perpendicular to the mean camber line itself. The most forward and rearward points of the mean camber line are the leading and trailing edges, respectively. The straight line connecting the leading and trailing edges is the chord line of the airfoil, and the distance from the leading to the trailing edge measured along the chord line is simply designated the chord of the airfoil. The thickness of the airfoil is the distance from the upper to the lower surface, measured perpendicular to the chord line, and varies with distance along the chord [11].

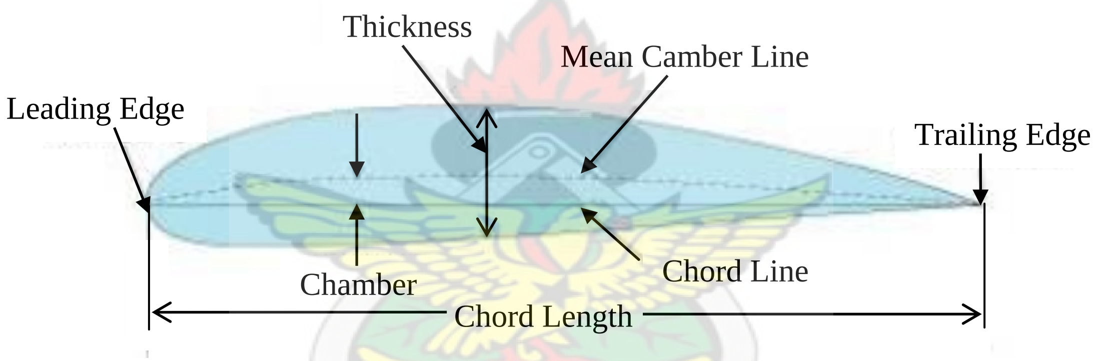

Figure 2.1: Wind Turbine Blade Nomenclature
Source: Walker, J. and Jenkins, N. (1997).

The maximum thickness, and where it occurs along the chord, is an important design feature of the turbine blade. The camber is the maximum distance between the mean camber line and the chord line, measured perpendicular to the chord line. Both the maximum thickness and the camber are usually expressed in terms of a percentage of the chord length; for example, a 12% thick airfoil has a maximum thickness equal to 0.12 multiplied by the chord length [5].

The aerodynamics of a horizontal-axis wind turbine is not straightforward. The air speed at the blades is not the same as the air speed far away from the turbine.

The very nature of the way in which energy is extracted from the air also causes air to be deflected by the turbine. In addition the aerodynamics of a wind turbine at the rotor surface exhibit phenomena that are rarely seen in other aerodynamic fields [9].

2.3 Classes of Wind Turbine

A wind turbine is a generic term for machines with rotating blades that convert the kinetic energy of wind into useful power. The basic idea has been around for a long time but modern wind turbines are a far cry from the original designs. Wind turbines can rotate about either on a horizontal or vertical axis, the former being more common. [8]

Modern turbines evolved from the early designs and are typically classified as two or three blade rotors. Most of the turbines used today have three blades. The rotational speed is also a very important design factor. Turbines operating at a constant rotor speed have been fomenting up to now, but turbines with variable rotational speed are becoming increasingly more common with the desire to optimize the energy captured, to lower stress, and to obtain better power quality. [7]

2.3.1 Horizontal Axis Wind Turbine Concept

Horizontal-axis wind turbine has the main rotor shaft and electrical generator at the top of a tower, and must be pointed into the wind as shown in Figure 2.2. Small turbines are pointed by a simple wind vane, while large turbines generally use a wind sensor coupled with a servo motor. Most have a gearbox, which turns the slow rotation of the blades into a quicker rotation that is more suitable to drive an electrical generator.

Figure 2.2: Horizontal Axis Wind Turbine
Source: Walker, J. and Jenkins, N. (1997).

Turbine blades are made stiff to prevent the blades from being pushed into the tower by high winds. Additionally, the blades are placed a considerable distance in front of the tower and are sometimes tilted forward into the wind a small amount. Downwind machines have been built, despite the problem of turbulence because they don't need an additional mechanism for keeping them in line with the wind, and because in high winds the blades can be allowed to bend which reduces their swept area and thus their wind resistance. Since cyclic or repetitive turbulence may lead to fatigue failures most Horizontal wind turbine are upwind machines [9].

2.3.2 Vertical Axis Wind Turbine Concept

Vertical Axis Wind Turbines have the main rotor shaft arranged vertically as shown in Figure 2.3. Key advantages of this arrangement are that the turbine does not need to be pointed into the wind to be effective. This is an advantage on sites where the wind direction is highly variable.

Figure 2.3: Vertical Axis Wind Turbine
Source: Walker, J. and Jenkins, N. (1997).

With a vertical axis, the generator and gearbox can be placed near the ground, so the tower doesn't need to support it, and it is more accessible for maintenance. Drawbacks are that some designs produce pulsating torque. It is difficult to mount vertical-axis turbines on towers, meaning they are often installed nearer to the base on which they rest, such as the ground or a building rooftop [9].

The wind speed is slower at a lower altitude, so less wind energy is available for a given size turbine. Air flow near the ground and other objects can create turbulent flow, which can introduce issues of vibration, including noise and bearing wear which may increase the maintenance or shorten the service life. However, when a turbine is mounted on a rooftop, the building generally redirects wind over the roof and these can double the wind speed at the turbine. If the height of the rooftop mounted turbine tower is approximately 50% of the building height, this is near the optimum for maximum wind energy and minimum wind turbulence [10].

2.4 Wind Speed Analysis on Horizontal and Vertical Axis Wind Turbine

The calculated wind speed for Horizontal Axis Wind Turbines is in the limits of 12 m/s to 15 m/s because of strength requirements for inertial loading. If the starting speed will be changed from 4.5 m/s to 7.5 m/s, then the energy production will be reduced on 2%. The influence of calculated nominal speed on the energy production is high. For instance the increase of calculated wind speed from 10.4 m/s to 20 m/s makes the energy production higher by four times. It means that for regions with high wind potential the calculated wind speed, taken for normal conditions, is smaller than it should be. Big wind power resources will not be used. The operating range of wind speed for low speed Vertical Axis Wind Turbine's is increased up to 20 m/s to 25 m/s, comparing with Horizontal Axis Wind Turbine which is 12 m/s to 15 m/s. It means that Vertical Axis Wind Turbines are preferable for regions with high wind potential [11].

2.5 Wind Resources in Ghana

One of the most important considerations in wind turbine design is the environment where it will be installed. Wind turbines can work in almost all the places, but the design dimensions would be different depending conditions of the place. Winds are large scale movements of air masses in the atmosphere. The movements are created on a global scale primarily by different solar heating of the earth's atmosphere. Wind speeds, of up to about 13 m/s can be harnessed by wind turbines to provide sufficient power in remote areas. The Metrological service department has installed a cup counter anemometer and dines pressure tube anemometer to measure instantaneous wind speed and direction. They have since recorded wind speed and direction data at 12 m above ground level from all their 22 synoptic stations sited within every latitude and longitude of the country. The data obtained from the Metrological service department indicate wind speeds of approximately 2.4 m/s at 12 m above ground level at stations set up with objectives other than for energy applications. The sites were deliberately selected for their low wind regimes as the measurements were made for meteorological and agricultural applications. The obtained data could therefore not be used as a true assessment of the wind energy potential in the country. For a long time, the lack of dependable countrywide data on wind energy has been the main obstacles for harnessing wind energy. Nonetheless, it is quite obvious that Ghana has some winds that could be tapped to supplement her energy requirements

The Energy Commission in 1999 started wind energy resource measurement along the coast of Ghana with the view to develop adequate, accurate and reliable wind energy data and evaluation tools as an integral part of Ghana's energy planning and policy framework. Measurements were taken at 11 sites East and West of the Meridian. The sites east of the Meridian were Tema, Adafoah, Lolonya, Pute, and Kpone with the sites west of the Meridian being Asemkow in Takoradi, Warabeba in Winneba, Mankoadze, Bortianor, GomoaFetteh and Aplaku. These studies and others made by private concerns at six coastal sites east of Tema in 1999 indicated the existence of fairly strong winds that could be utilized for power generation. The data collected included average wind speed, average wind direction and standard deviation. The monthly average wind speed measurement at 12 m above ground varied in the range of 4.8 m/s to 5.5 m/s. The data somehow validated a six year satellite-borne measurement provided by the U.S National Renewable Energy Laboratory (NREL), which suggested that Ghana has appreciable wind resource for power generation.

A wind energy system usually needs an average annual wind speed of at least 4 m/s to be practical. Table 2.1 shows the average wind speeds for coastal Ghana; between Latitude 5^o–6^o N and Longitude 0^o-1^o E. Over the last decade, there has been a marked change towards offshore wind as a key energy resource. Increased wind speed and reduced wind turbulence offshore are much more appreciated now, and this in conjunction with more cost effective infrastructure has reduced the predicted cost of energy from offshore projects. Offshore Ghana has a considerable high potential for wind energy from the conducted studies undertaken by National Renewable Energy Laboratory.

These are monthly average wind speeds at Tema and four other surrounding coastal towns, namely; Kpone, Lolonya, Adafoah and Pute in 1999 compiled by the Energy Commission. The average wind speed measured about 10 km off the coastline in the direction of the sea is about 5.5 m/s. It is about the same in the western and central regions which constitute about two thirds of the total coastline of Ghana. The offshore wind energy potential is huge and worth pursuing.

Table 2.1: Average wind speeds for coastal Ghana; between Latitude 5^o–6^oN and Longitude 0^o -1^o E

Sensor Height*(m/s)	**July**	**Aug**	**Sept**	**Oct**	**Nov**	**Dec**
12 meters	4.56	5.41	5.49	6.36	5.08	4.74
40 meters	5.41	6.31	6.54	7.54	6.02	5.18
Satellite(NREL)	5.4-6.0	4.6-5.2	4.8-5.3	4.5-5.0	3.5-3.7	3.6-4.2

Over the land, the wind speed is averagely between 2 m/s and 9 m/s. With the wind speeds recorded for medium power turbines could be operated as alternative to large-scale turbines. Some investors have shown considerable interest in the exploitation of wind energy in Ghana. Indeed, some private firms are already in touch with the Energy Commission on the possibility of setting up wind farms for power generation. The average wind speed of the extrapolated data for all the 22 synoptic stations were in the range of 2 m/s to 5.1 m/s at 12 m above ground and 3.5 m/s to 8.4 m/s at 50 m above ground level.

The average wind speed along the coast was in the range of 4 m/s to 5.1 m/s at 12 m above the ground and 6 m/s to 6.4 m/s at 50 m above the ground level along the coast, west of the meridian. Mankoadze recorded the highest mean speed of 6.08 m/s whilst Oshiyie recorded the lowest of 3.33 m/s. Figure 2.4, 2.5, and 2.6 all show the wind distribution at onshore areas at 12 m and 50 m above ground levels respectively.

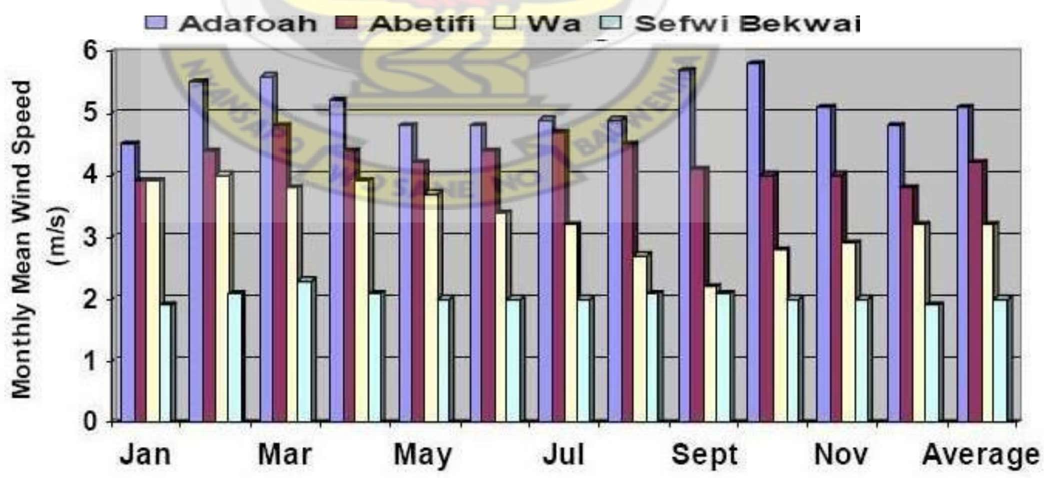

Figure 2.4: Wind Speed Distribution at 12 m above ground level in Ghana
Source: SWERA Ghana project, (2005)

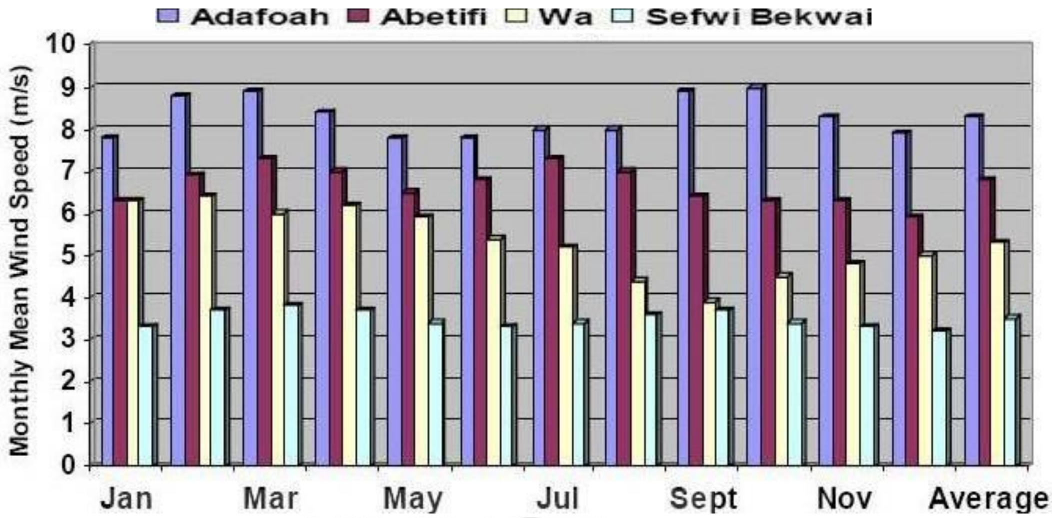

Figure 2.5: Wind Speed Distribution at 50 m above ground level in Ghana
Source: SWERA Ghana project, (2005)

On the east coast of the meridian, Lolonya gave the highest wind speed of 5.43 m/s and the predominant direction of the wind speed was 240^o with a corresponding mean wind speed of 5.66 m/s and frequency 47%. For Adafoah the mean wind speed was 5.33 m/s and the predominant direction of the wind speed was 240^o with a corresponding mean wind speed of 5.52 m/s and frequency of 47% followed by 210^o with mean speed of 5.69 m/s and frequency of 31%.

The analyses of the available wind data indicate that the mean wind speed for Mankoadze, Lolonya, Adafoah, Petu, and Aklaku were in the range of 5 m/s to 6.1 m/s at 12 m above ground with corresponding power densities of 119 to 410 W/m^2. With these speeds electric power generation is favorable. Aerial survey by an international team on the SWERA project identified some spots inland Ghana with high wind regimes [11].

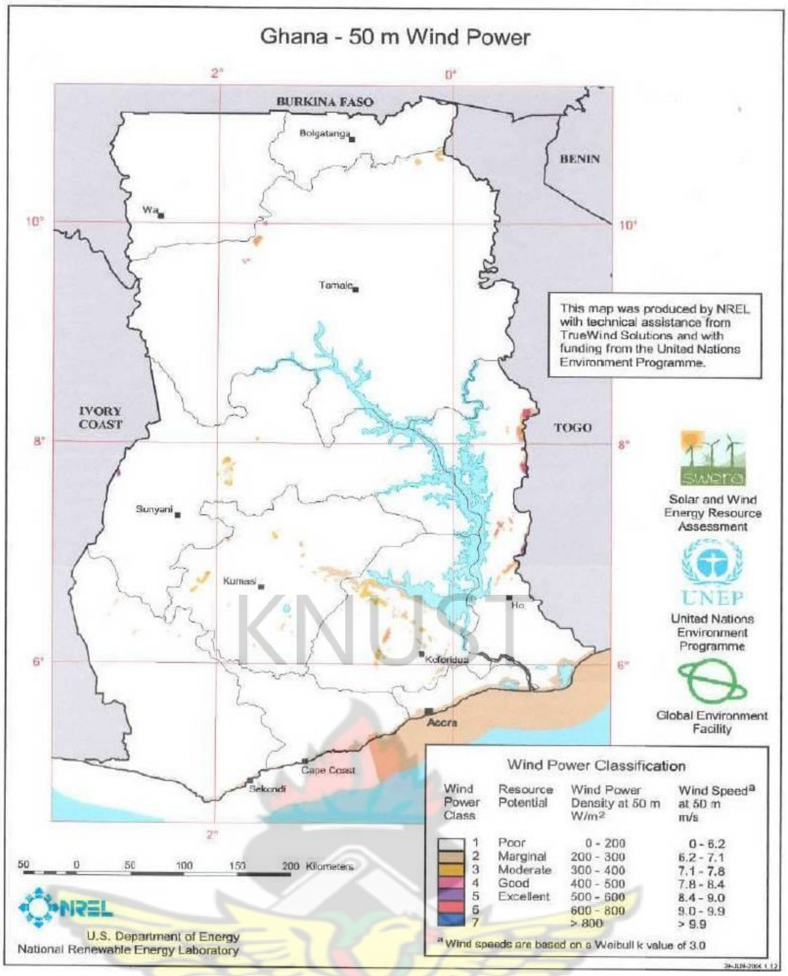

Figure 2.6: Wind Power Classification Map at 50 m

Source: SWERA Ghana project, (2005)

CHAPTER THREE

3.0 Model of Aerodynamic Parameters and Calculation

In this chapter, the application of blade element momentum theory on horizontal axis wind turbine and the analysis on the aerodynamic performance of the blade profile would be computed and explained. Finally, the blade designed procedure would be used to design a blade profile with optimum performance.

3.1 Blade Element Momentum Theory

The principle of the blade element theory is to consider the forces experienced by the blades of the rotor in their motion through the air and this theory is therefore intimately concerned with the geometrical shape of the blade. That is, the blade-element theory method will be used in analysing the behaviour of blades due to their motion through air. Blade element momentum theory relates rotor performance to rotor geometry and particularly important, prediction of this theory is the effect of finite blade number [12, 13].

The first assumption in Blade element momentum theory is that individual stream tubes can be analysed independently of the rest of the flow. A second assumption associated with the development of blade element momentum theory is that span wise flow is negligible, and therefore airfoil or profile data taken from two-dimensional section tests are acceptable. A third assumption is that flow conditions do not vary in the circumferential direction. With this assumption the stream tube to be analysed is a uniform annular ring centred on the axis of revolution [12, 15].

Blade Element Momentum Theory equates two methods of examining how a wind turbine operates. The first method is to use a momentum balance on a rotating annular stream tube passing through a turbine. The second is to examine the forces generated by the airfoil lift and drag coefficients at various sections along the blade. These two methods then give a series of equations that can be solved iteratively [16, 17].

3.2 Equations under Blade Momentum Theory

3.2.1 Axial Force

The blade momentum theory assumes a control volume, in which the control volume boundaries are the surface of a stream tube. The turbine in the tube creates a discontinuity of pressure in the stream tube of air flowing through it. Considering the stream tube around a wind turbine shown in Figure 3.1, there are four points shown in the Figure. Point (1) is the upstream of the turbine, point (2) just before the turbine blades, point (3) just after the blades and point (4), downstream of the blades. Between point (2) and point (3), energy is extracted from the wind and there is a change in pressure as a result [13, 18].

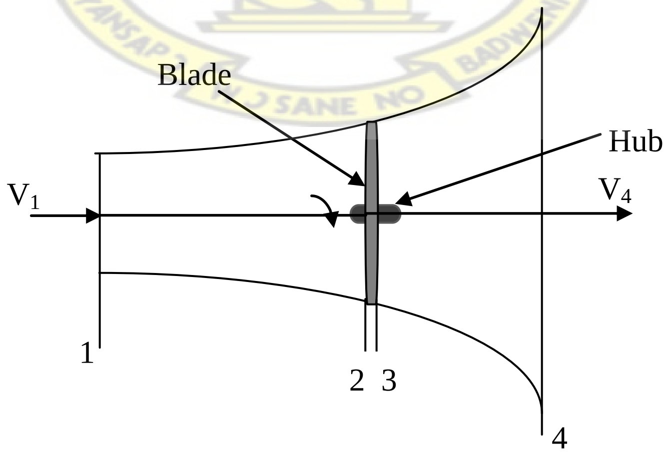

Figure 3.1: Axial Stream tube around a Wind Turbine

From the assumption that the continuity of velocity through the turbine exists, Assume $p_1 = p_4$ and that $V_2 = V_3$.

We can also assume that between points (1) and (2) and between points (3) and (4) the flow is frictionless so we can apply Bernoulli's equation to arrive at.

$$p_2 - p_3 = \frac{1}{2}\rho\,(V_1^2 - V_4^2) \quad (1)$$

It is also known that force is the product of pressure and area, so we find that;

$$dF_x = (p_2 - p_3)dA \quad (2)$$

$$dF_x = \frac{1}{2}\rho\,(V_1^2 - V_4^2)dA \quad (3)$$

If an axial induction factor, a is defined as the fractional decrease in the wind velocity between the free stream and the rotor plane, then a, can be defined as;

$$a = \frac{(V_1 - V_2)}{V_1} \quad (4)$$

It can also be shown from equation (4) and (6) that:

$$V_2 = V_1(1 - a) \quad (5)$$

$$V_4 = V_1(1 - 2a) \quad (6)$$

Substituting equation (6) into equation (3) yields:

$$dF_x = \frac{1}{2}\rho V_1^2\,[4a(1 - a)]2\pi r dr \quad (7)$$

3.2.2 Rotating Annular Stream tube

Consider the conservation of angular momentum in this annular stream tube. A side and an end view are shown in Figure 3.2 and Figure 3.3 respectively.

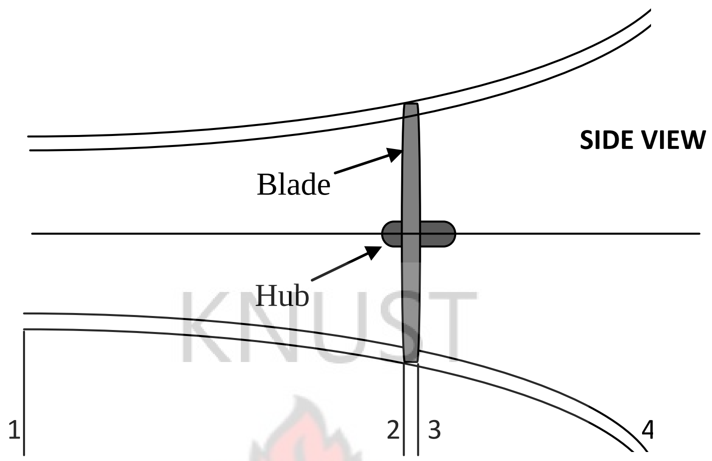

Figure 3.2: A Side View of Rotating Annular Stream Tube

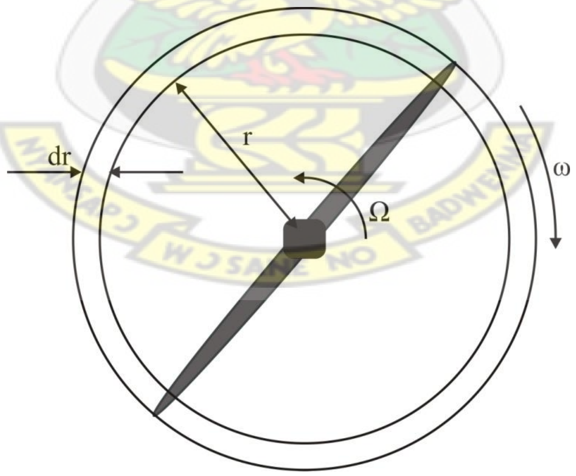

Figure 3.3: An End View of Rotating Annular Stream Tube

The blade wake rotates with an angular velocity ω, and the blades rotate with an angular velocity, Ω. For steady state flow, air mass flow rate through the disk can be written as:

Moment of Inertia of an annulus,

$$I = mr^2 \tag{8}$$

Angular Moment,

$$L = I\omega \tag{9}$$

Torque,

$$T = \frac{dL}{dt} \tag{10}$$

$$T = \frac{dI\omega}{dt} = \frac{d(mr^2\omega)}{dt} = \frac{dm}{dt}r^2\omega \tag{11}$$

So for a small element the corresponding torque will be:

$$dT = d\dot{m}\omega r^2 \tag{12}$$

For steady state flow, air mass flow rate through the disk can be written as;

$$d\dot{m} = \rho\, AV_2 \tag{13}$$

$$d\dot{m} = \rho 2\pi r dr V_2\omega\, r^2 \tag{14}$$

$$d\dot{m} = \rho V_2\, \omega r^2 2\pi r dr \tag{15}$$

Define angular induction factor a':

$$a' = \frac{\omega}{2\Omega} \tag{16}$$

From Equation (5), $V_2 = V(1 - a)$ so:

$$dT = 4\, a' (1 - a)\rho V \Omega r^3 \pi dr \tag{17}$$

Momentum theory has therefore yielded equations for the axial Equation (7) and tangential force Equation (17) on an annular element of fluid.

3.2.3 Blade Element Theory

Blade element theory relies on two key assumptions [19]:

- There are no aerodynamic interactions between different blade elements.
- The forces on the blade elements are solely determined by the lift and drag coefficients.

Consider a blade divided up into N elements as shown in Figure 3.4.

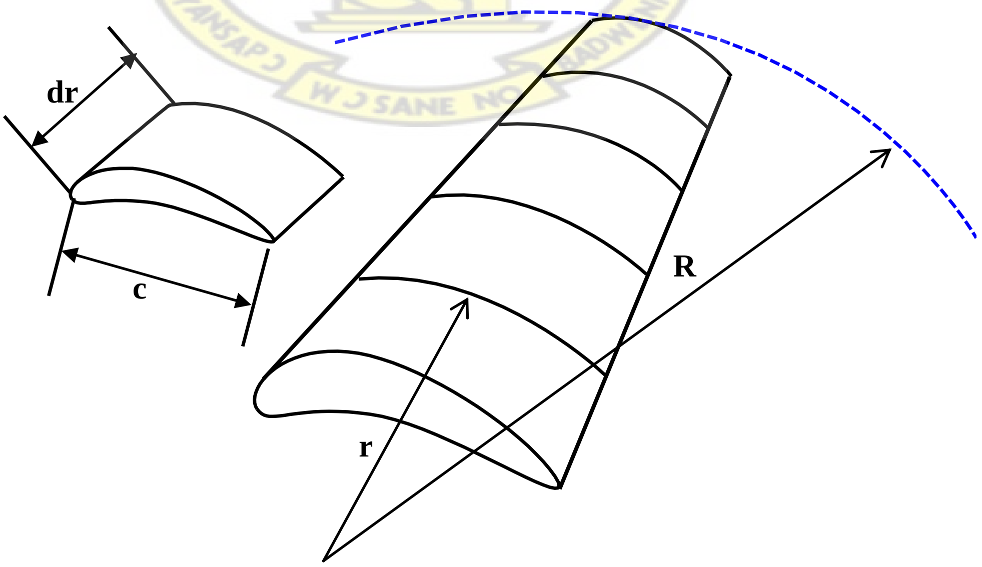

Figure 3.4: The Blade Element Model

Each of the blade elements will experience a slightly different flow as they have a different rotational speed (Ωr), a different chord length (c) and a different twist angle ($\boldsymbol{\gamma}$). Blade element theory involves dividing up the blade into a sufficient number of elements and calculating the flow at each one. The overall performance characteristics are determined by numerical integration along the blade span [13, 20].

3.2.4 Relative Flow

In practice the flow of wind over a turbine blade is turned slightly as it passes over it. In order to obtain a more accurate estimate of turbine blade performance, an average of inlet and exit flow conditions is used to estimate performance.

The flow around the blades starts at station (2) as shown in Figures 3.1 and 3.2 and ends at station (3). At inlet to the blade the flow is not rotating, at exit from the blade row the flow rotates at rotational speed ω. That is over the blade row wake rotation has been introduced. The average rotational flow over the blade due to wake rotation is therefore $\omega/2$. The average tangential velocity which the blade experiences is shown in Figure 3.5.

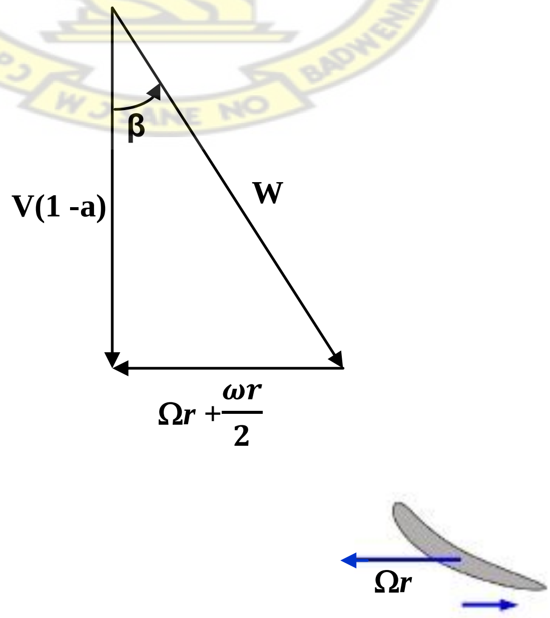

Figure 3.5: Flow onto the Turbine Blade

Examining Figure 3.5 we can immediately note that:

$$\Omega r + \frac{\omega r}{2} = \Omega r(1 + a') \tag{18}$$

From Equation (11), $V_2 = V_1(1 - a)$ and so:

$$\tan \beta = \frac{\Omega r\,(1+a')}{V(1-a)} \tag{19}$$

Where V is used to represent the incoming flow velocity. The value of β will vary from blade element to blade element. The local tip speed ratio, λ is defined as:

$$\lambda = \frac{\Omega r}{V} \tag{20}$$

So the expression for tan β can be further simplified:

$$\tan \beta = \frac{\lambda(1+a')}{(1-a)} \tag{21}$$

From Figure 3.5 the following relation is apparent:

$$W = \frac{V(1-a)}{\cos \beta} \tag{22}$$

3.2.5 Blade Elements

The forces on the blade element are shown in Figure 3.6. Note that by definition the lift and drag forces are perpendicular and parallel to the incoming flow.

For each blade element one can see:

$$dF_\theta = dL\cos\beta - dD\sin\beta \qquad (23)$$

$$dF_x = dL\sin\beta - dD\cos\beta \qquad (24)$$

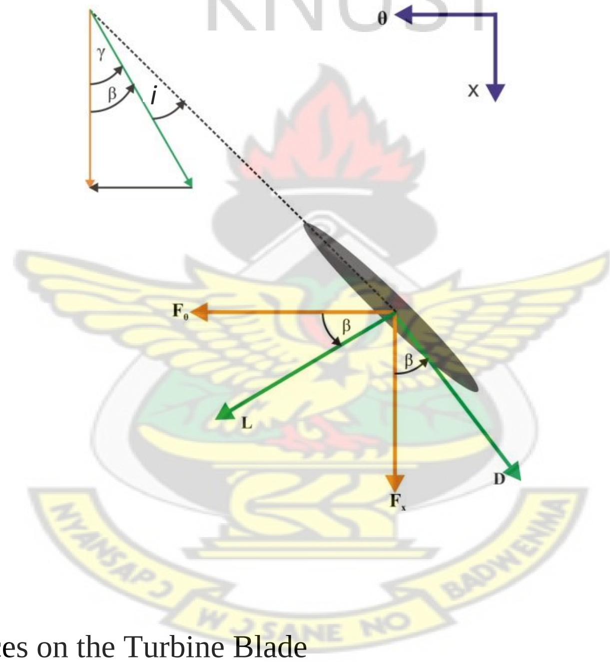

Figure 3.6: Forces on the Turbine Blade

Where dL and dD are the lift and drag forces on the blade element respectively. dL and dD can be found from the definition of the lift and drag coefficients as follows:

$$dL = \frac{1}{2} C_L \cdot \rho \cdot c \cdot W^2 dr \qquad (25)$$

$$dD = \frac{1}{2} C_D \cdot \rho \cdot c \cdot W^2 dr \qquad (26)$$

If there are B blades, combining equation (23) and equation (24) it can be shown that:

$$dF_x = B\frac{1}{2}\rho W^2(C_L\sin\beta + C_D\cos\beta)cdr \qquad (27)$$

$$dF_\theta = B\frac{1}{2}\rho W^2(C_L\cos\beta + C_D\sin\beta)cdr \qquad (28)$$

The Torque on an element, dT is simply the tangential force multiplied by the radius.

$$dT = B\frac{1}{2}\rho W^2(C_L\cos\beta + C_D\sin\beta)crdr \qquad (29)$$

The effect of the drag force is clearly seen in the equations, an increase in thrust force on the machine and a decrease in torque and power output.

These equations can be made more useful by noting that β and W can be expressed in terms of induction factors etc. Substituting and carrying out some algebra yields:

$$dF_x = \sigma'\pi\rho\frac{V^2(1-a)^2}{\cos^2\beta}(C_L\sin\beta + C_D\cos\beta)rdr \qquad (30)$$

$$dT = \sigma'\pi\rho\frac{V^2(1-a)^2}{\cos^2\beta}(C_L\cos\beta + C_D\sin\beta)r^2dr \qquad (31)$$

Where σ′ is called the local solidity and is defined as:

$$\sigma' = \frac{Bc}{2\Pi r} \qquad (32)$$

3.2.6 Tip Loss Correction

At the tip of the turbine blade losses are introduced in a similar manner to those found in wind tip vortices on turbine blades. These can be accounted for in BEM theory by means of a correction factor. This correction factor Q varies from 0 to 1 and characterizes the reduction in forces along the blade [20].

$$Q = \frac{2}{\pi} cos^{-1}\left[exp\left\{-\left(\frac{B/2[1-r/R}{(r/R)cos\beta}\right)\right\}\right] \quad (33)$$

The results from $\cos^{-1}$ must be in radians. The tip loss correction is applied to Equation (7) and Equation (17) to give:

$$dF_x = Q\rho V_1^2[4a(1-a)]\pi rd\boldsymbol{r} \quad (34)$$

$$dT = Q4a^{'}(1-a)\rho V\Omega r^3\pi dr \quad (35)$$

3.2.7 Blade Element Momentum Equations

We now have four equations; two derived from momentum theory which expresses the axial thrust and the torque in terms of flow parameters Equations (7) and (17).

$$dF_x = Q\rho V_1^2[4a(1-a)]\pi rdr \quad (36)$$

$$dT = Q4a^{'}(1-a)\rho V\Omega r^3\pi dr \quad (37)$$

We also have two equations derived from a consideration of blade forces which express the axial force and torque in terms of the lift and drag coefficients of the airfoil from Equations (30) and (31) as follow:

$$dF_x = \sigma^{'}\pi\rho\frac{V^2(1-a)^2}{cos^2\beta}(C_L sin\beta + C_D cos\beta)rdr \quad (38)$$

$$dT = \sigma^{'}\pi\rho\frac{V^2(1-a)^2}{cos^2\beta}(C_L cos\beta - C_D sin\beta)r^2dr \quad (39)$$

To calculate rotor performance, Equations (35) and (34) from a momentum balance are equated with Equations (30) and (31). Once this is done the following useful relationships arise:

$$\frac{a}{1-a} = \frac{\sigma' [C_L sin\beta + C_D cos\beta]}{4Q cos^2\beta} \quad (40)$$

$$\frac{a'}{1-a} = \frac{\sigma' [C_L \cos\beta + C_D \sin\beta]}{4Q\lambda_r \cos^2\beta} \quad (41)$$

Equation (40) and (41) are used in the blade design procedure.

3.2.8 Power Output

The contribution to the total power from each annulus is:

$$dP = \Omega dT \quad (42)$$

The total power from the rotor is:

$$P = \int_{rh}^{R} dPdr \quad (43)$$

$$P = \int_{\boldsymbol{rh}}^{\boldsymbol{R}} \Omega dTdr \quad (44)$$

Where r_h is the hub radius. The power coefficient C_P is given by:

$$C_P = \frac{P}{P_{wind}} \quad (45)$$

$$C_P = \frac{\int_{rh}^{R} \Omega dT}{\frac{1}{2}\rho\pi R^2 V^3} \quad (46)$$

Using Equation (31) it is possible to develop an integral for the power coefficient directly. After some algebra:

$$C_P = \frac{8}{\lambda^2}\int_{\lambda h}^{\lambda} \lambda_r^3 \, a'(1-a)\left[1 - \frac{C_D}{C_L} tan\beta\right] d\lambda_r \quad (47)$$

For a selected airfoil type and for a specified tip-speed ratio and blade length, the blade shape can be designed for optimum blade airfoil for maximum circulation. Also, from the deduction of power coefficient maximum power and lift force can then be calculated to see the performance of the rotor in an average wind velocity of 3 m/s.

3.3 Blade Design

3.3.1 Introduction

Designing a blade shape from a known airfoil or profile type for an optimum blade means determining the blade shape parameters such as the chord length distribution and twist distribution along the blade length for a certain tip-speed ratio at which the power coefficient and of the rotor is maximum. To achieve this, the change of the power coefficient of the rotor with respect to tip-speed ratio should be figured out in order to determine the design tip-speed ratio at which the rotor has a maximum power coefficient. The blade design parameters are then obtained accordingly using the design tip-speed ratio. Since the airfoil type is selected before, the glide ratio included in this term can be chosen so as to it gets maximum value [21].

All the airfoils were chosen based on its performance and its ability to circulate at low wind speed to generate both power and lift at its maximum. A spread sheet is used to determine the maximum power coefficient for each blade element (elemental power coefficient) for any set of values of local tip-speed ratio [22].

3.3.2 Blade Design Procedure

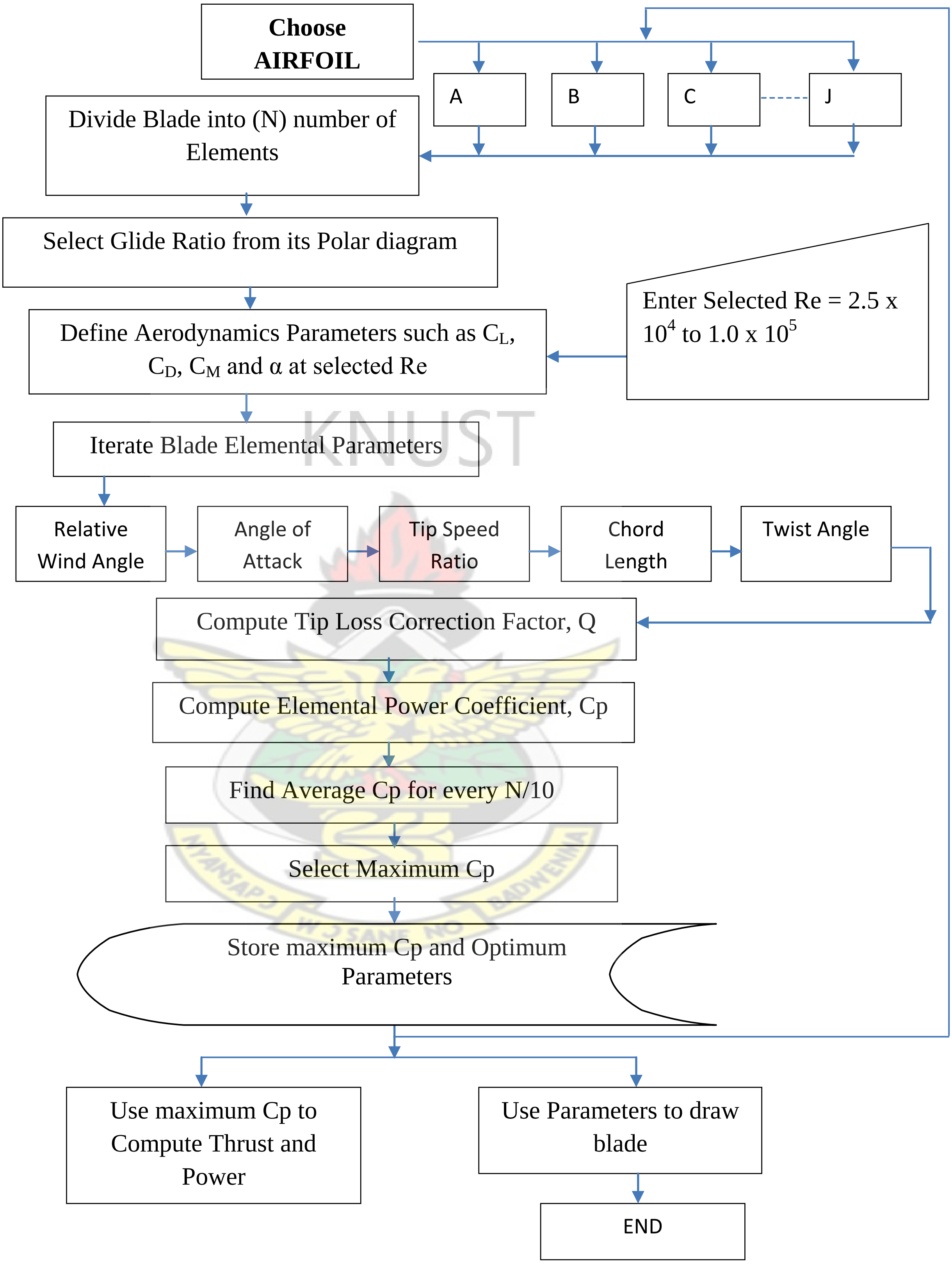

Figure 3.7: Flow Chart for Wind Turbine Blade Design Using the BEM Approach

The blade design procedure shown in Figure 3.7 gives a summary on how all the ten blade profiles are first designed for maximum performance within low wind speed. The airfoils were chosen based on its maximum performance in low wind speed with appreciable Reynolds number in the order of 1 million. In each case of the design, the power coefficient was iterated to obtain a maximum value at which the corresponding blade parameters were stored. These parameters are taken as the optimum blade parameters. Some of the blade parameters include the chord width, the tip speed ratio, twist angle, blade angle, angle of attack, lift coefficient, drag coefficient and moment coefficient. The design begins with airfoil NACA 4412 followed by WorthmannFx 63-137, Selig 1210, Ara-D 6%, Selig 2091, Selig Donovan 7032, Selig Donovan 7037, Selig Donovan 8000, Selig 3021, and Ara-D 10%.

Aerodynamic parameters with optimum performance with good features from the ten designed profiles in Figure 3.7 are stored. The stored values as well as some good features from the ten profiles are used to redesign a new blade profile called low wind speed **(LWS)** Blade profile which would comparatively give an appreciable power coefficient at low wind speed. The redesign process is shown in Figure 3.8.

In designing the LWS blade profile for maximum circulation and power generation, the existing ten blade profiles are selected one after the other and its stored aerodynamics parameters (Figure 3.7) tested and optimized.

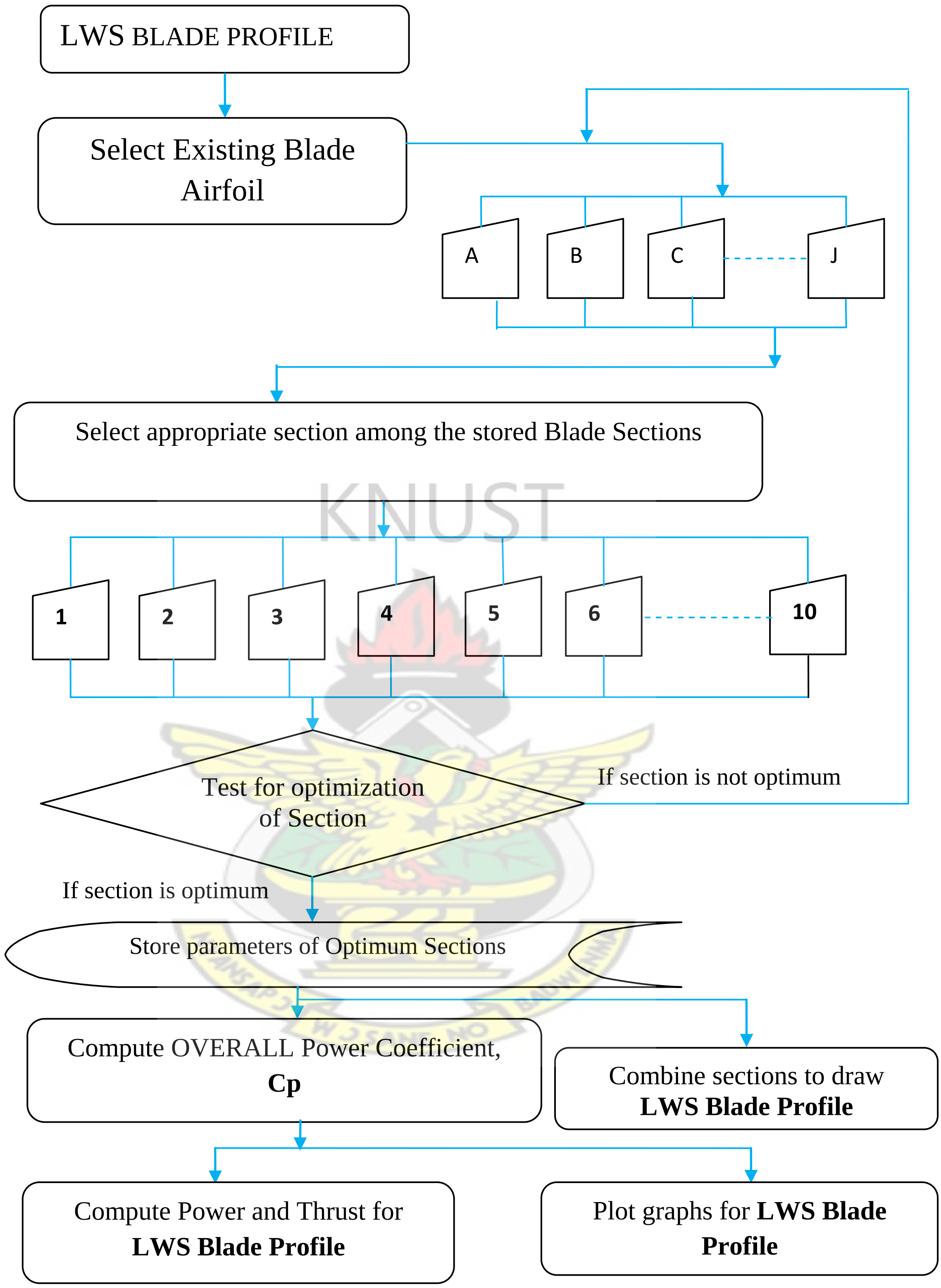

Figure 3.8: Flow Chart for Optimized LWS Blade Profile

CHAPTER FOUR

Results and Discussion

4.1 Introduction

The design procedures shown in Figures 3.7 and 3.8 (chapter three) are used to obtain graphs and drawings for analysis and discussions. The designed process in Figure 3.7 gives the design analysis of all the ten air foils which were selected and their parameters and or features examined through an iterative process to obtain optimum parameters. Appendix I give detailed information of the iterative process of one of the profiles. In the analysis of these profiles, several graphs were drawn to show the various effects that aerodynamic parameters have on the performances of the blade.The elemental blade profile as well as two dimensional views of each blade profile was generated. The results are illustrated in Figures 4.1 through to Figure 4.79.

The performance of the blade profile greatly depends on the power coefficient of the airfoil and this factor is directly proportional to the power output of the blade profile [9]. Therefore, in designing a blade profile that performs best at low wind speed, the blade parameters and features that tend to give a higher power coefficient are critically tested and stored for the design of a new blade profile called the LWS blade profile. Figure 3.8 systematically depicts how the LWS blade profile is obtained. Similarly graphs and drawings are obtained for the LWS blade profile to substantiate its pattern and profile shape in Figure 4.80 through to Figure 4.90.

The parameters of the optimized LWS blade profile are then compared with the existing profiles. The power of the optimized LWS blade profile is validated with standard Power versus Wind speed data of the Evance Wind Turbine Limited, a recognized and accredited wind turbine company.

4.2 Blade Design Results

The aerodynamic properties of all ten blade profiles in Appendix II and III are used in the design process to obtain a number of plots and drawings for the profiles. Some of the graphs plotted to assess the profiles for its performance are the variation of elemental power coefficient with respect to relative wind angles for values of local tip-speed ratio, power coefficient against relative wind angles, power coefficient against chord-length distribution, power coefficient against tip-speed ratio, twist, torque and thrust distributions for the designed blade.

4.2.1 Blade design results for NACA 4412

Both Figure 4.1 and Figure 4.2 show an elemental blade section and a set of elemental blade sections up to 50th element to substantiate the pattern of the dimensional views of the blade profile.The plot in Figure 4.3 clearly shows the elemental power coefficient versus relative wind angles for values of local tip speed ratios of λ_1= 4, λ_2=5 ….., λ_5= 8. The highest elemental power coefficient as well as the generalized power coefficient, C_P of 0.55 occurred at a relative wind angle of 10.20^o as shown in Figures 4.3. For each of the profiles the coefficient of lift increased by 0.11 from the reference value for every extra degree of angle of attack up to some maximum lift limit when the airflow separated from the airfoil and lift suddenly dropped and whiles drag increased.

Moreover, when the power coefficient was plotted against various chord length ratios, the optimum power and hence lift occurred at a chord length ratio (c/R) of 0.44 at the same C_P of 0.55. Similarly, a tip speed ratio of 7.44 occurred at the same power coefficient as indicated in Figure 4.6

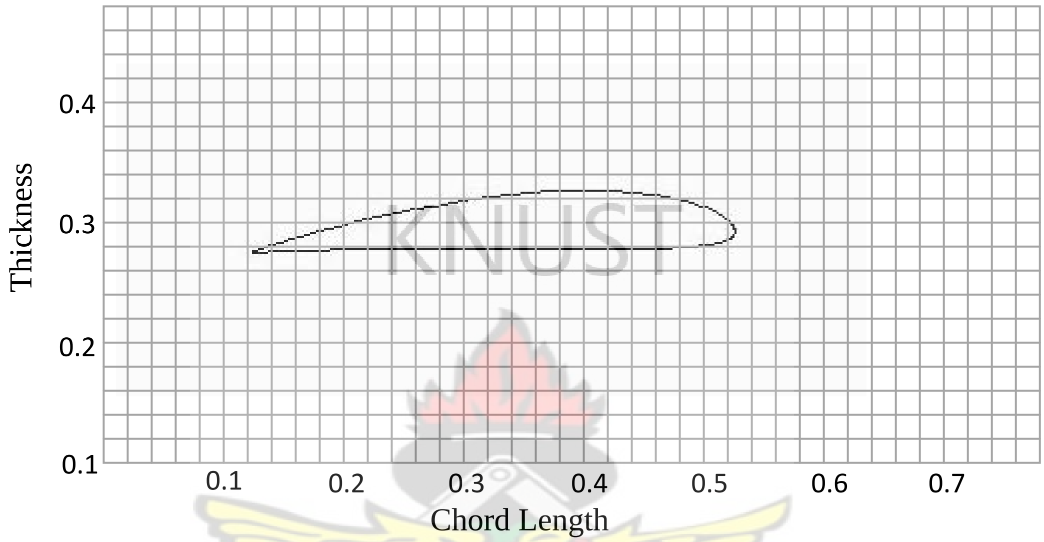

Figure 4.1: 2-D Sectional View of NACA 4412 Designed Blade Profile Element

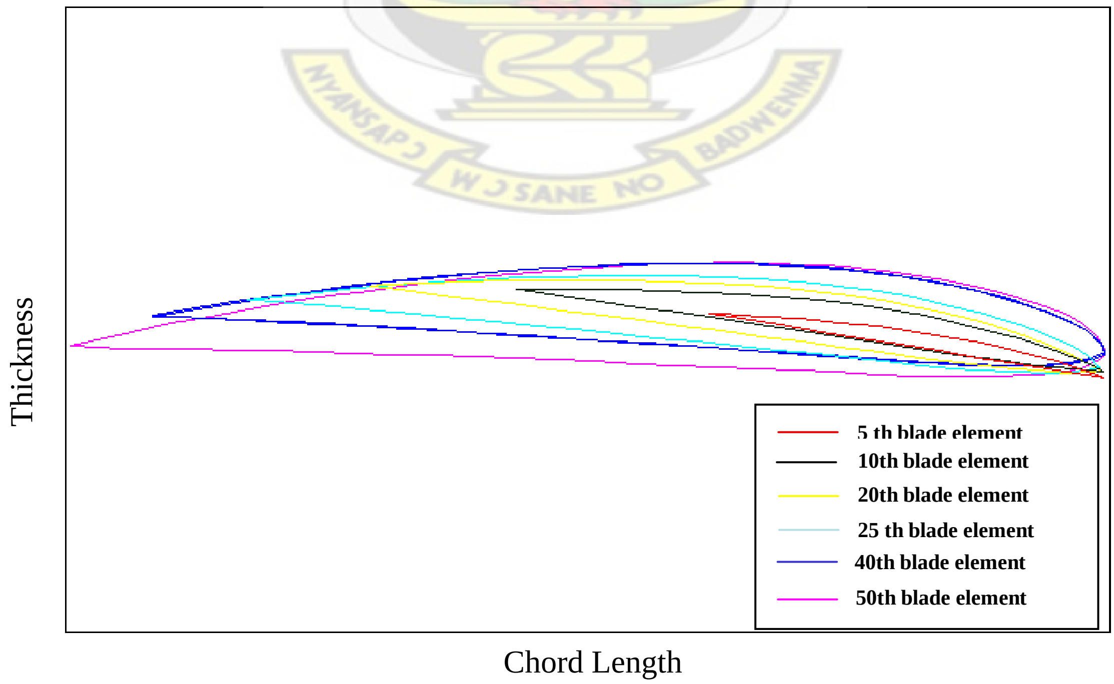

Figure 4.2: 2-D Sectional View of NACA 4412 Designed Blade Profile for Set of Blade Elements

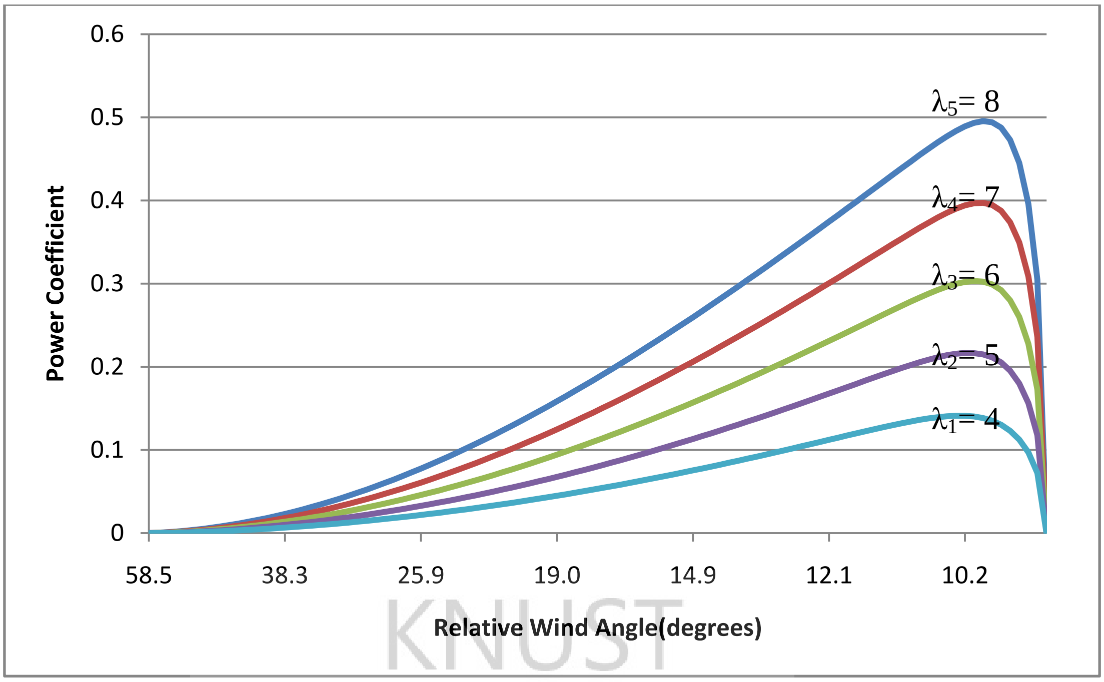

Figure 4.3: Variation of Elemental Power Coefficient with Relative Wind Angles for Values of Local Tip-Speed Ratio for NACA 4412

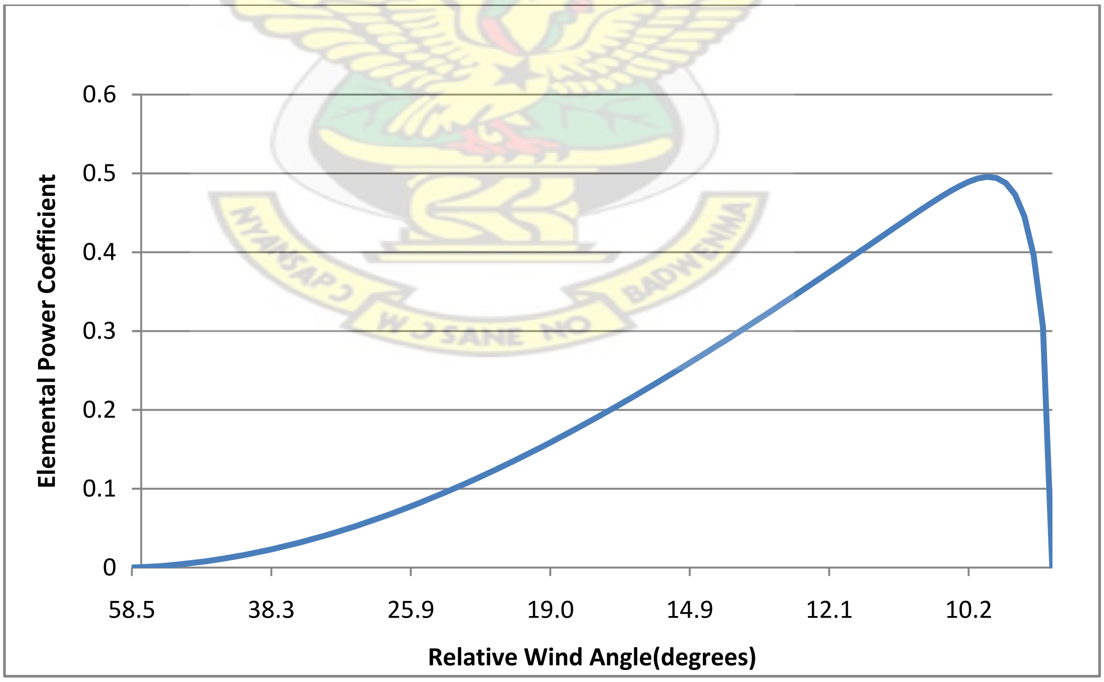

Figure 4.4: A Graph of Power Coefficient against Relative Wind Angle for NACA 4412

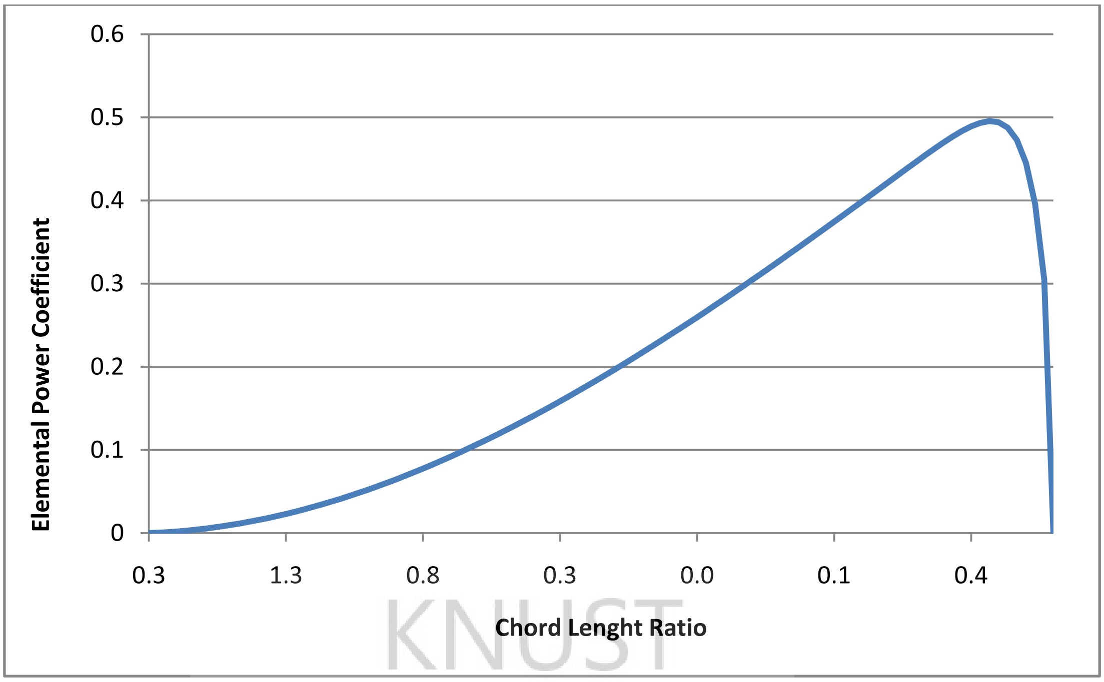

Figure 4.5: Variation of Power Coefficient to Chord Length Ratio for NACA 4412

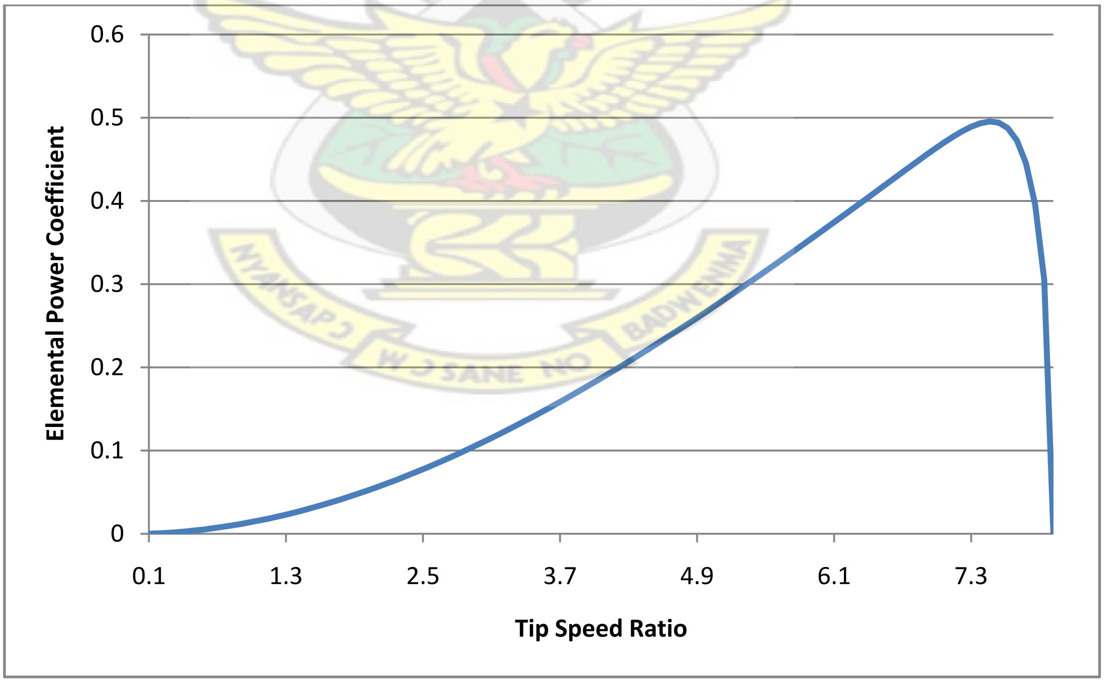

Figure 4.6: Variation of Elemental Power Coefficient to Elemental Tip Speed Ratio for NACA 4412

From Figure 4.7, the twist distribution for the designed blade showed a normalized outline. It could be observed from the aforementioned Figure that as the twist distribution reaches zero the radial locations gives a negative twist angle pattern starting from (r/R) 0.81. This has a higher probability of stalling the blade at that point. It could also be seen that the twist angle is highest at the root and least at the tip of the blade as radial location increases accordingly.

Figure 4.8 also shows how power coefficient relates to torque and thrust distribution along the blade profile. It depicts when the maximum thrust and torque occurred along the blade against the required power coefficient. The maximum thrust and torque were considered in the design of the blade profile.

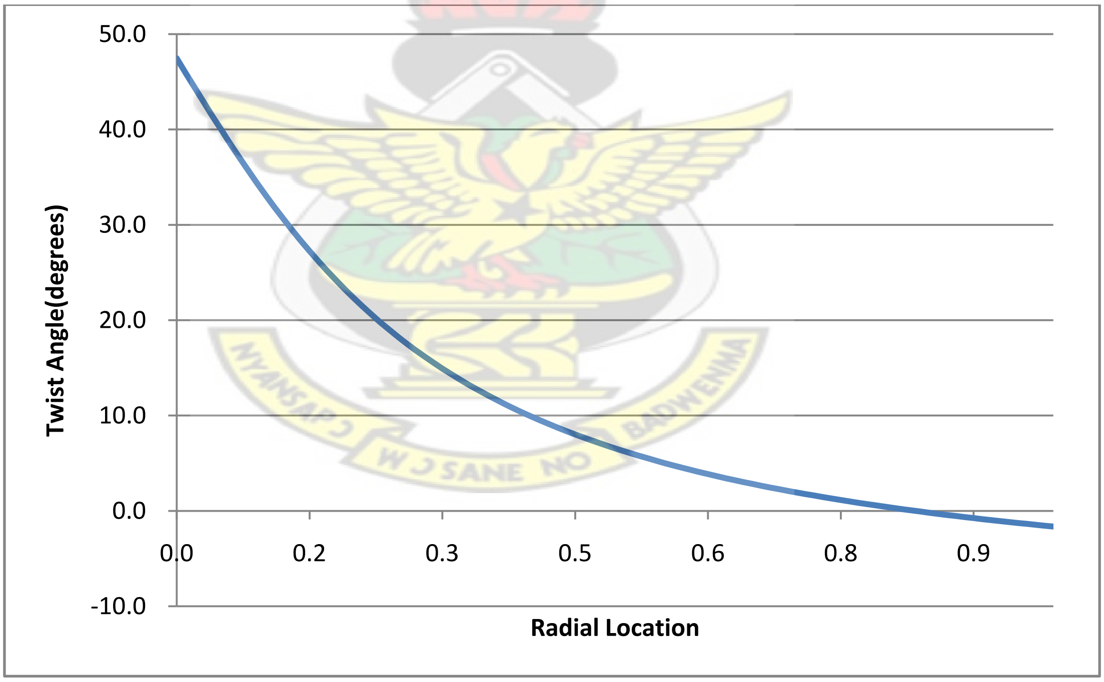

Figure 4.7: Twist Distributions for the Designed Bladefor NACA 4412

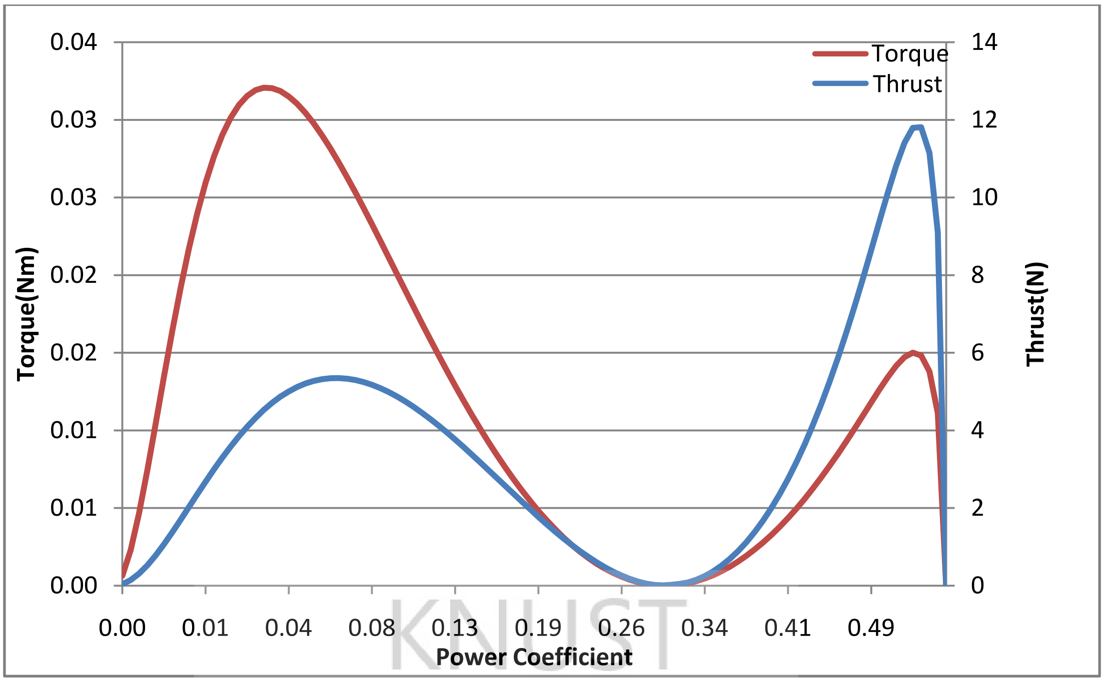

Figure 4.8: Power Coefficient against Torque and Thrust Distribution for NACA 4412

4.2.2 Blade design results for Selig 1210

Both Figure 4.9 and Figure 4.10 show an elemental blade section and a set of elemental blade sections up to 50th element to substantiate the pattern of the dimensional views of the blade profile.The plot in Figure 4.11 clearly shows the elemental power coefficient versus relative wind angles for values of local tip speed ratios of λ_1= 4, λ_2=5 ……., λ_5= 8. The highest elemental power coefficient as well as the generalized power coefficient, C_P of 0.5961 occurred at a relative wind angle of 9.80^o as shown in Figures 4.12.

Moreover, when the power coefficient was plotted against various chord length ratios, the optimum power and hence lift occurred at a chord length ratio (c/R) of 0.2118 at the same C_P of 0.5961 as shown in Figure 4.13. Similarly, a tip speed ratio of 7.52 occurred at the same power coefficient as indicated in Figure 4.14.

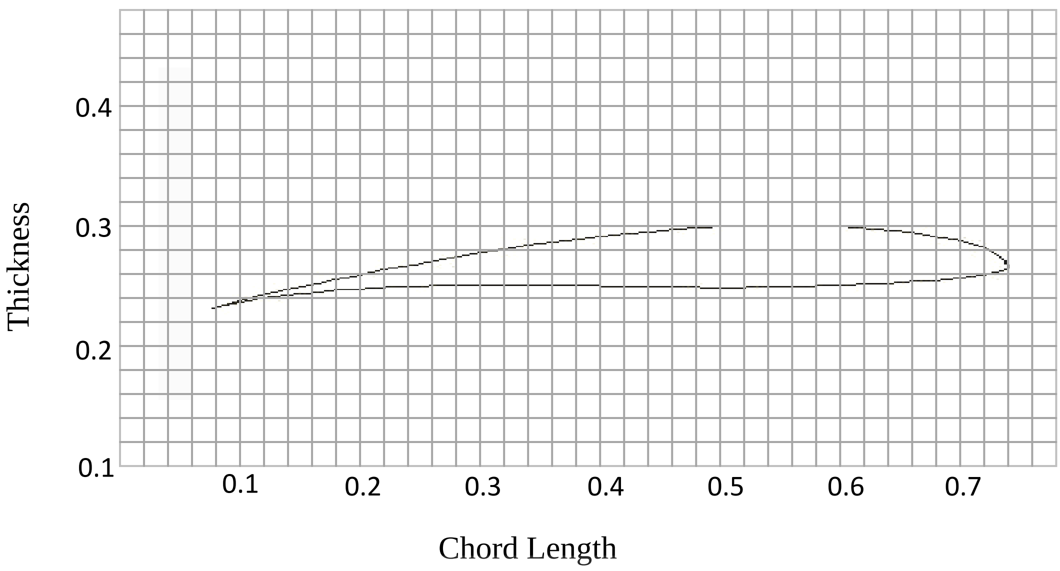

Figure 4.9: 2-D Sectional View of Selig 1210 Designed Blade Profile Element

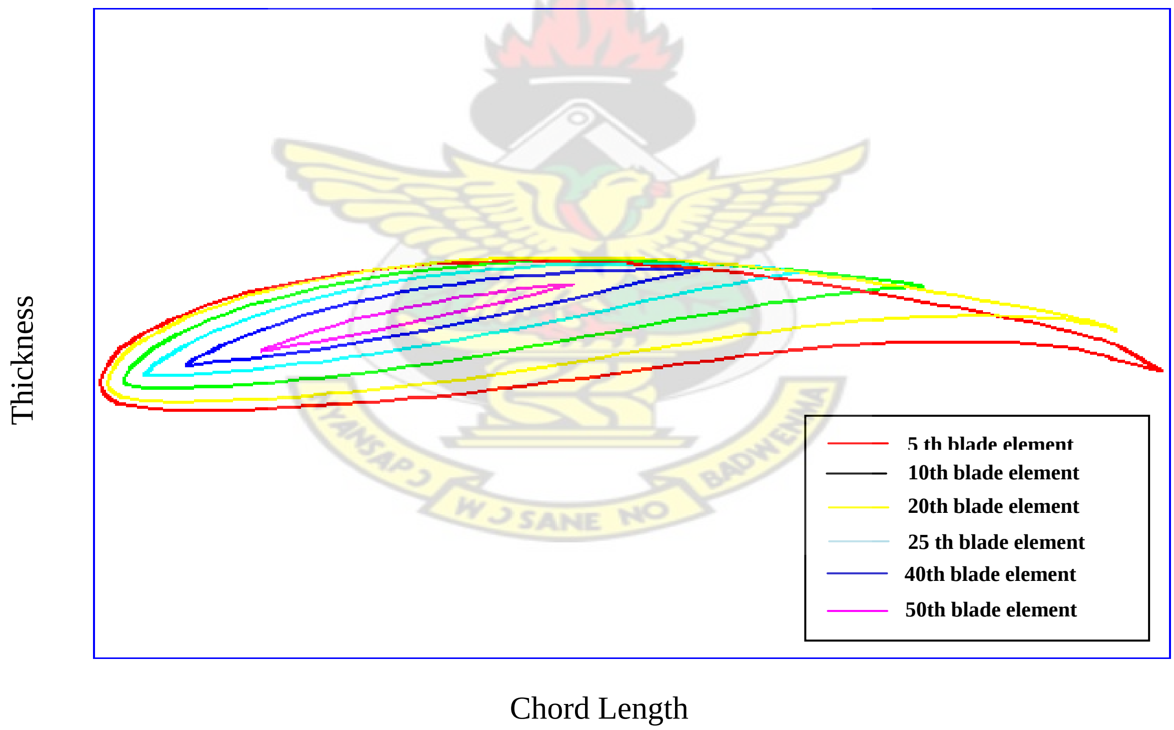

Figure 4.10: 2-D Sectional View of Selig1210 Designed Blade Profile for Set of Blade Elements

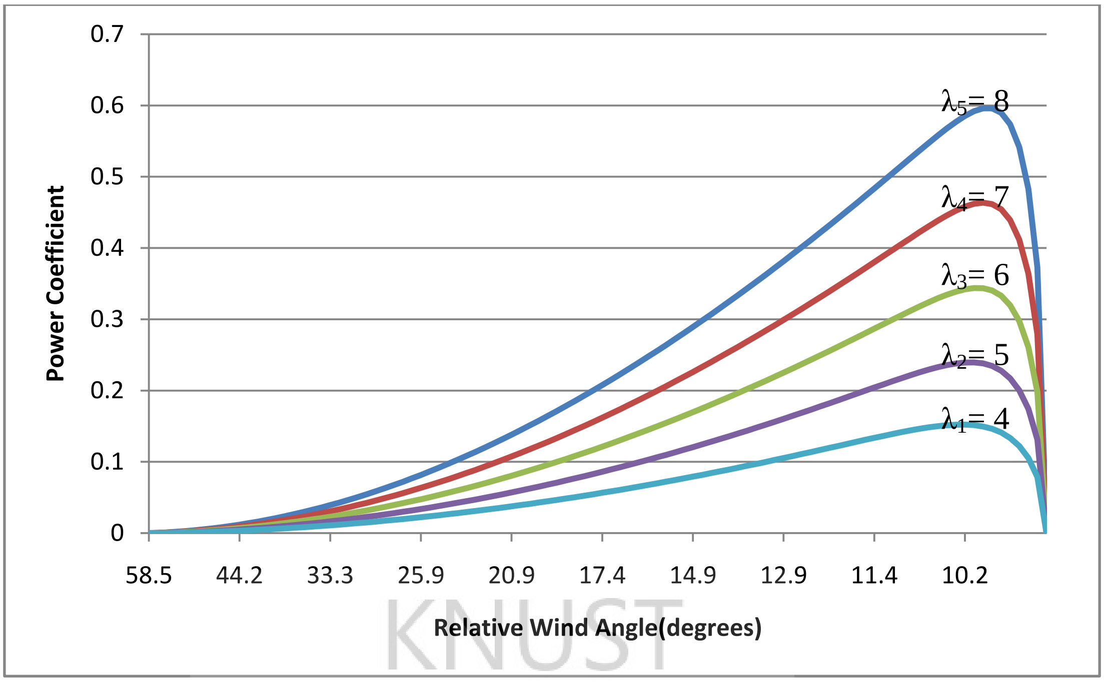

Figure 4.11: Variation of Elemental Power Coefficient with Relative Wind Angles for Values of Local Tip-Speed Ratio for Selig 1210

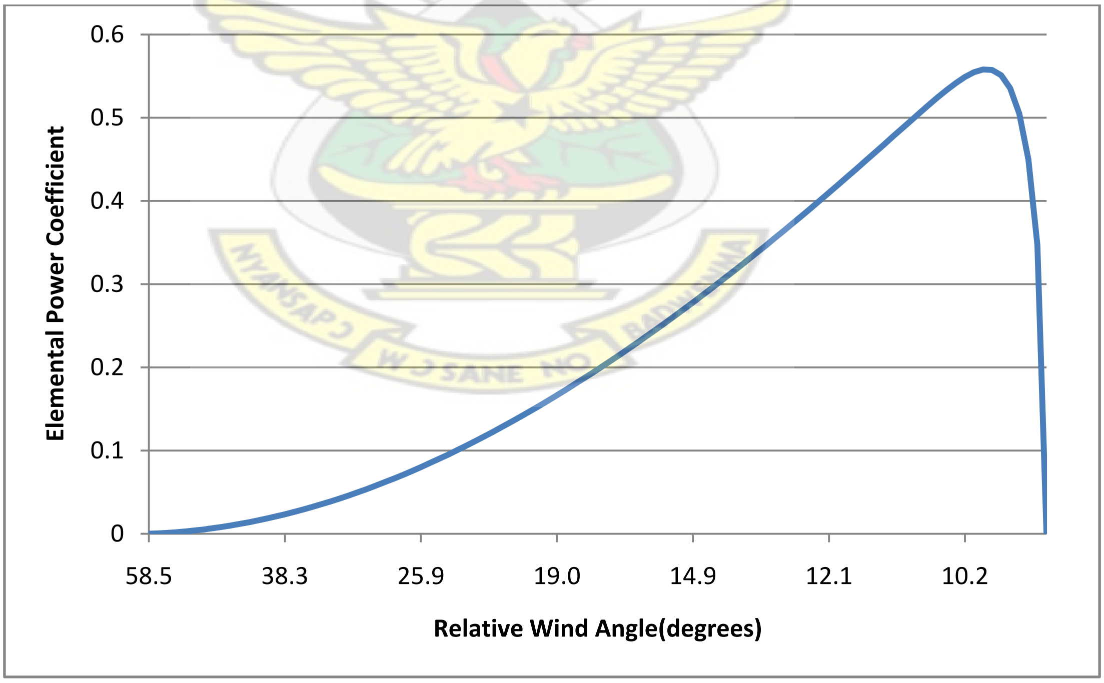

Figure 4.12: A Graph of Power Coefficient against Relative Wind Angle for Selig 1210

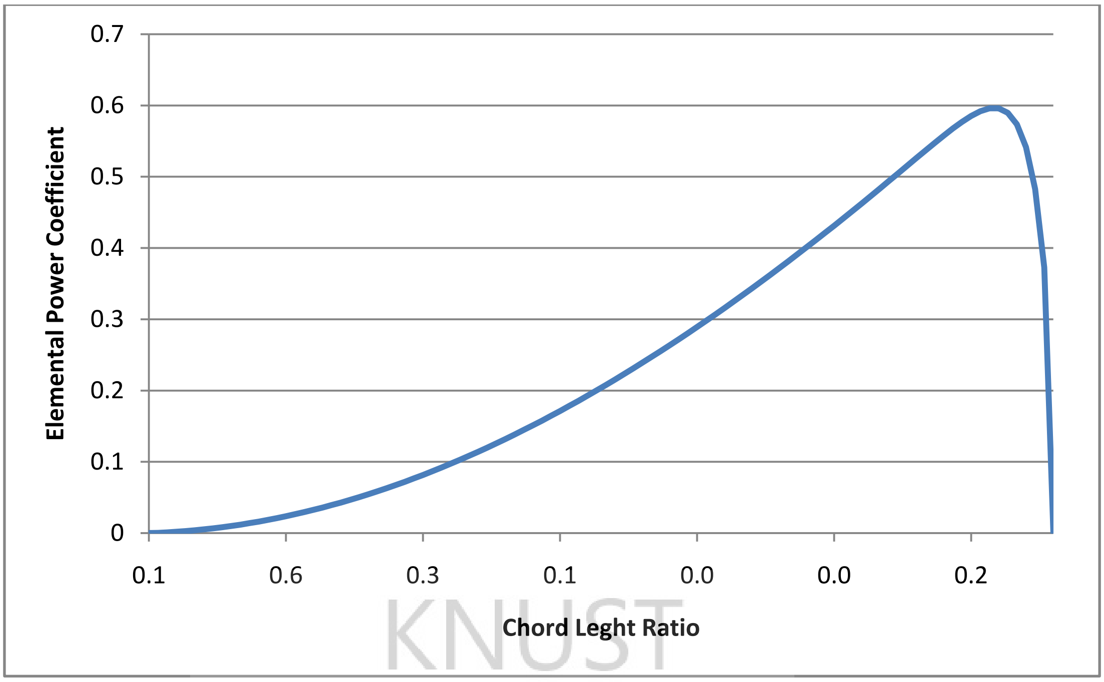

Figure 4.13: Variation of Power Coefficient to Chord Length Ratio for Selig 1210

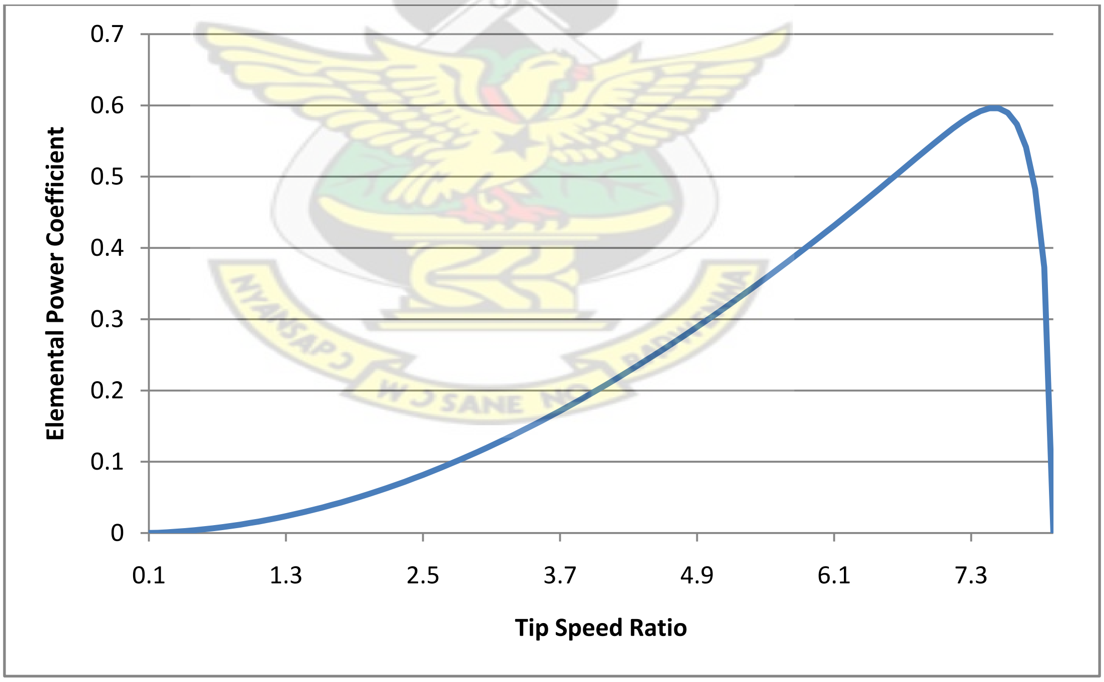

Figure 4.14: Variation of Elemental Power Coefficient to Elemental Tip Speed Ratio for Selig 1210

From Figure 4.15, the twist distribution for the designed blade shows a normalized outline as the various radial locations gave a positive twist angle pattern. This could be observed in the aforementioned Figure that the twist angle is highest at the root and least at the tip of the blade as radial location increases accordingly.

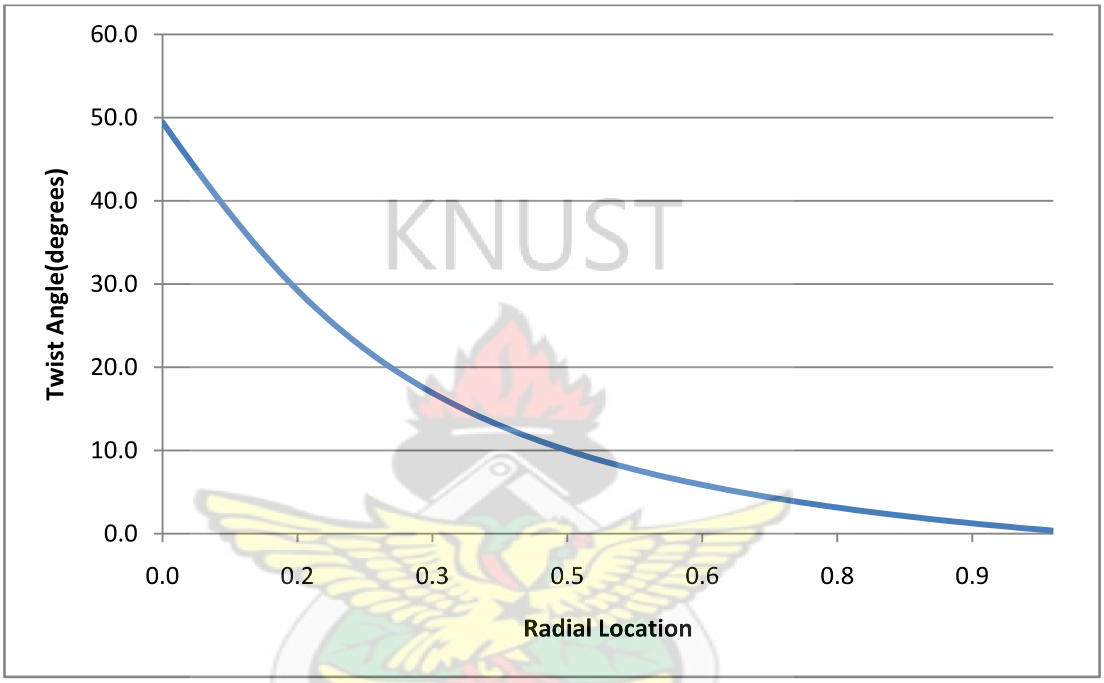

Figure 4.15: Twist Distribution for the Designed Blade for Selig 1210

Figure 4.16 also shows how power coefficient relates to torque and thrust distribution along the blade profile. It depicts when the maximum thrust and torque occurred along the blade against the required power coefficient. The maximum thrust and torque were considered in the design of the blade profile.

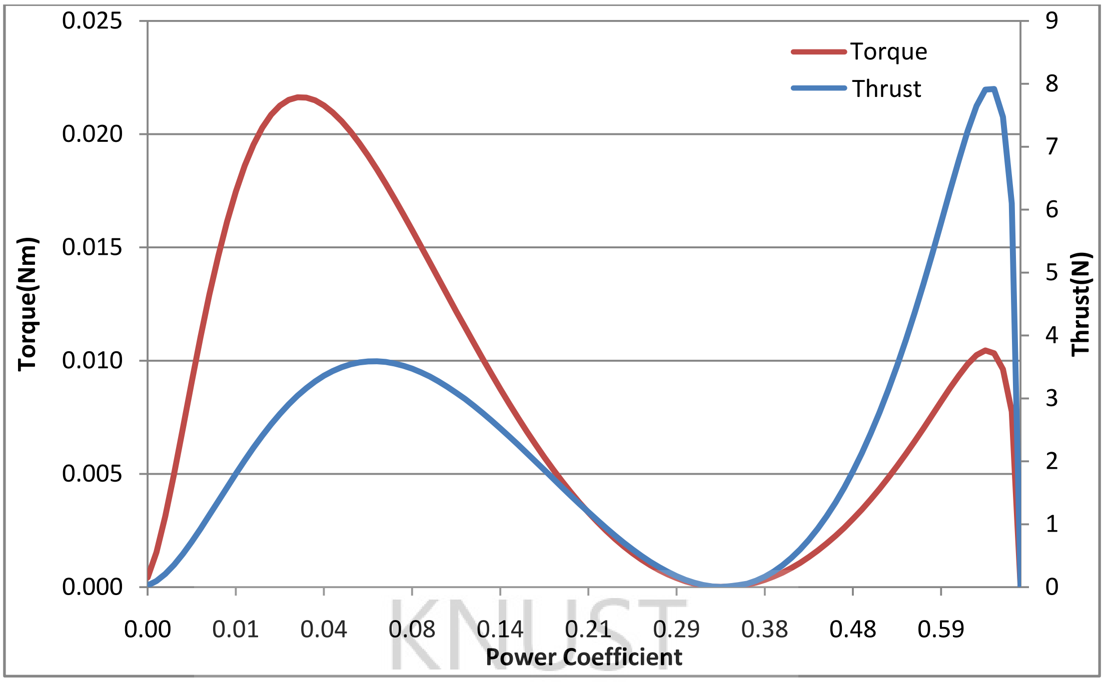

Figure 4.16: Power Coefficient against Torque and Thrust Distribution for Selig 1210

4.2.3 Blade design Results for Worthmann FX 63-137

Both Figure 4.17 and Figure 4.18 show an elemental blade section and a set of elemental blade sections up to 50th element to substantiate the pattern of the dimensional views of the blade profile. The plot in Figure 4.19 clearly shows the elemental power coefficient versus relative wind angles for values of local tip speed ratios of λ_1= 4, λ_2=5 ……, λ_5= 8. The highest elemental power coefficient as well as the generalized power coefficient, C_P of 0.5581 occurred at a relative wind angle of 10.03° as shown in Figures 4.20.

Moreover, when the power coefficient was plotted against various chord length ratios, the optimum power and hence lift occurred at a chord length ratio (c/R) of 0.25 at the same C_P of 0.5581 as shown in Figure 4.21. Similarly, a tip speed ratio of 7.44 occurred at the same power coefficient as indicated in Figure 4.22.

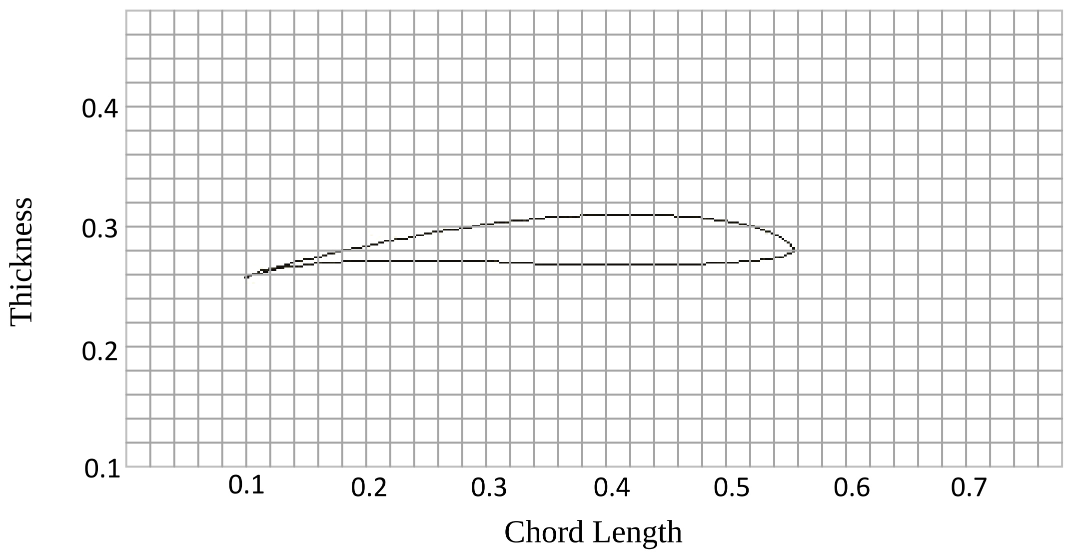

Figure 4.17: 2-D Sectional View of Worthmann FX63-137 Designed Blade Profile

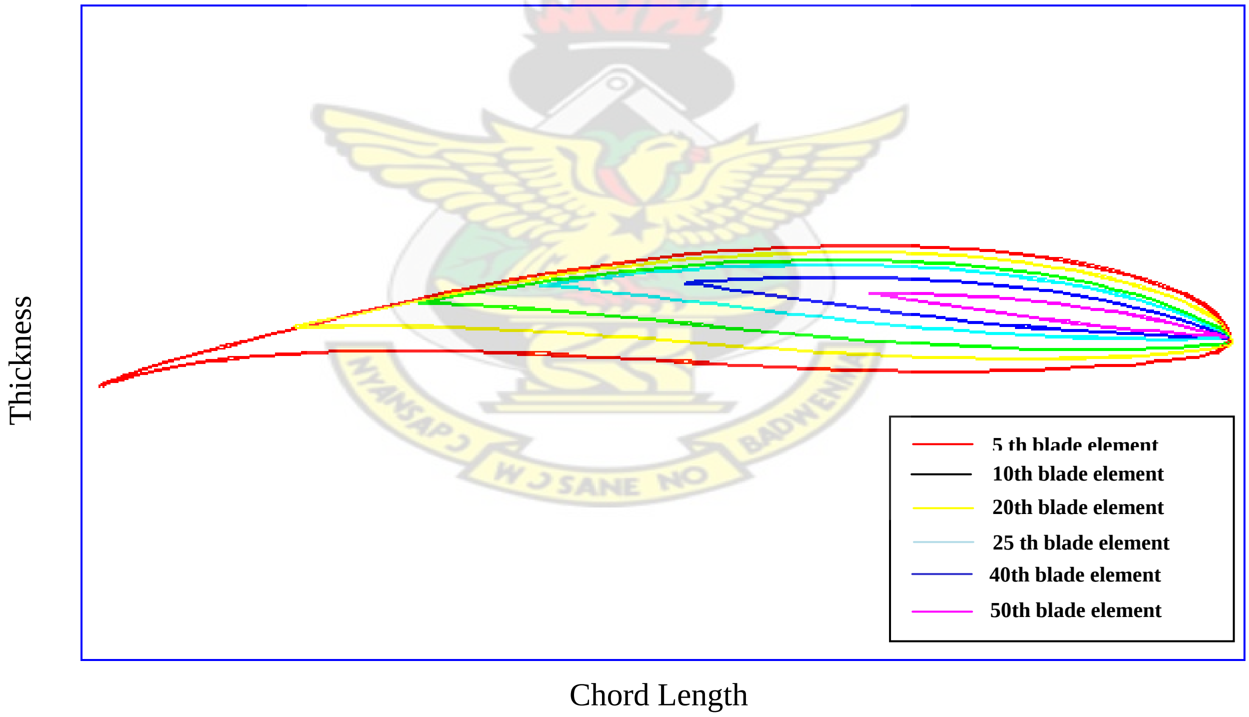

Figure 4.18: 2-D Sectional View of Worthmann FX63-137 Designed Blade Profile for Set of Blade Elements

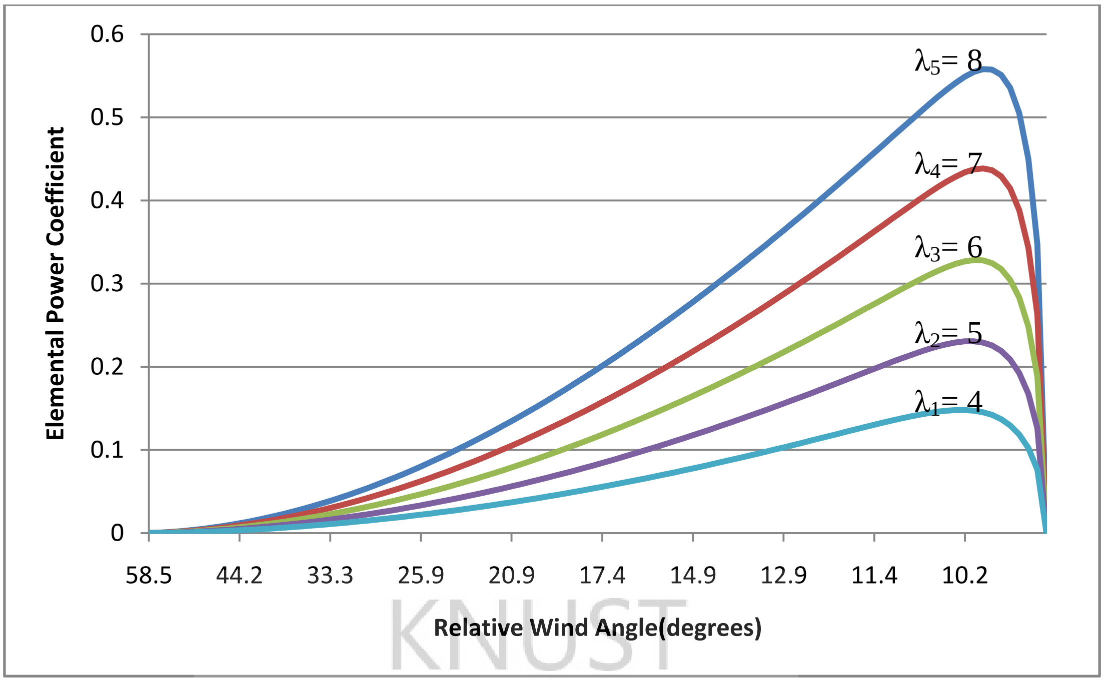

Figure 4.19: Variation of Elemental Power Coefficient with Relative Wind Angles for Values of Local Tip-Speed Ratio for Worthmann FX63-137

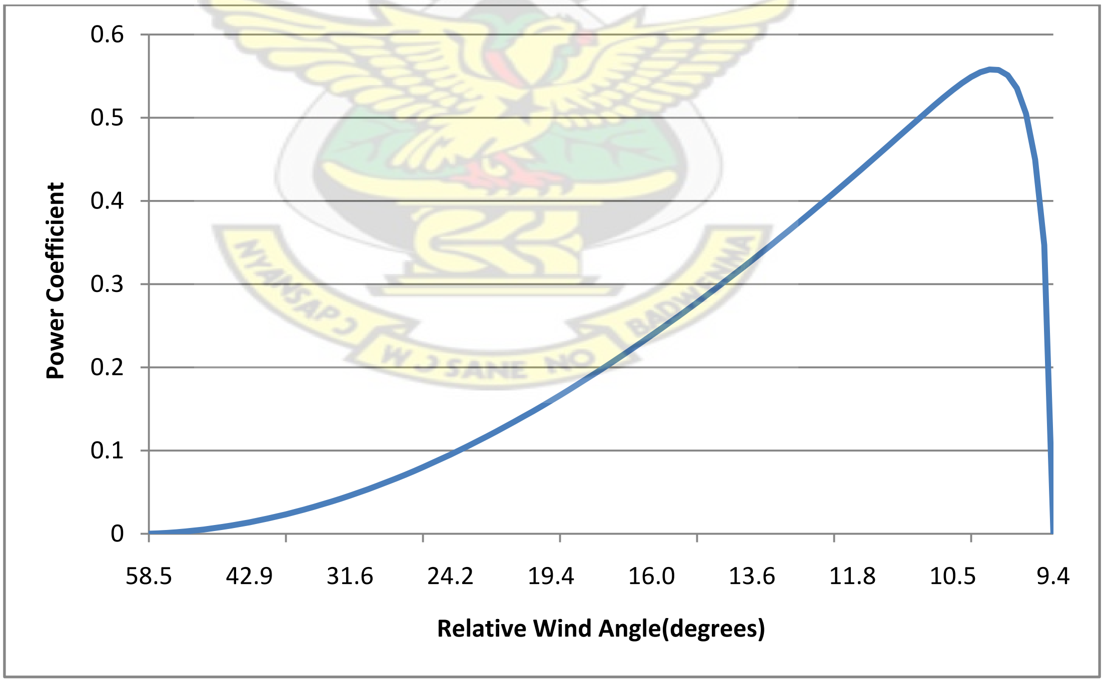

Figure 4.20: A Graph of Power Coefficient against Relative Wind Angle for Worthmann FX 63-137

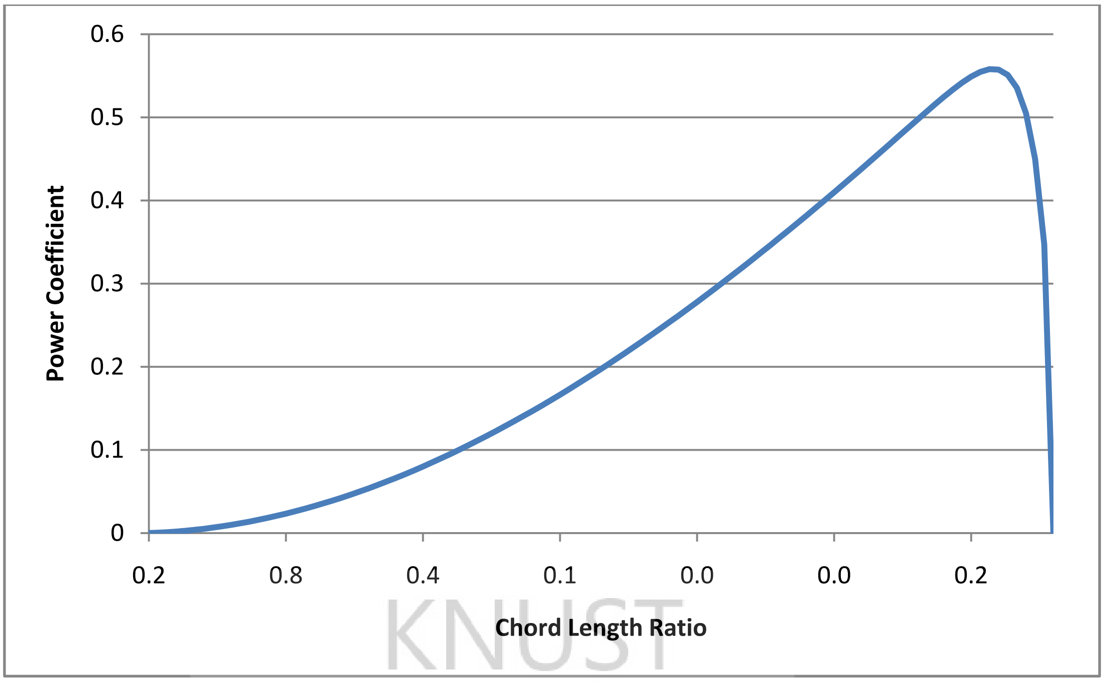

Figure 4.21: Variation of Power Coefficient to Chord Length Ratio for Worthmann FX63-137

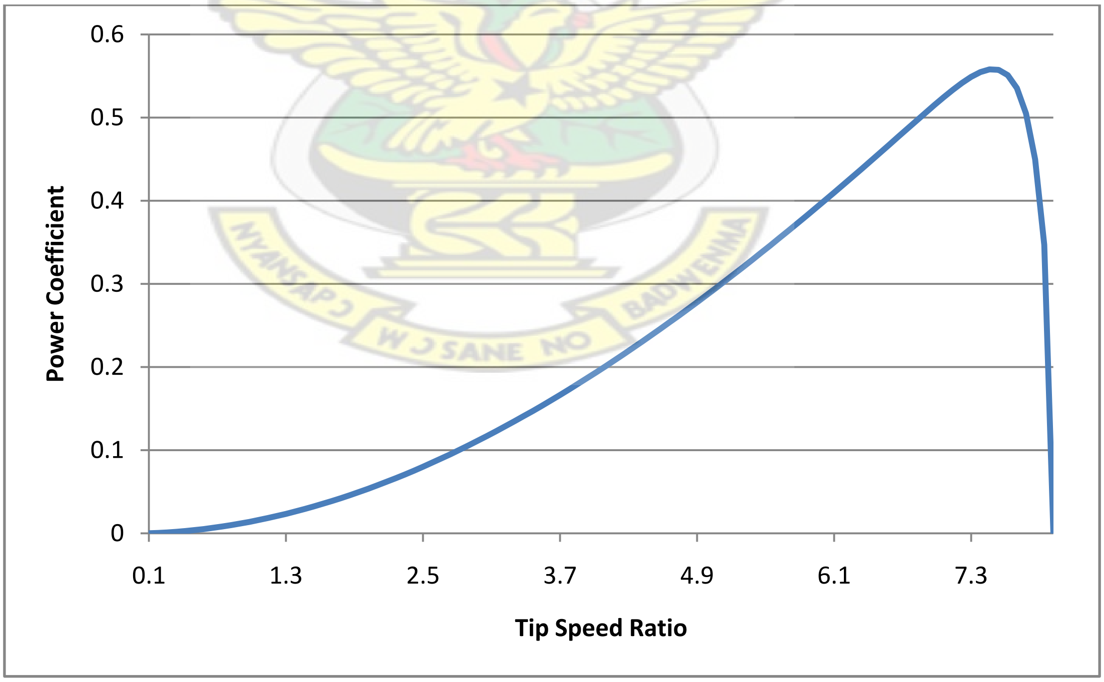

Figure 4.22: Variation of Elemental Power Coefficient with respect to Elemental Tip Speed Ratio for Worthmann FX63-137.

Figure 4.23 also shows the twist distribution for the designed blade which 4gives a normalized outline as the various radial locations gave a positive twist angle pattern. This could be observed from the Figure that the twist angle is highest at the root and least at the tip of the blade as radial location increases accordingly.

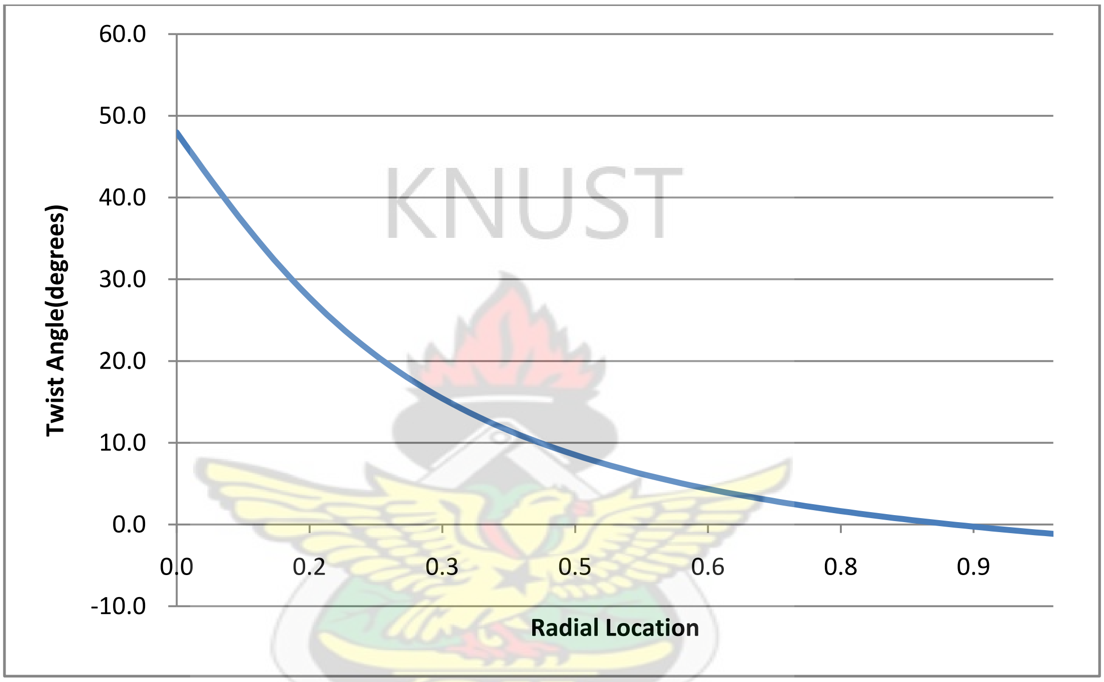

Figure 4.23: Twist Distribution for the Designed Blade for Worthmann FX63-137

Figure 4.24 also shows how power coefficient relates to torque and thrust distribution along the blade profile. It depicts when the maximum thrust and torque occurred along the blade against the required power coefficient. The maximum thrust and torque were considered in the design of the blade profile.

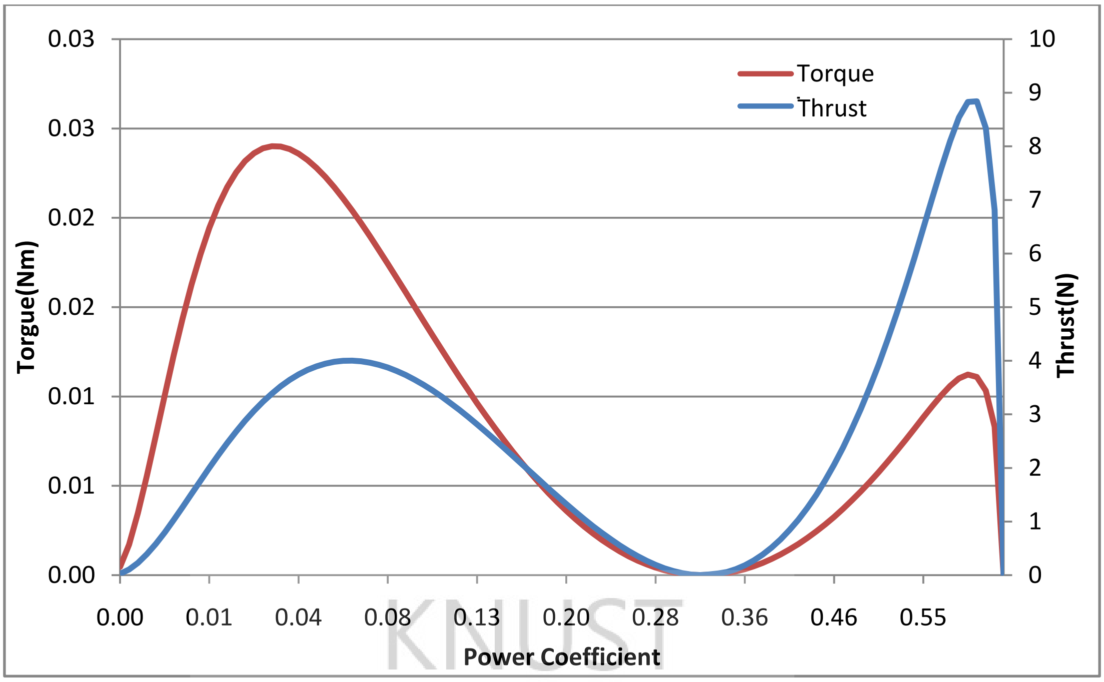

Figure 4.24: Power Coefficient against Torque and Thrust Distribution for Worthmann FX 63-137

4.2.4 Blade design Results for Ara-D 6%

Both Figure 4.25 and Figure 4.26 show an elemental blade section and a set of elemental blade sections up to 50th element to substantiate the pattern of the dimensional views of the blade profile. The plot in Figure 4.27 clearly shows the elemental power coefficient versus relative wind angles for values of local tip speed ratios of $\lambda_1 = 4$, $\lambda_2 = 5$ ……, $\lambda_5 = 8$. The highest elemental power coefficient as well as the generalized power coefficient, C_P of 0.5503 occurred at a relative wind angle of 10.03^o as shown in Figures 4.28.

Moreover, when the power coefficient was plotted against various chord length ratios, the optimum power and hence lift occurred at a chord length ratio (c/R) of 0.40 at the same C_P of 0.5503 as shown in Figure 4.30. Similarly, a tip speed ratio of 7.44 occurred at the same power coefficient as indicated in Figure 4.31.

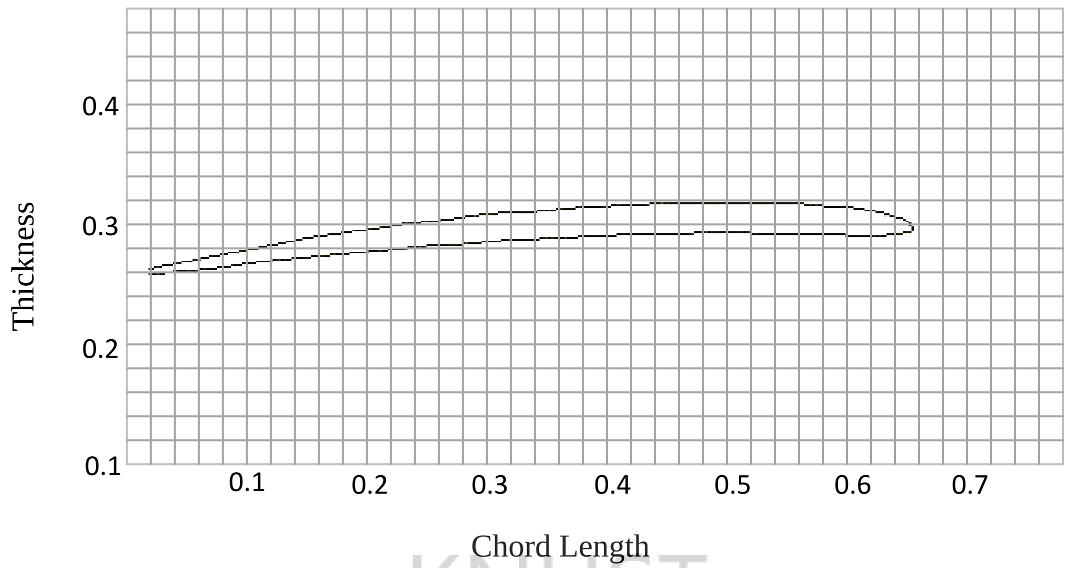

Figure 4.25: 2-D Sectional View of Ara-D 6% Designed Blade Profile Element

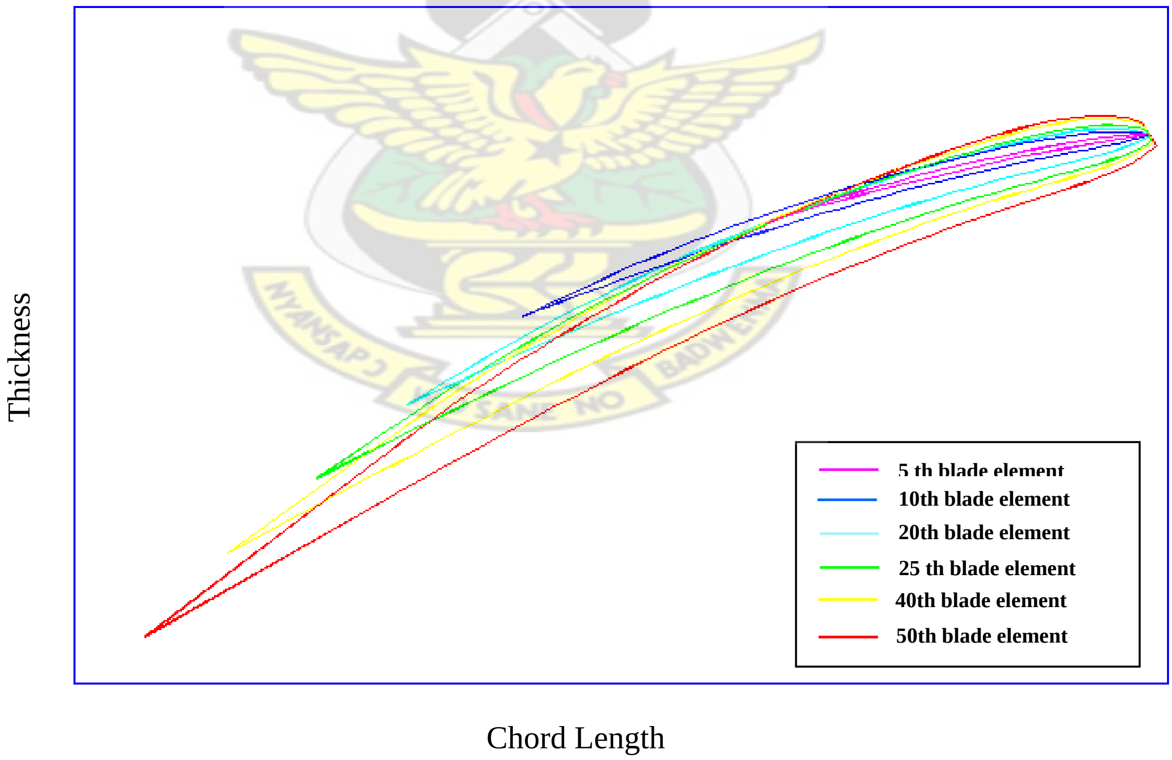

Figure 4.26: 2-D Sectional View of Ara-D 6% Designed Blade Profile for a Set of Blade Elements

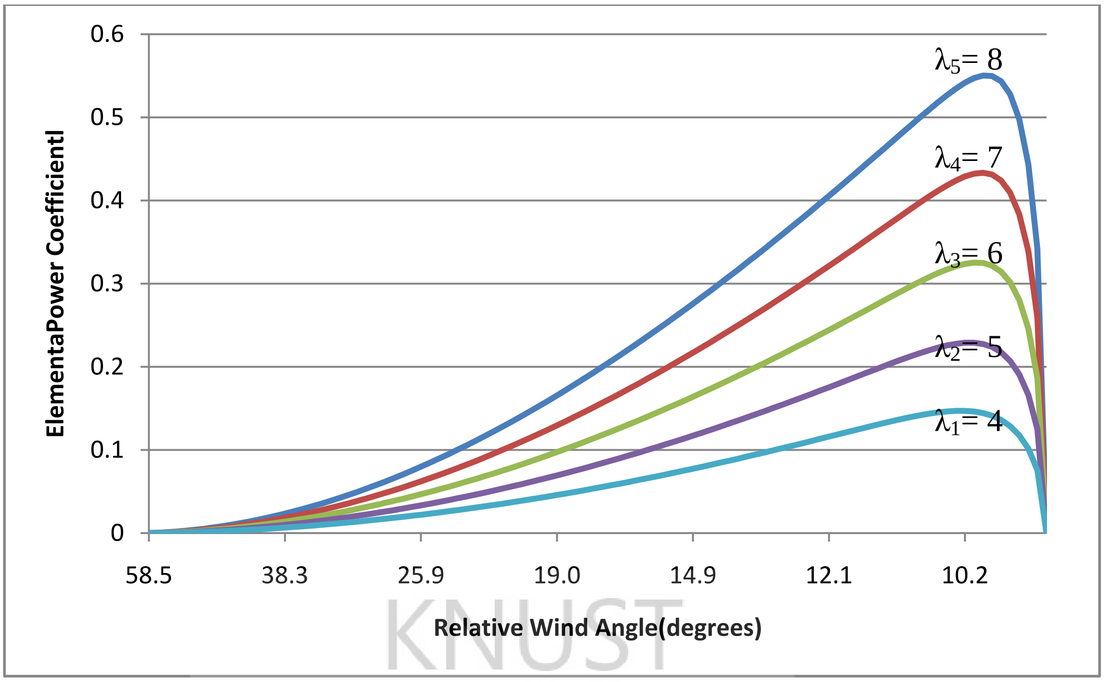

Figure 4.27: Variation of Elemental Power Coefficient with Relative Wind Angles for Values of Local Tip-Speed Ratio for Ara-D 6%.

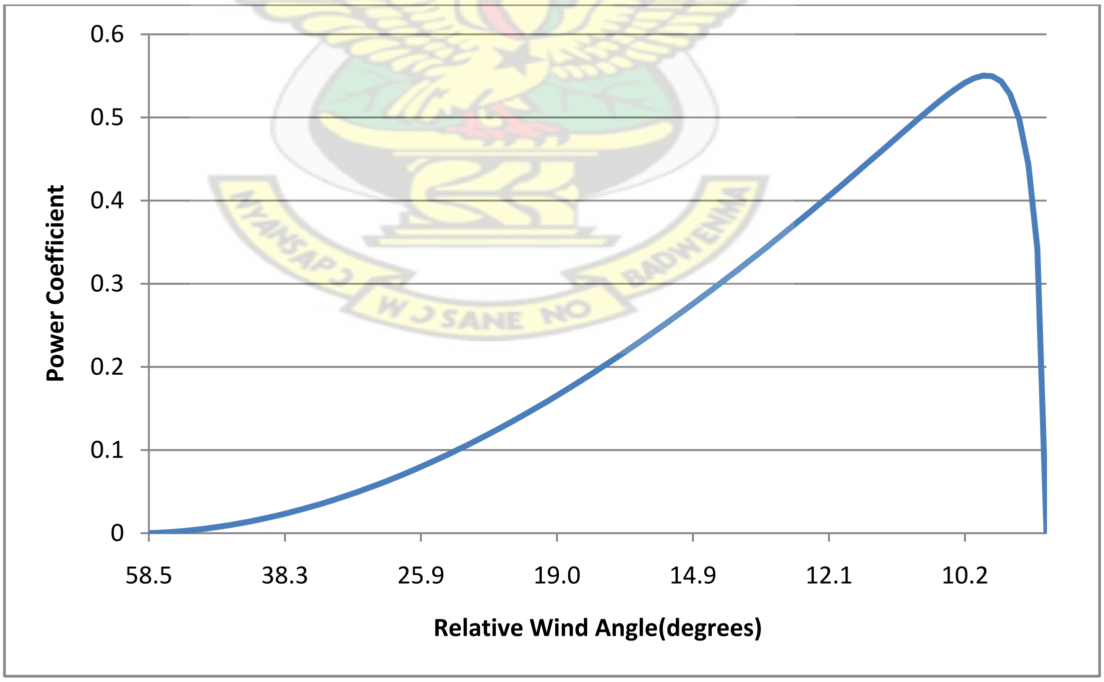

Figure 4.28: A Graph of Power Coefficient against Relative Wind Angle for Ara-D 6%.

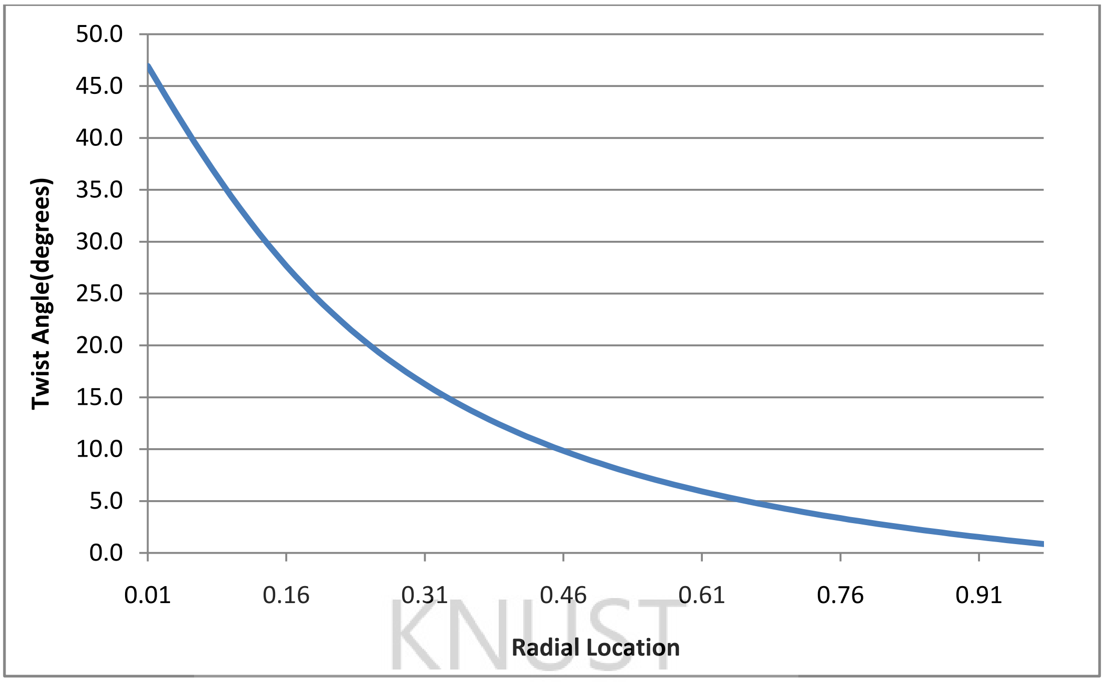

Figure 4.29: Twist Distribution for the Designed Blade for Ara-D 6%.

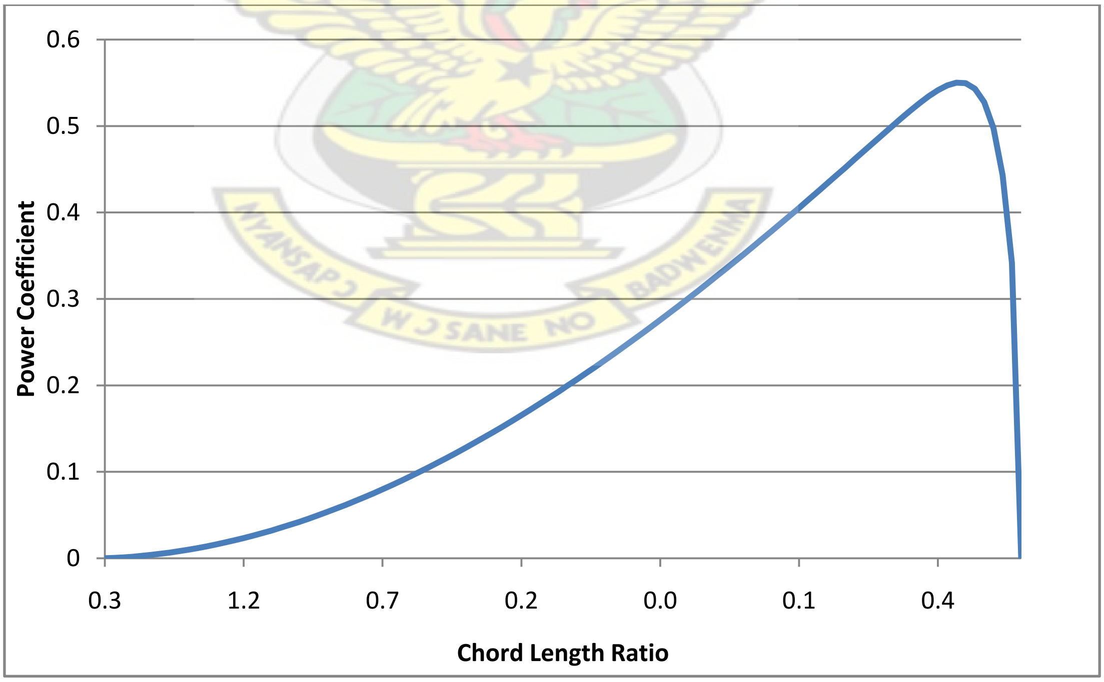

Figure 4.30: Variation of Power Coefficient to Chord Length Ratio for Ara-D 6%.

Figure 4.29 also shows the twist distribution for the designed blade which gives a normalized outline as the various radial locations gave a positive twist angle pattern. This could be observed from the Figure that the twist angle is highest at the root and least at the tip of the blade as radial location increases accordingly.

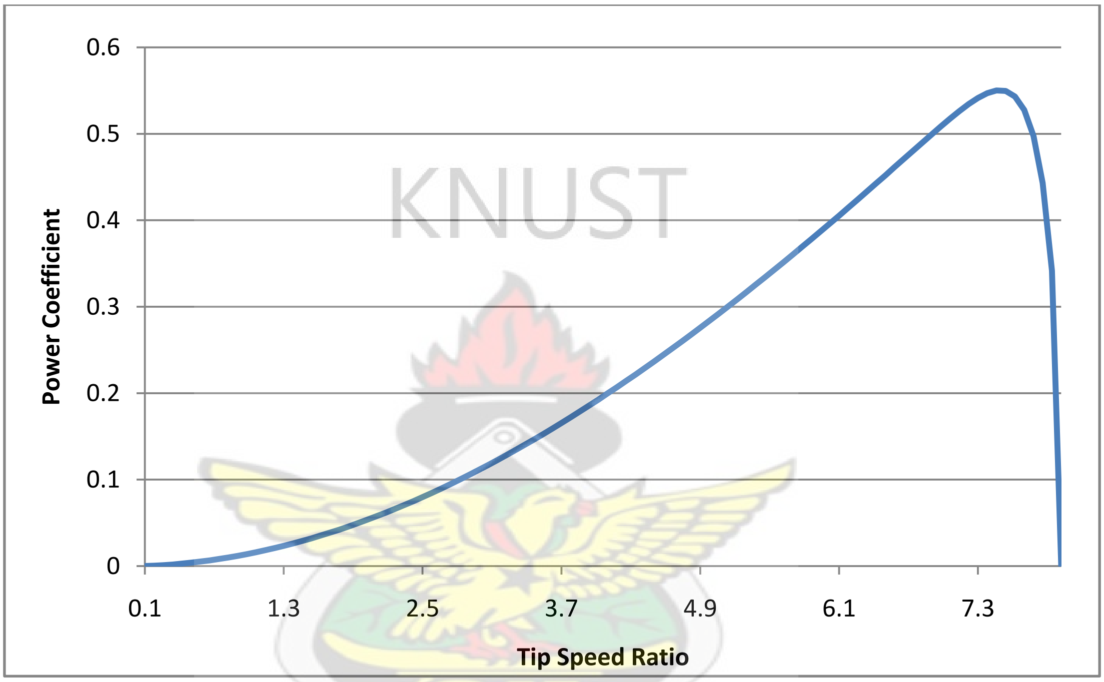

Figure 4.31: Variation of Elemental Power coefficient to Elemental Tip Speed Ratio for Ara-D 6%.

Figure 4.32 also shows how power coefficient relates to torque and thrust distribution along the blade profile. It depicts when the maximum thrust and torque occurred along the blade against the required power coefficient. The maximum thrust and torque were considered in the design of the blade profile.

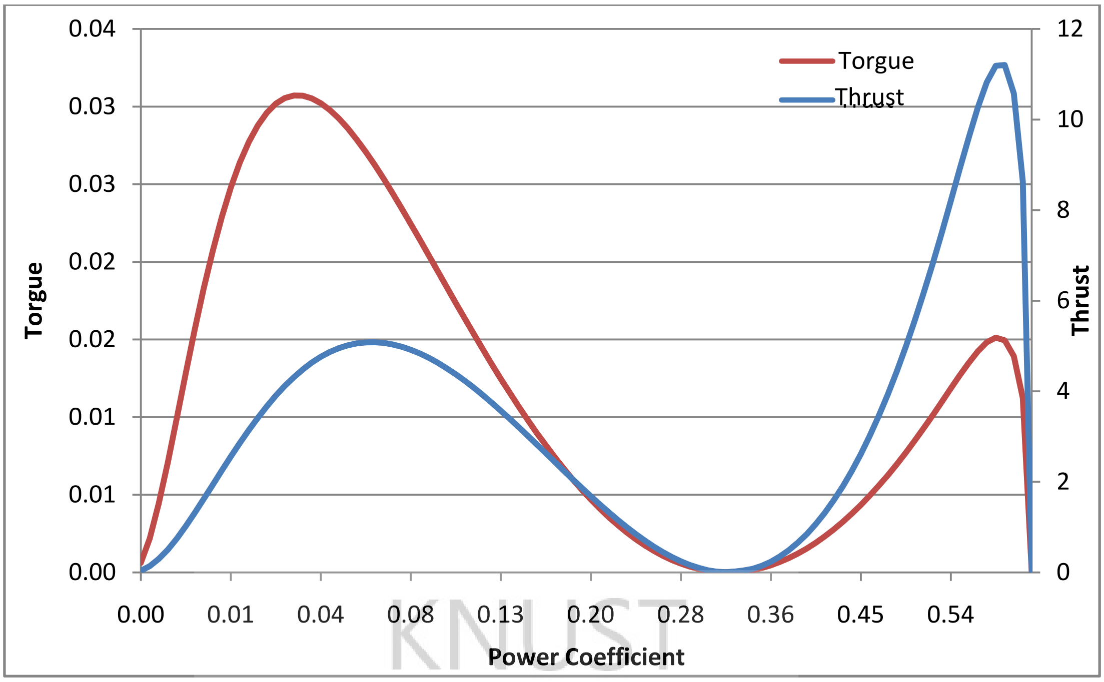

Figure 4.32: Power Coefficient against Torque and Thrust Distribution for Ara-D 6%.

4.2.5 Blade design Results for Selig 2091

Both Figure 4.33 and Figure 4.34 show an elemental blade section and a set of elemental blade sections up to 50th element to substantiate the pattern of the dimensional views of the blade profile. The plot in Figure 4.35 clearly shows the elemental power coefficient versus relative wind angles for values of local tip speed ratios of λ_1= 4, λ_2=5 ….., λ_5= 8. The highest elemental power coefficient as well as the generalized power coefficient, C_P of 0.0266 occurred at a relative wind angle of 24.22^o as shown in Figures 4.36.

Moreover, when the power coefficient was plotted against various chord length ratios, the optimum power and hence lift occurred at a chord length ratio (c/R) of 0.7981 at the same C_P of 0.0266 as shown in Figure 4.38. Similarly, a tip speed ratio of 2.72 occurred at the same power coefficient as indicated in Figure 4.39.

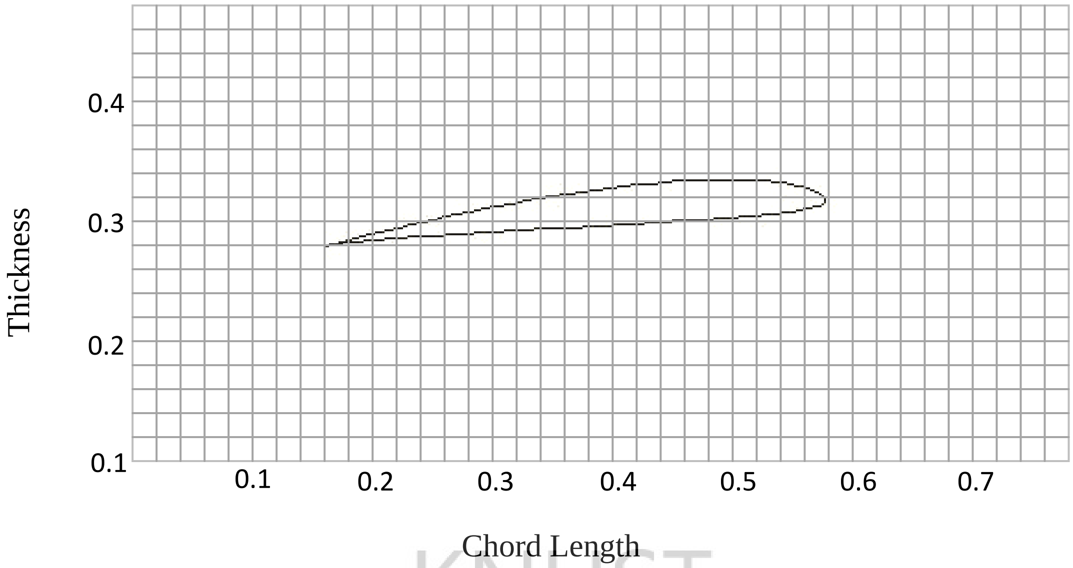

Figure 4.33: 2-D Sectional View of Selig 2091 Designed Blade Profile Element

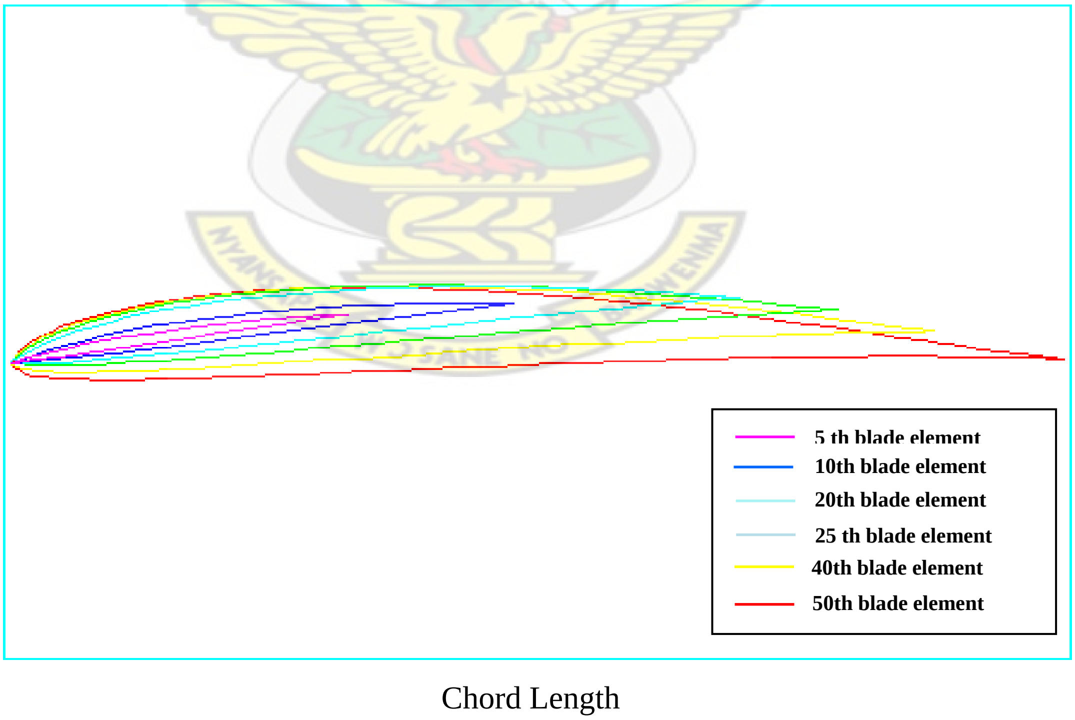

Figure 4.34: 2-D Sectional View of Selig 2091 Designed Blade Profile for Set of Blade Elements

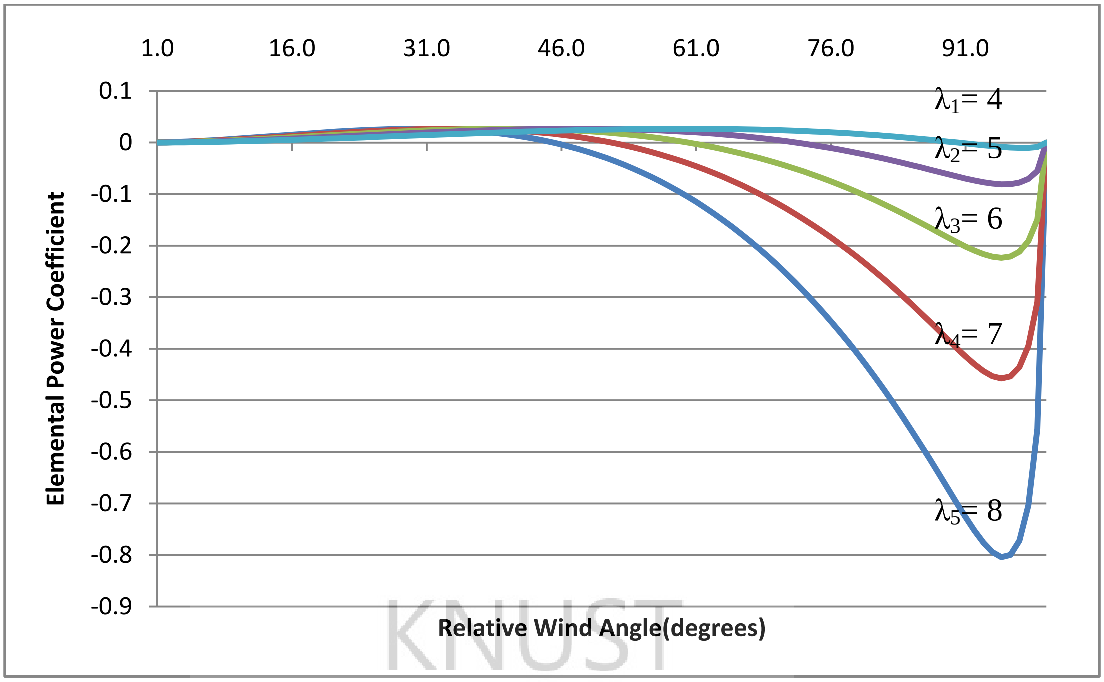

Figure 4.35: Variation of Elemental Power Coefficient with Relative Wind Angles for Values of Local Tip-Speed Ratio for Selig 2091

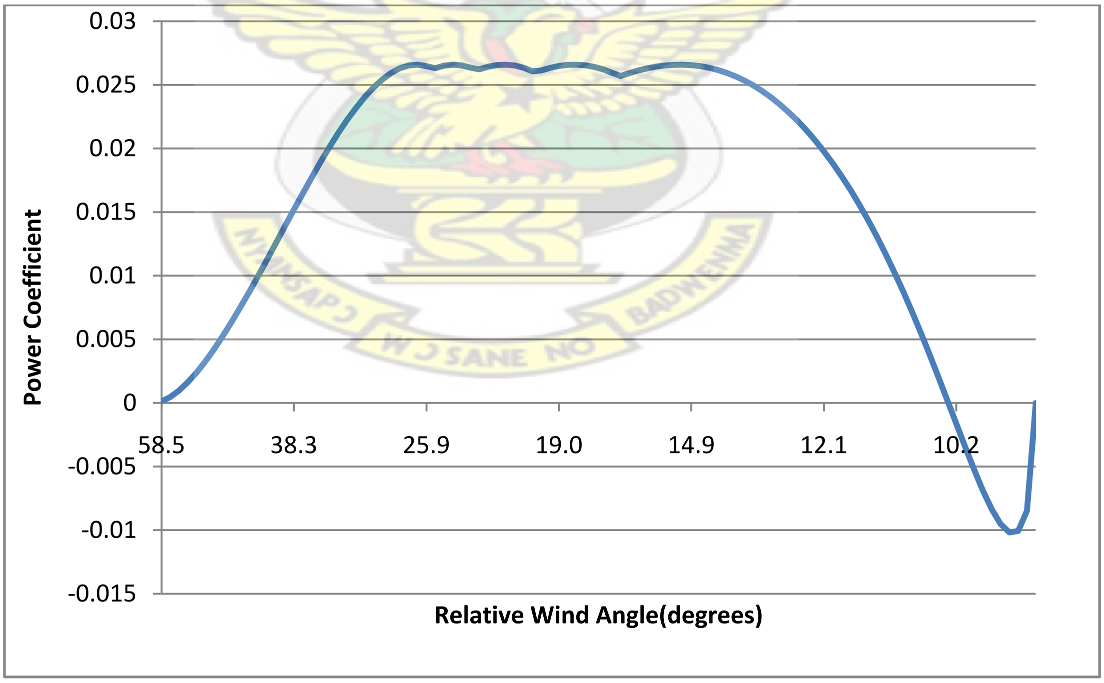

Figure 4.36: A Graph of Power Coefficient against Relative Wind Angle for Selig 2091

Figure 4.37 also shows the twist distribution for the designed blade which gives a normalized outline. It could also be seen from the Figure that, the blade performs very well at a twist angle of 5^o and a radial location greater than 0.80. The blade has a high probability to stall as it gives negative twist angle pattern beyond radial location value of 0.80. It could also be observed that the twist angle is highest at the root and least at the tip of the blade as radial location increases accordingly.

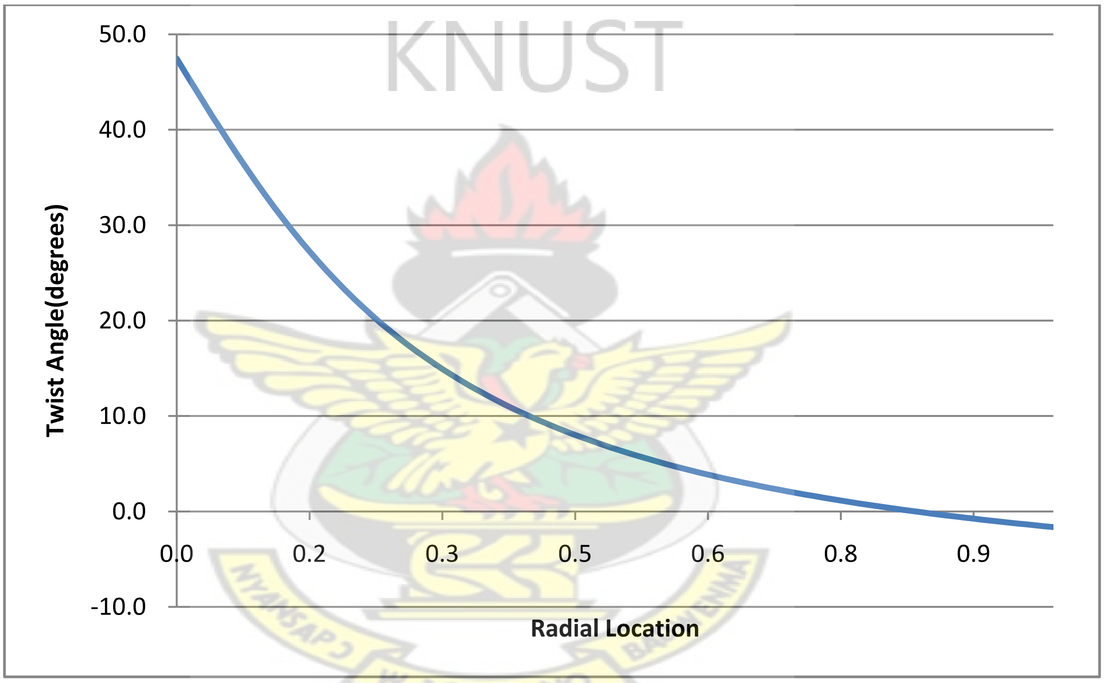

Figure 4.37: Twist Distribution for the Designed Blade for Selig 2091

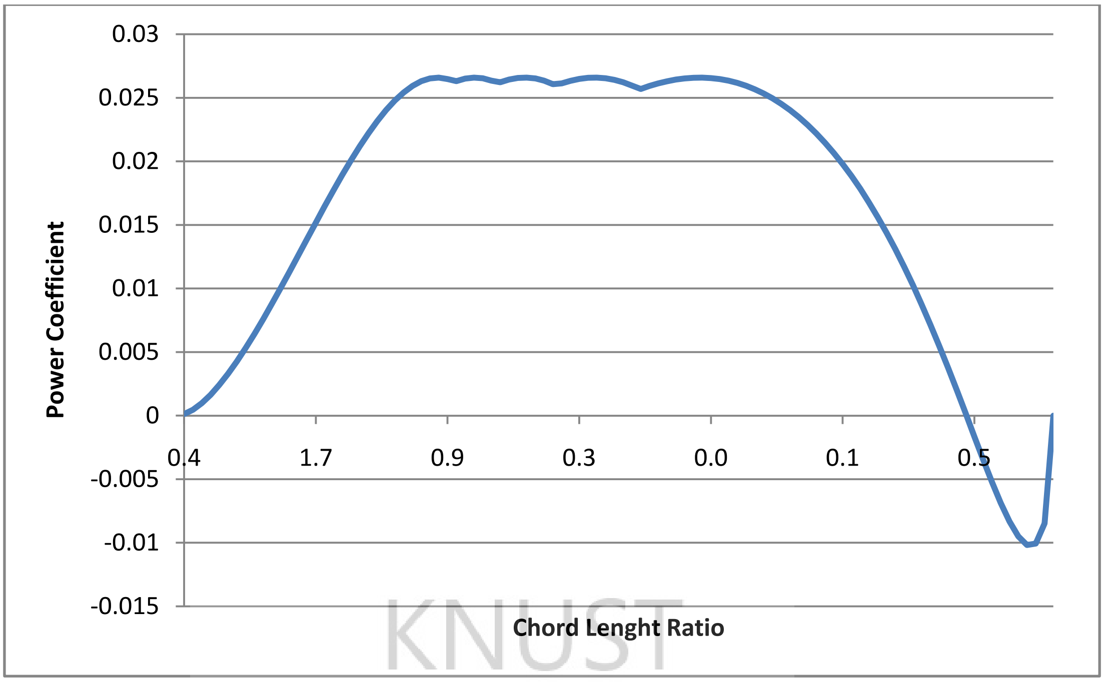

Figure 4.38: Variation of Power Coefficient to Chord Length Ratio for Selig 2091

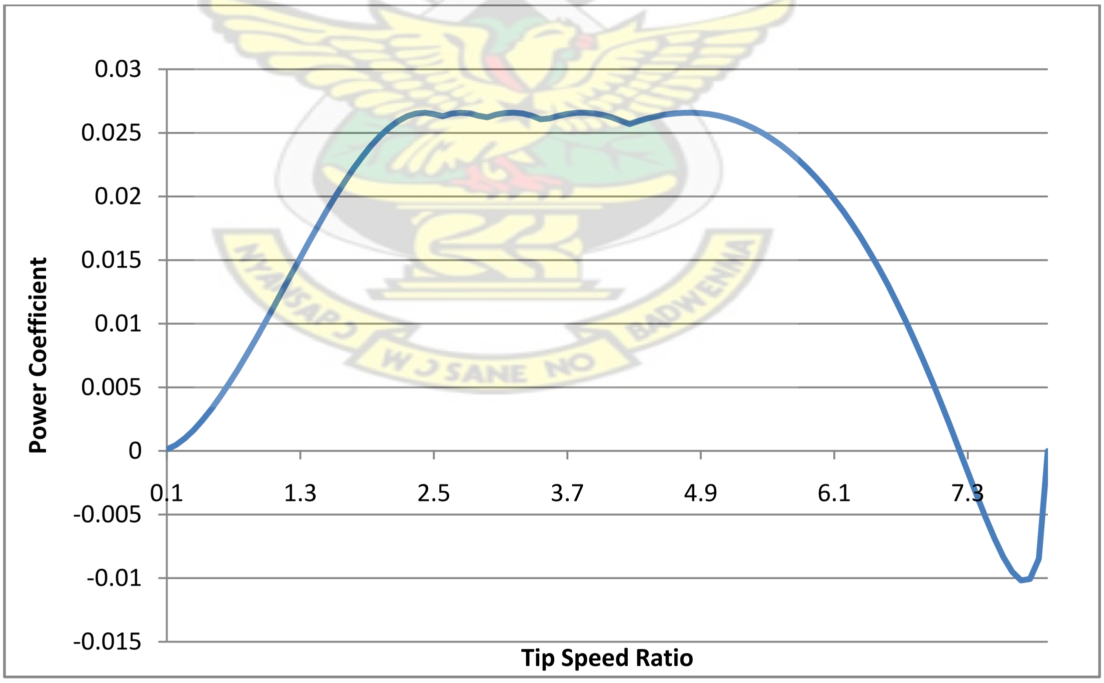

Figure 4.39: Variation of Elemental Power Coefficient with Respect to Elemental Tip Speed Ratio for Selig 2091

Figure 4.40 also shows how power coefficient relates to torque and thrust distribution along the blade profile. It depicts when the maximum thrust and torque occurred along the blade against the required power coefficient. The maximum thrust and torque were considered in the design of the blade profile.

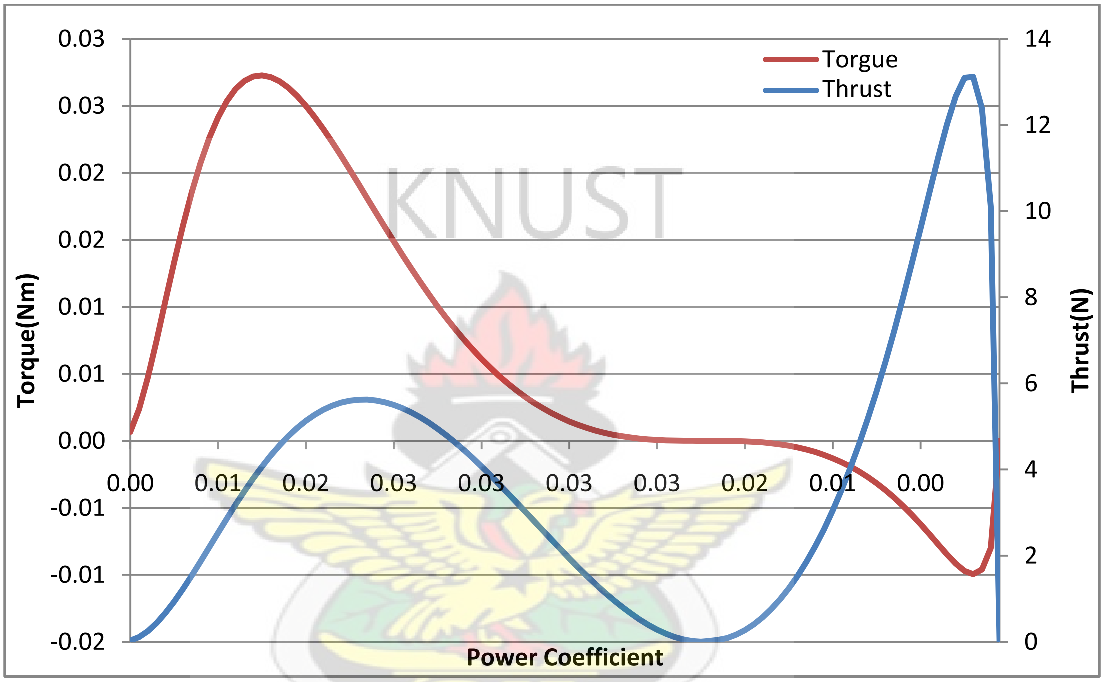

Figure 4.40: Power Coefficient against Torque and Trust Distribution for Selig 2091

4.2.6 Blade design Results for Selig Donovan 7032

Both Figure 4.41 and Figure 4.42 show an elemental blade section and a set of elemental blade sections up to 50th element to substantiate the pattern of the dimensional views of the blade profile. The plot in Figure 4.43 clearly shows the elemental power coefficient versus relative wind angles for values of local tip speed ratios of λ_1= 4, λ_2=5 ……, λ_5= 8. The highest elemental power coefficient as well as the generalized power coefficient, C_P of 0.5996 occurred at a relative wind angle of 10.03^o as shown in Figures 4.44.

Moreover, when the power coefficient was plotted against various chord length ratios in Figure 4.45, the optimum power and hence lift occurred at a chord length ratio (c/R) of 0.56 at the same C_P of 0.5996. Similarly, a tip speed ratio of 7.52 occurred at the same power coefficient as indicated in Figure 4.46.

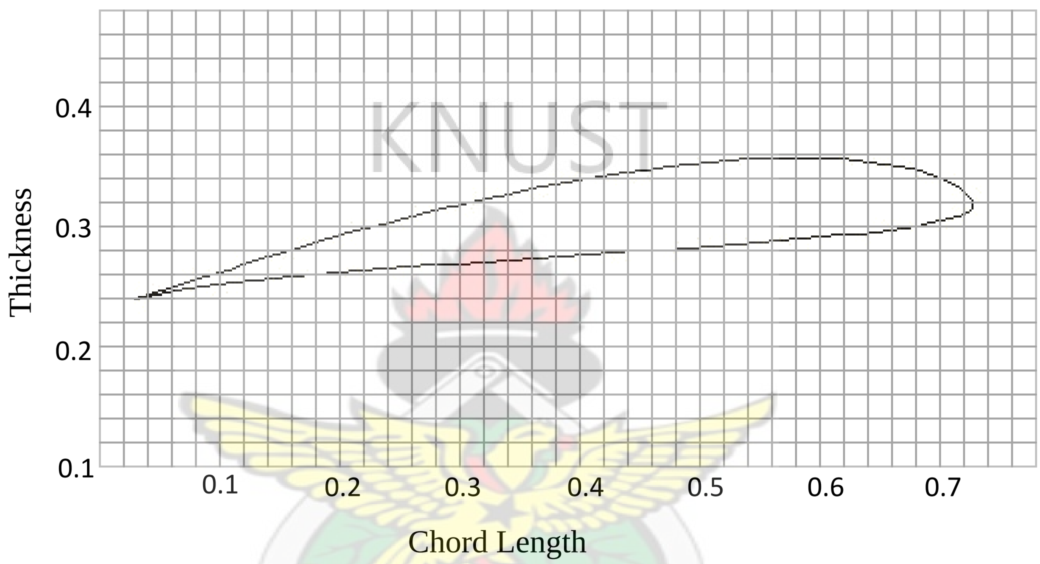

Figure 4.41: 2-D Sectional View of Selig Donovan 7032 Designed Blade Profile Element

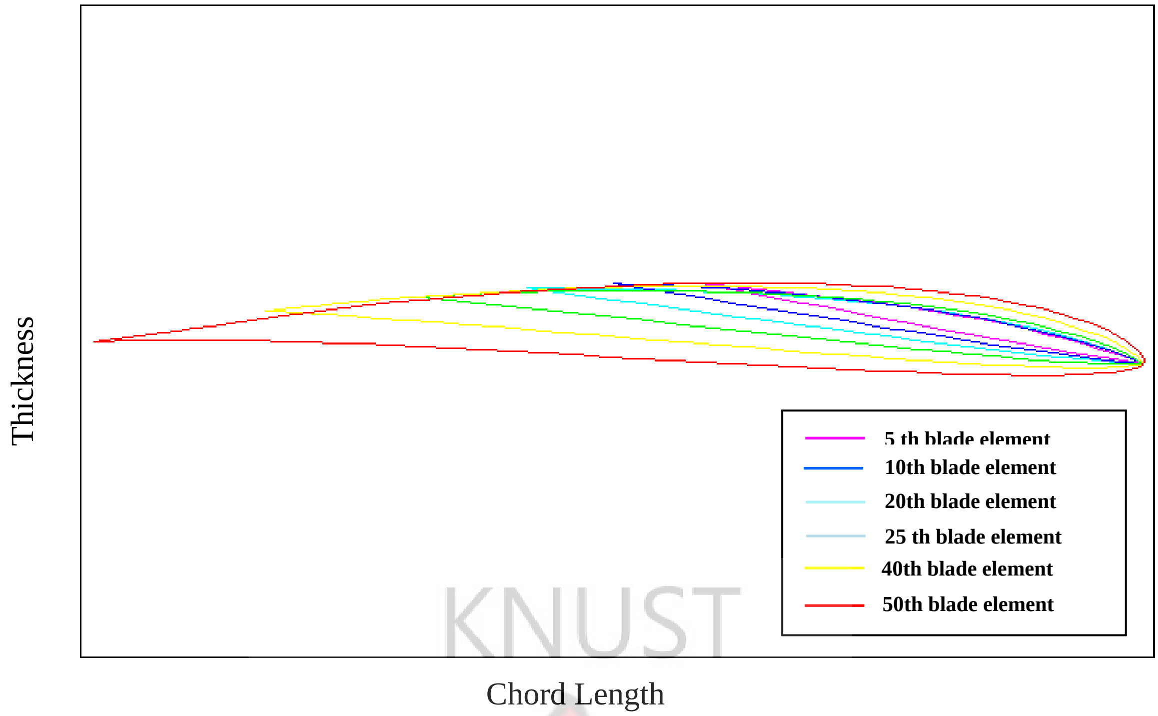

Figure 4.42:2-D Sectional View of Selig Donovan 7032 Designed Blade Profile for Set of Blade Elements

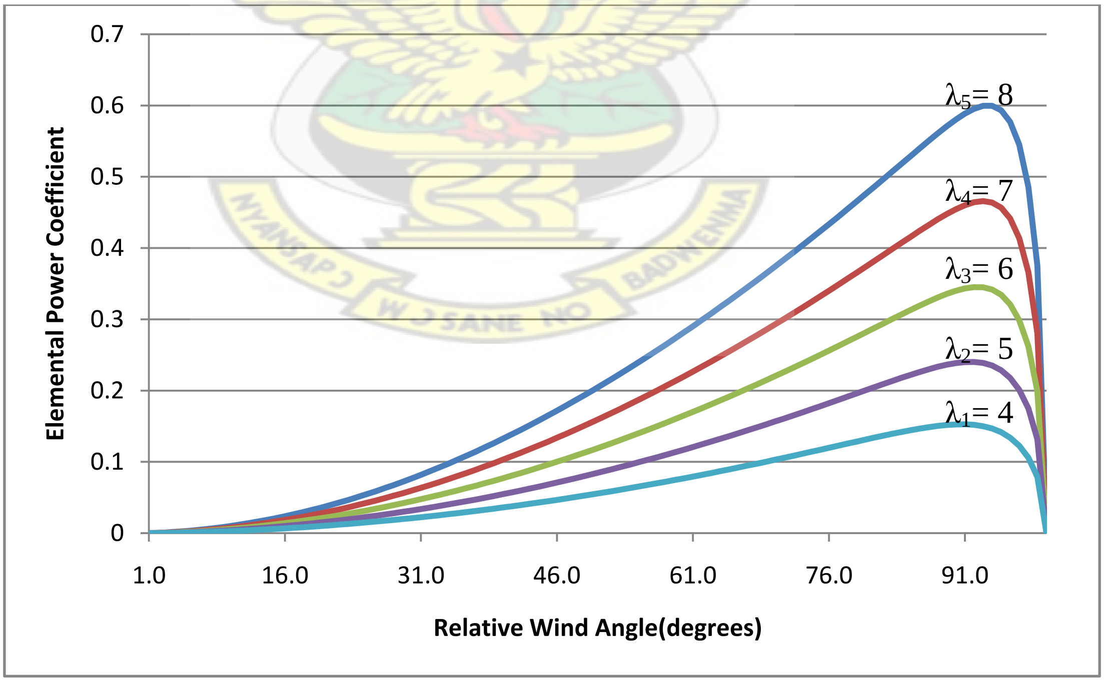

Figure 4.43: Variation of Elemental Power Coefficient with Relative Wind Angles for Values of Local Tip-Speed Ratio for Selig Donovan 7032

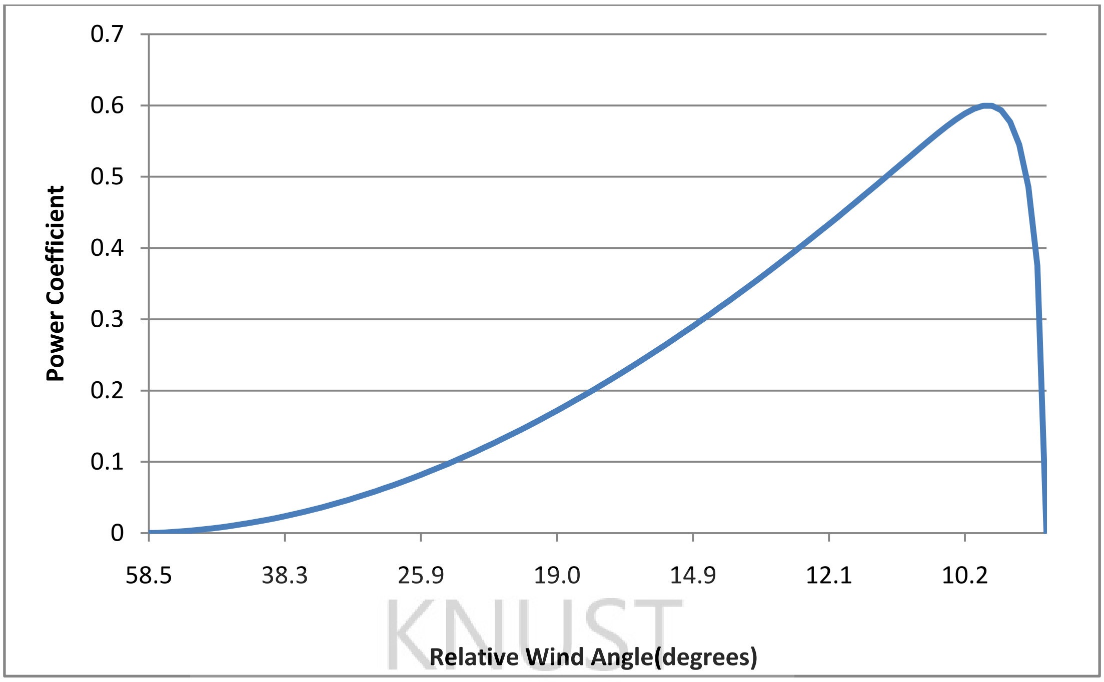

Figure **4.44:** A Graph of Power Coefficient against Relative Wind Angle for Selig Donovan 7032

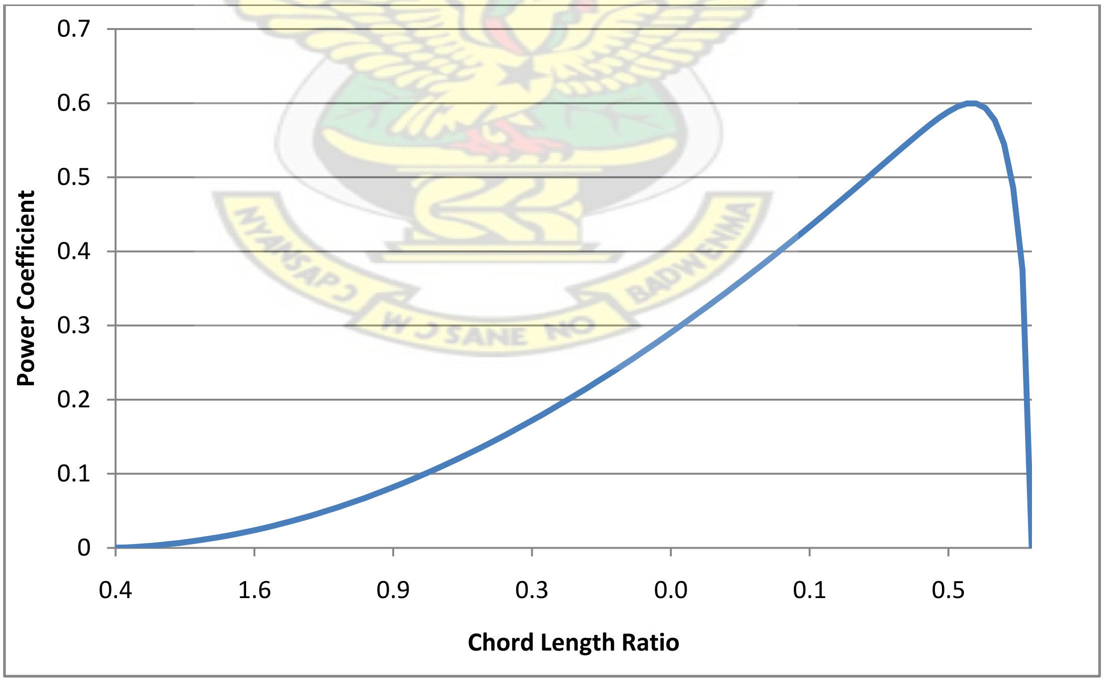

Figure 4.45: Variation of Power Coefficient to Chord Length Ratio Selig Donovan 7032

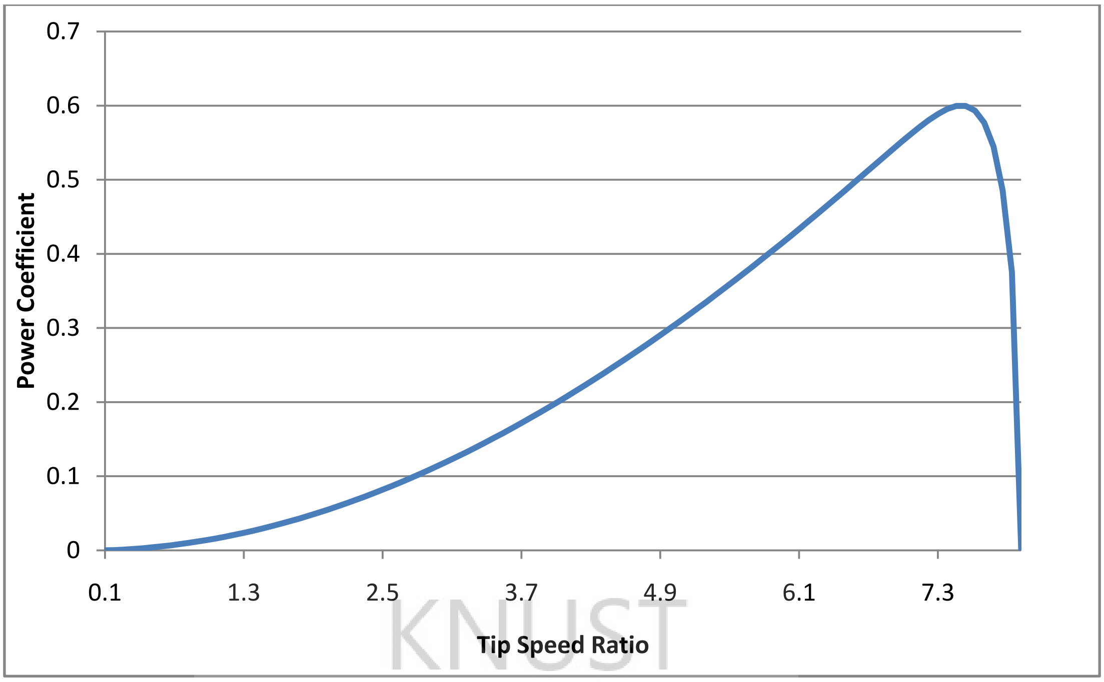

Figure 4.46: Variation of Elemental Power Coefficient with Respect to Elemental Tip Speed Ratio for Selig Donovan 7032

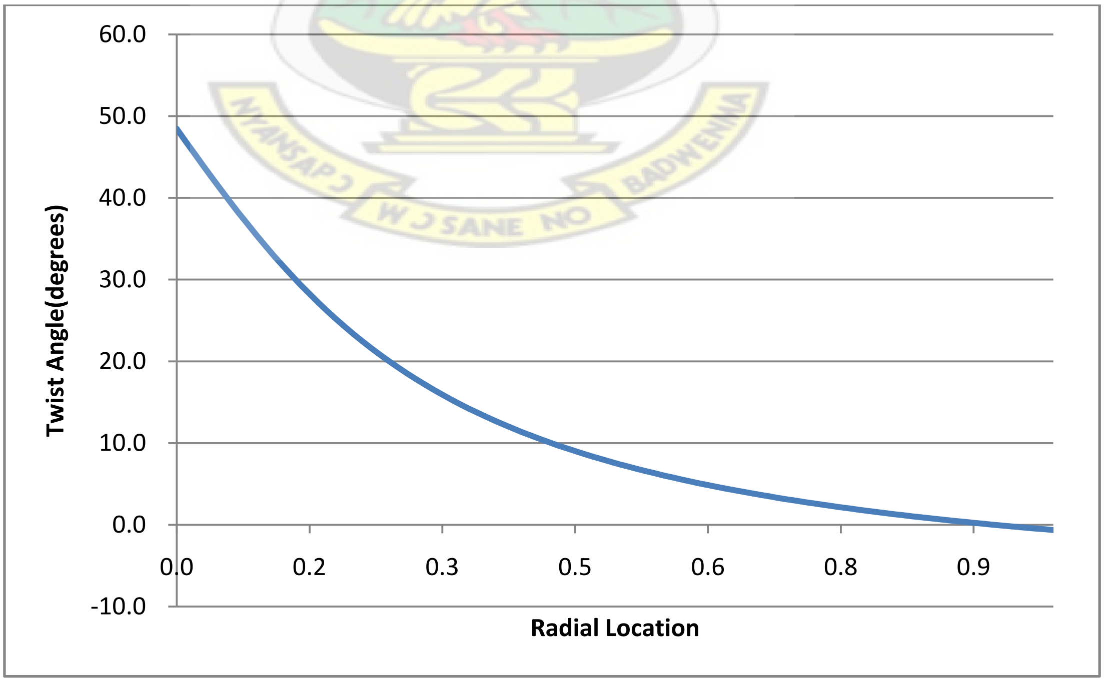

Figure 4.47: Twist Distribution for the Designed Blade for Selig Donovan 7032.

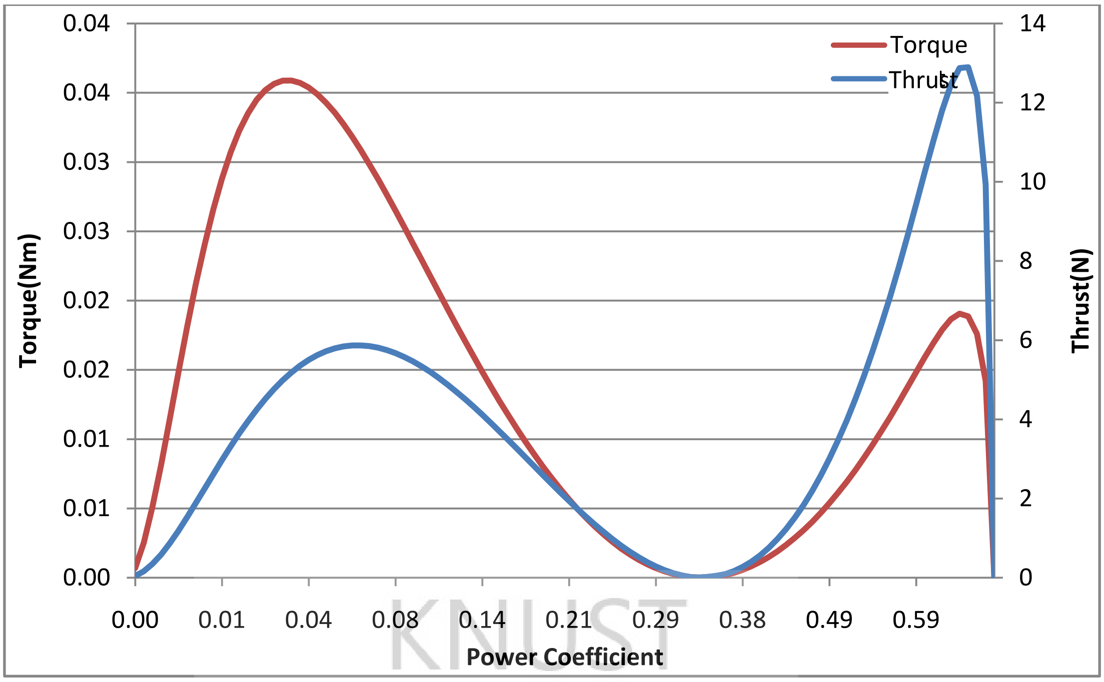

Figure 4.48: Power Coefficient against Torque and Thrust Distribution for Selig Donovan 7032

Figure 4.47 above also shows the twist distribution for the designed blade which gives a normalized outline as the various radial locations gave a positive twist angle pattern. This could be observed from the Figure that the twist angle is highest at the root and least at the tip of the blade as radial location increases accordingly.

Figure 4.48 above also shows how power coefficient relates to torque and thrust distribution along the blade profile. It depicts when the maximum thrust and torque occurred along the blade against the required power coefficient. The maximum thrust and torque were considered in the design of the blade profile.

4.2.7 Blade design Results for Selig Donovan 7037

Both Figure 4.49 and Figure 4.50 show an elemental blade section and a set of elemental blade sections up to 50th element to substantiate the pattern of the dimensional views of the blade profile. The plot in Figure 4.51 clearly shows the elemental power coefficient versus relative wind angles for values of local tip speed ratios of λ_1= 4, λ_2=5 ….., λ_5= 8. The highest elemental power coefficient as well as the generalized power coefficient, C_P of 0.5933 occurred at a relative wind angle of 10.03^o as shown in Figure 4.52.

Moreover, when the power coefficient was plotted against various chord length ratios as shown in Figure 4.53, the optimum power and hence lift occurred at a chord length ratio (c/R) of 0.63 at the same C_P of 0.5933. Similarly, a tip speed ratio of 7.44 occurred at the same power coefficient as indicated in Figure 4.54.

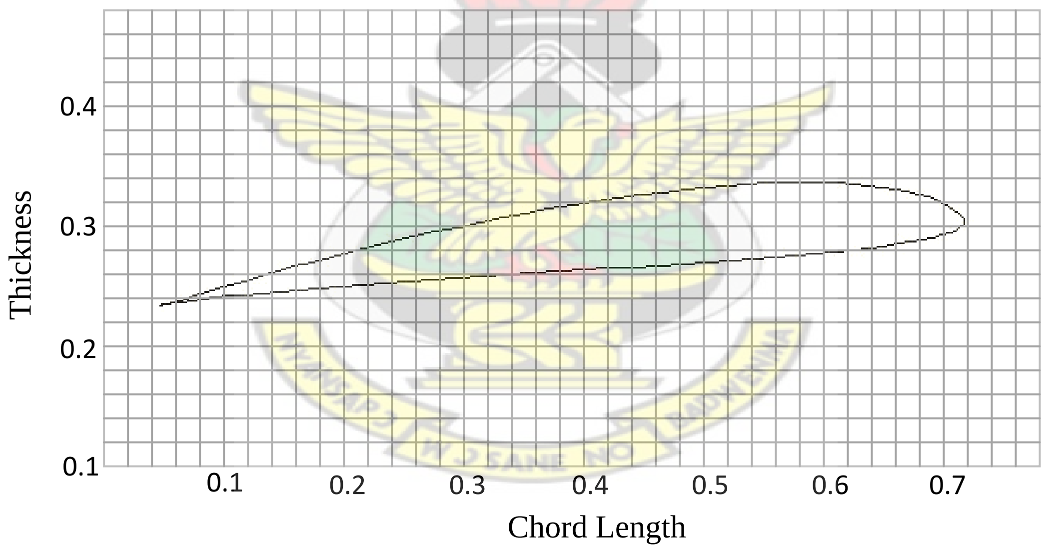

Figure 4.49: 2-D Sectional View of Selig Donovan 7037 Designed Blade Profile Element

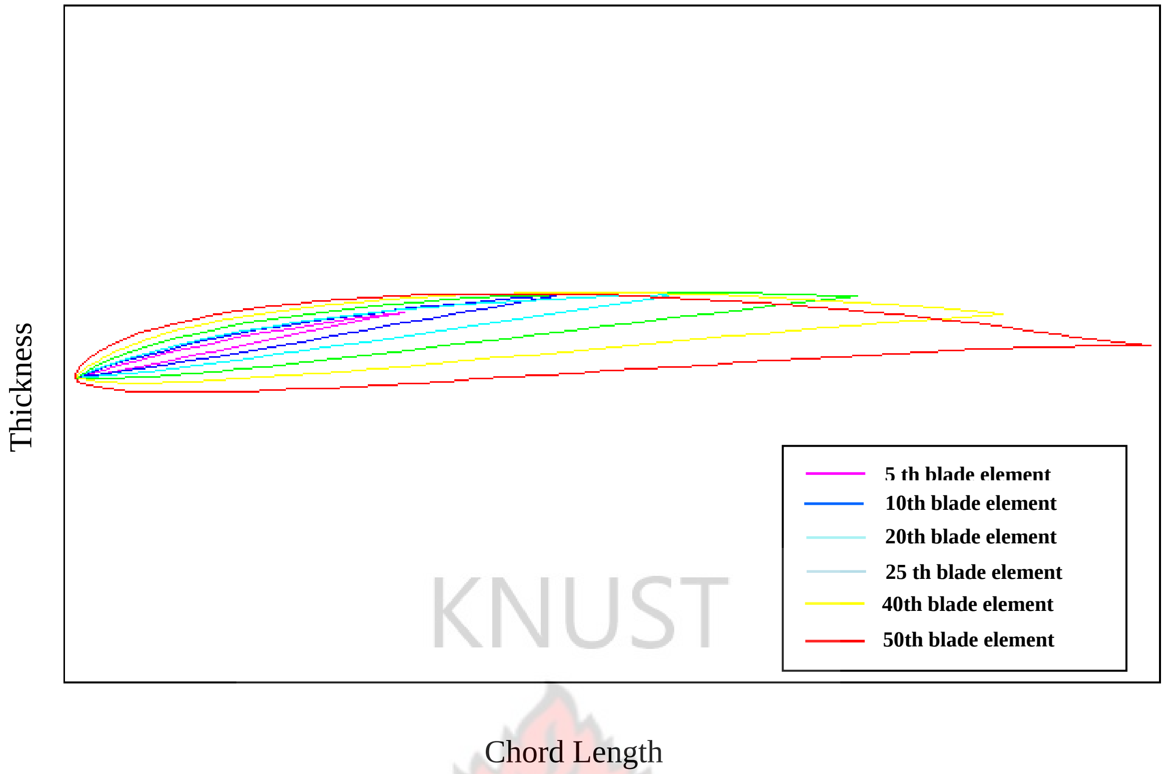

Figure 4.50: 2-D Sectional View of Selig Donovan 7037 Designed Blade Profile for a Set of Blade Elements

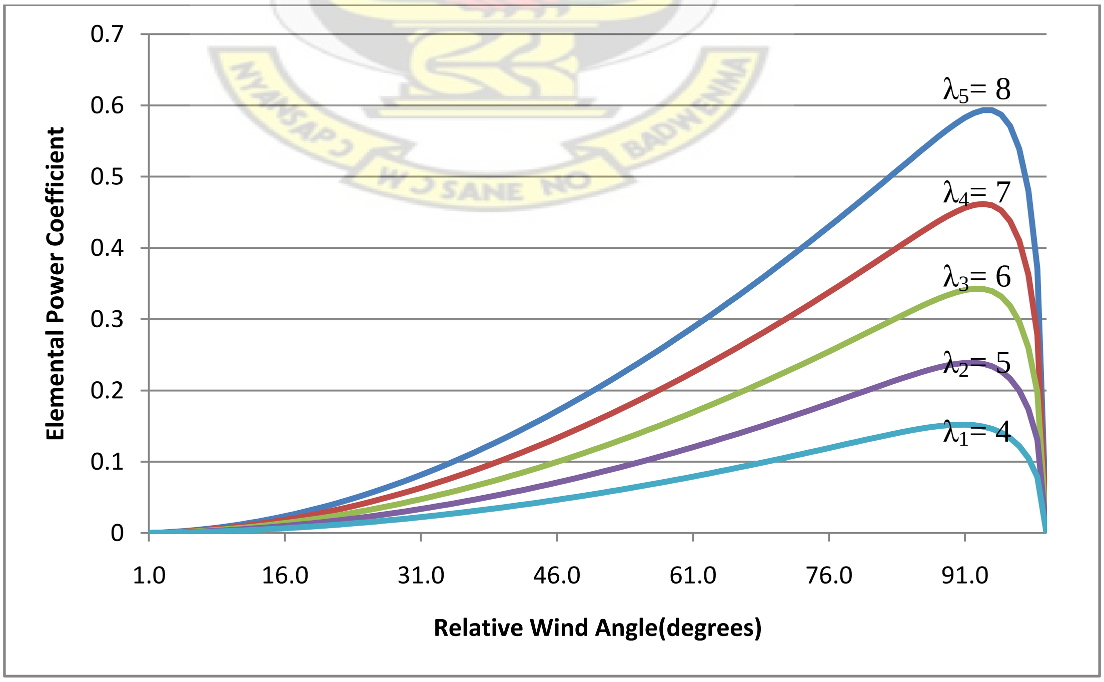

Figure 4.51: Variation of Elemental Power Coefficient with Relative Wind Angles for Values of Local Tip-Speed Ratio for Selig Donovan 7037

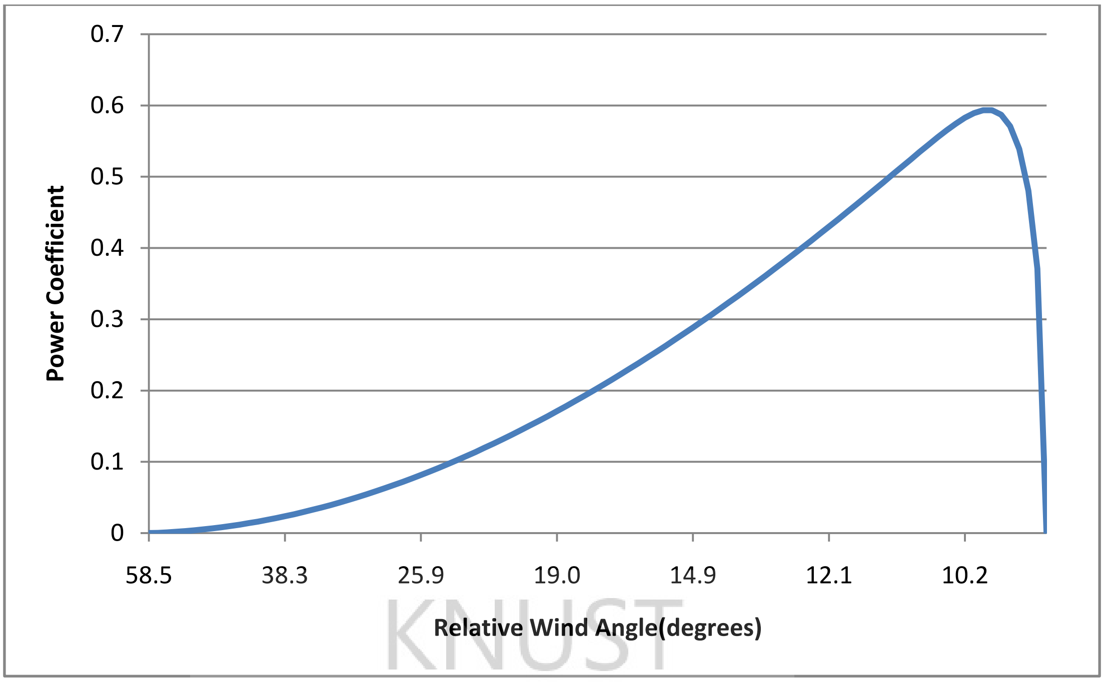

Figure 4.52: Variation of Power Coefficient to Relative Wind Angle for Selig Donovan 7037 Designed

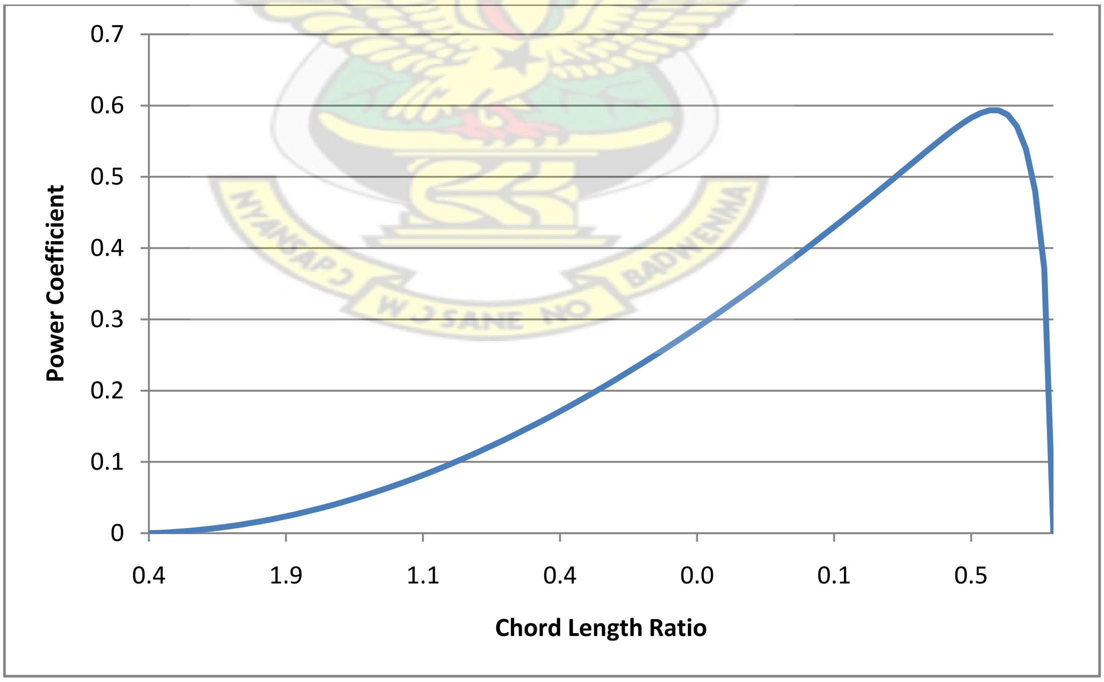

Figure 4.53: Variation of Power Coefficient to Chord Length Ratio for Selig Donovan 7037 Designed

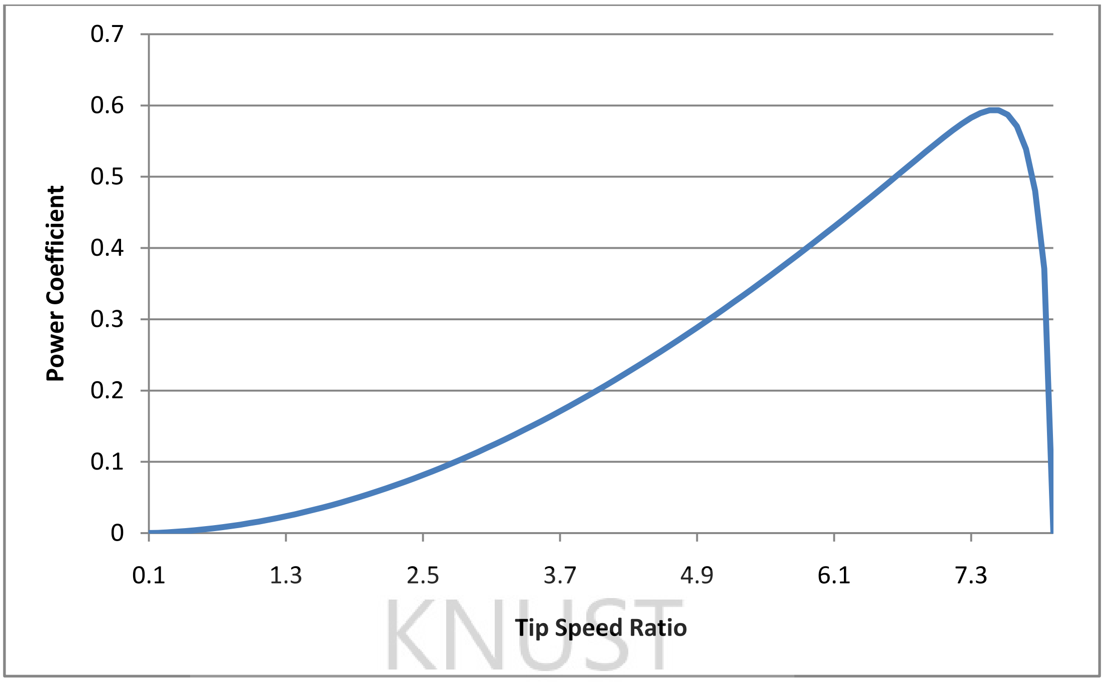

Figure 4.54: Variation of Elemental Power Coefficient to Elemental for Selig Donovan 7037 Designed Tip Speed Ratio

Figure 4.55 also shows the twist distribution for the designed blade which gives a normalized outline as the various radial locations gave a positive twist angle pattern. This could be observed from the Figure that the twist angle is highest at the root and least at the tip of the blade as radial location increases accordingly.

Figure 4.56 also shows how power coefficient relates to torque and thrust distribution along the blade profile. It depicts when the maximum thrust and torque occurred along the blade against the required power coefficient. The maximum thrust and torque were considered in the design of the blade profile.

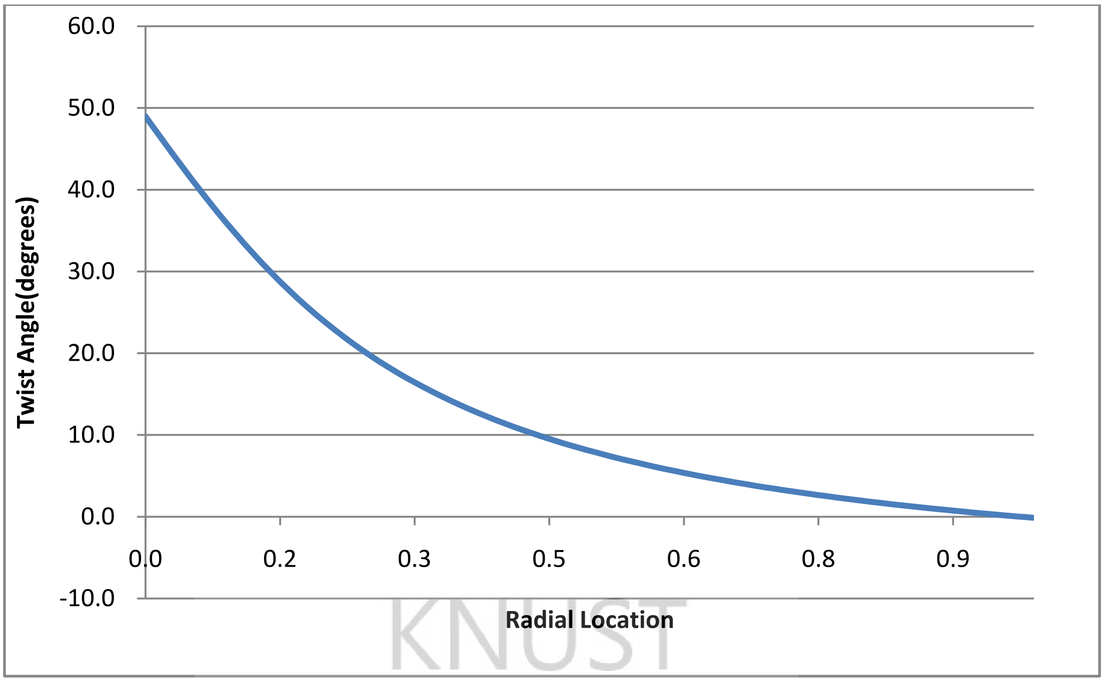

Figure 4.55: Twist Distribution for the Designed Blade for Selig Donovan7037 Designed

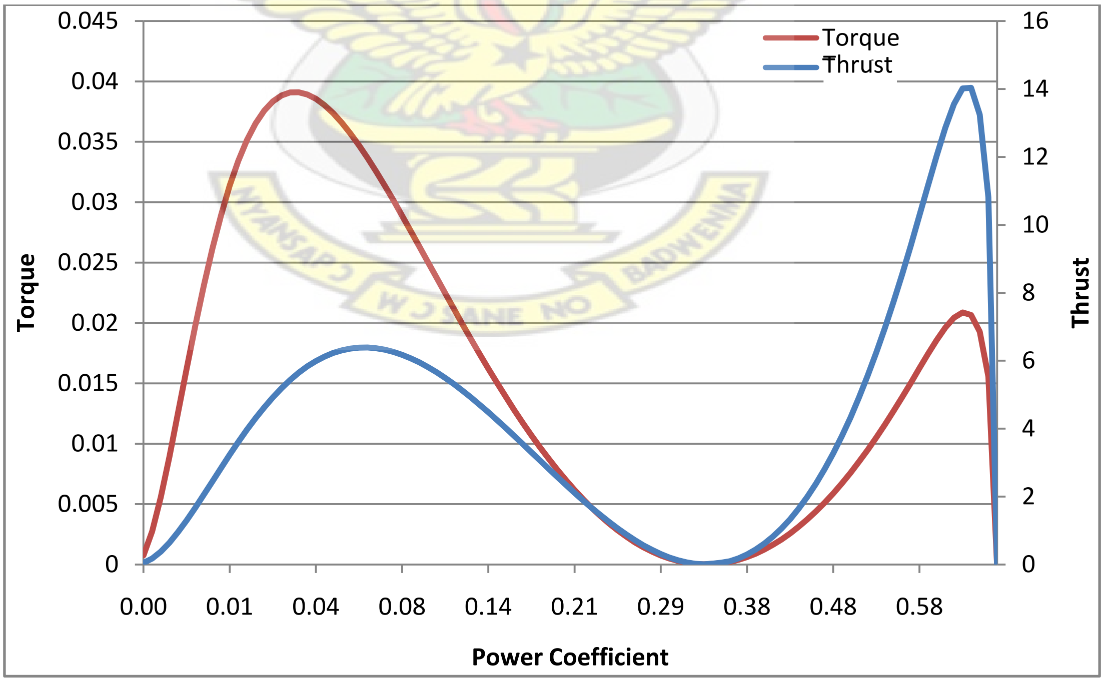

Figure 4.56: Power Coefficient against Torque and Thrust Distribution for Selig Donovan 7037

4.2.8 Blade design Results for Selig Donovan 8000

Both Figure 4.57 and Figure 4.58 show an elemental blade section and a set of elemental blade sections up to 50th element to substantiate the pattern of the dimensional views of the blade profile.The plot in Figure 4.59 clearly shows the elemental power coefficient versus relative wind angles for values of local tip speed ratios of λ_1= 4, λ_2=5 …., λ_5= 8. The highest elemental power coefficient as well as the generalized power coefficient, C_P of 0.5711 occurred at a relative wind angle of 10.03^o as shown in Figures 4.60.

Moreover, when the power coefficient was plotted against various chord length ratios, the optimum power and hence lift occurred at a chord length ratio (c/R) of 0.9052 at the same C_P of 0.5711 as shown in Figure 4.62. Similarly, a tip speed ratio of 7.44 occurred at the same power coefficient as indicated in Figure 4.63.

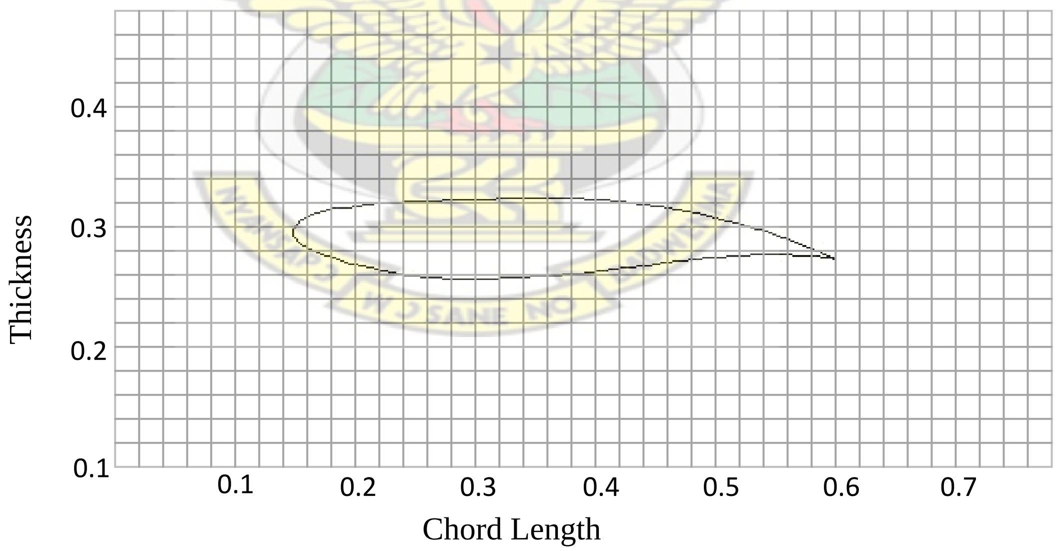

Figure 4.57: 2-D Sectional View of Selig Donovan 7037Designed Blade Profile Element

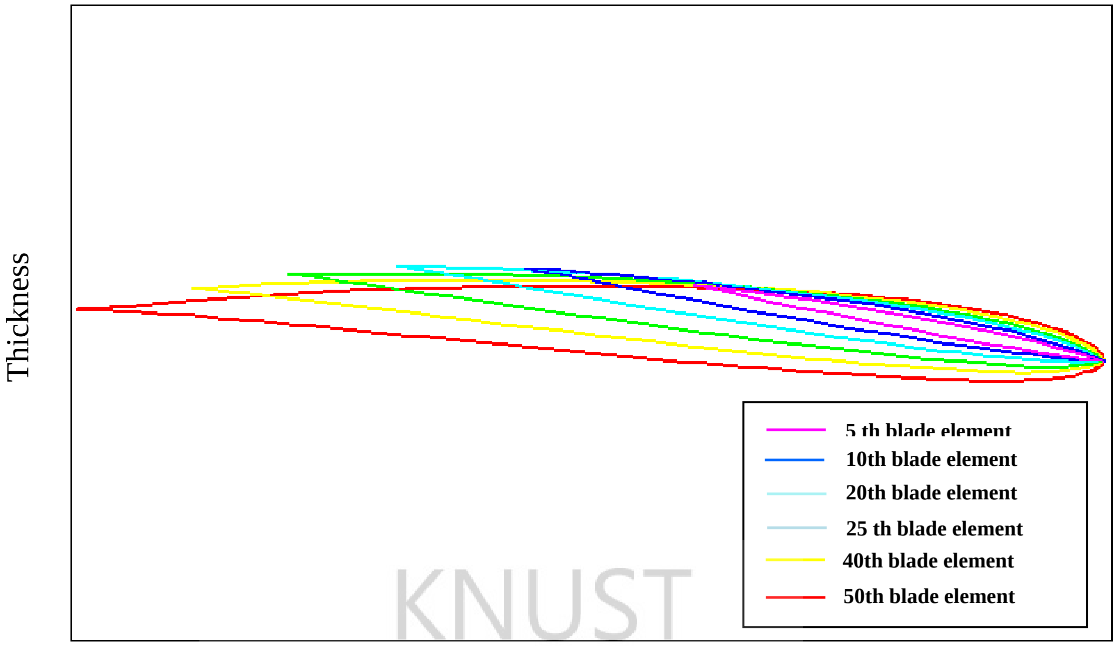

Figure 4.58: 2-D Sectional View of Selig Donovan 8000 Designed Blade Profile for a Set of Blade Elements

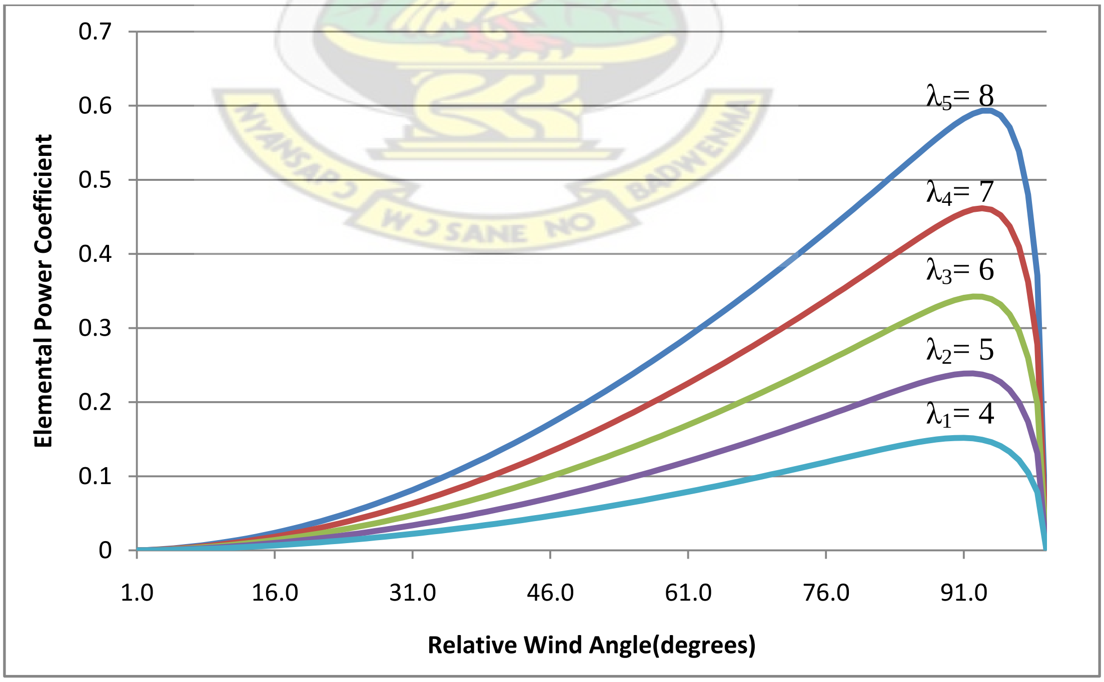

Figure 4.59: Variation of Elemental Power Coefficient with Relative Wind Angles for Values of Local Tip-Speed Ratio for Selig Donovan 8000.

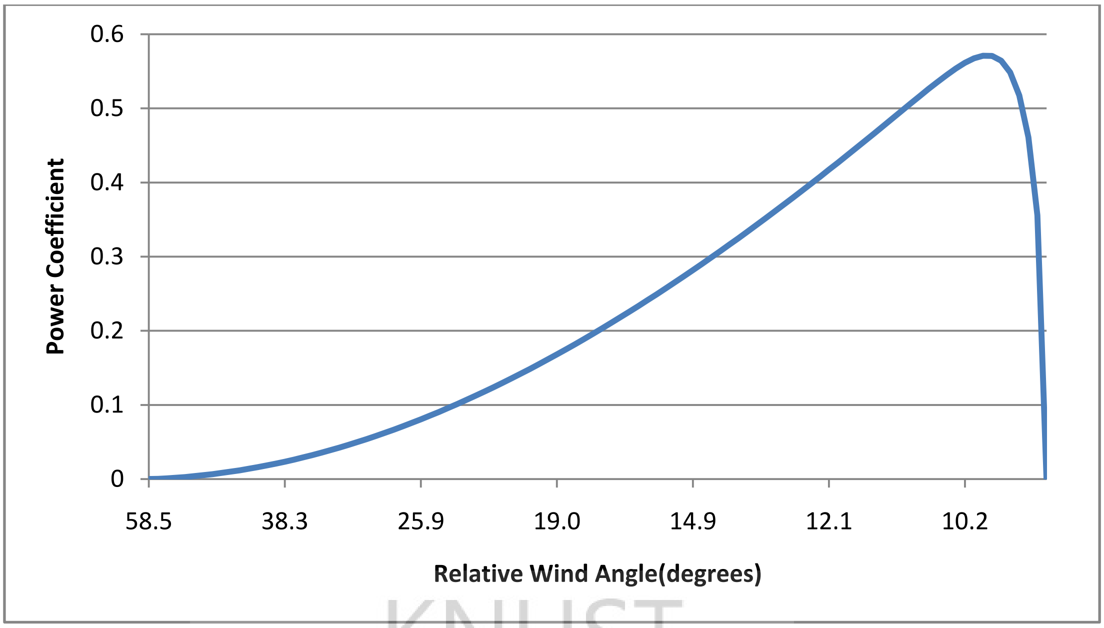

Figure 4.60: A Graph of Power Coefficient against Relative Wind Angle for Selig Donovan 8000

Figure 4.61 also shows the twist distribution for the designed blade which gives a normalized outline as the various radial locations gave a positive twist angle pattern. This could be observed from the Figure that the twist angle is highest at the root and least at the tip of the blade as radial location increases accordingly

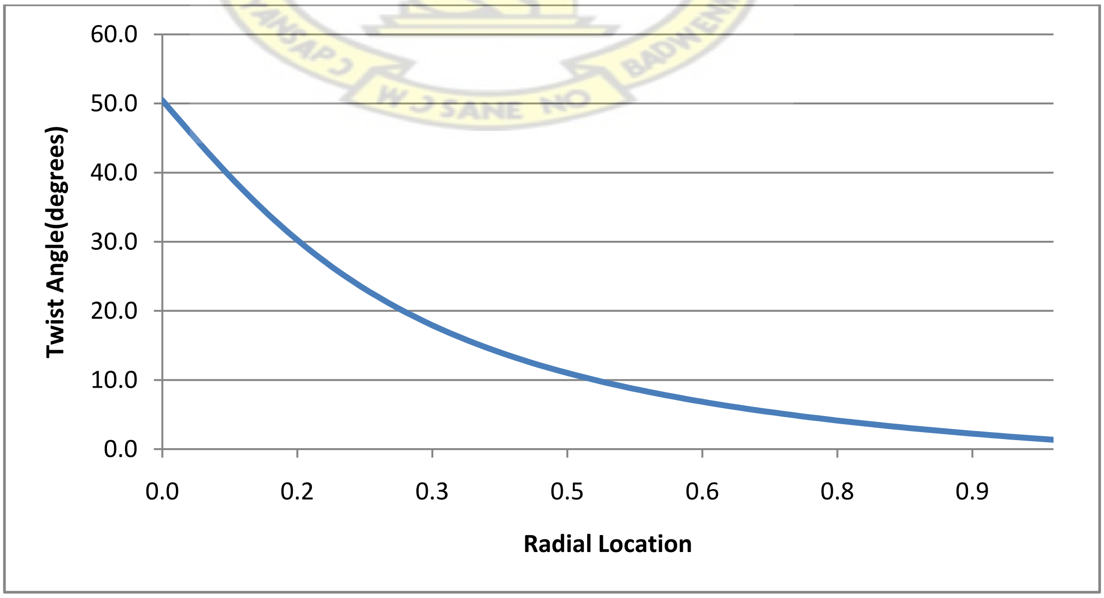

Figure 4.61: Twist distribution for the Designed Blade for Selig Donovan 8000

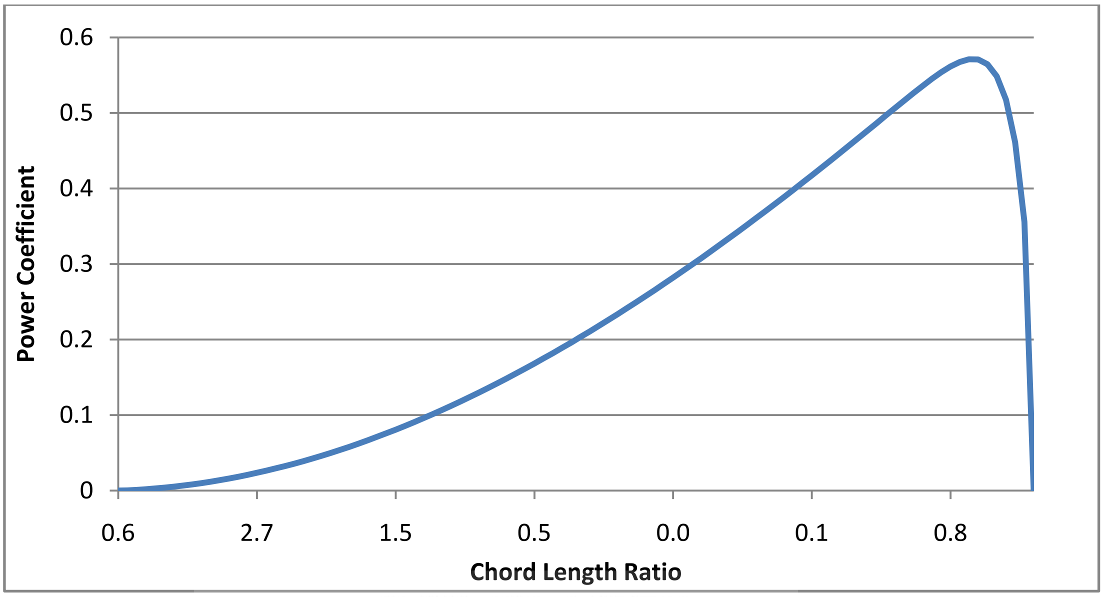

Figure 4.62: Variation of Power Coefficient to Chord Length Ratio for Selig Donovan 8000

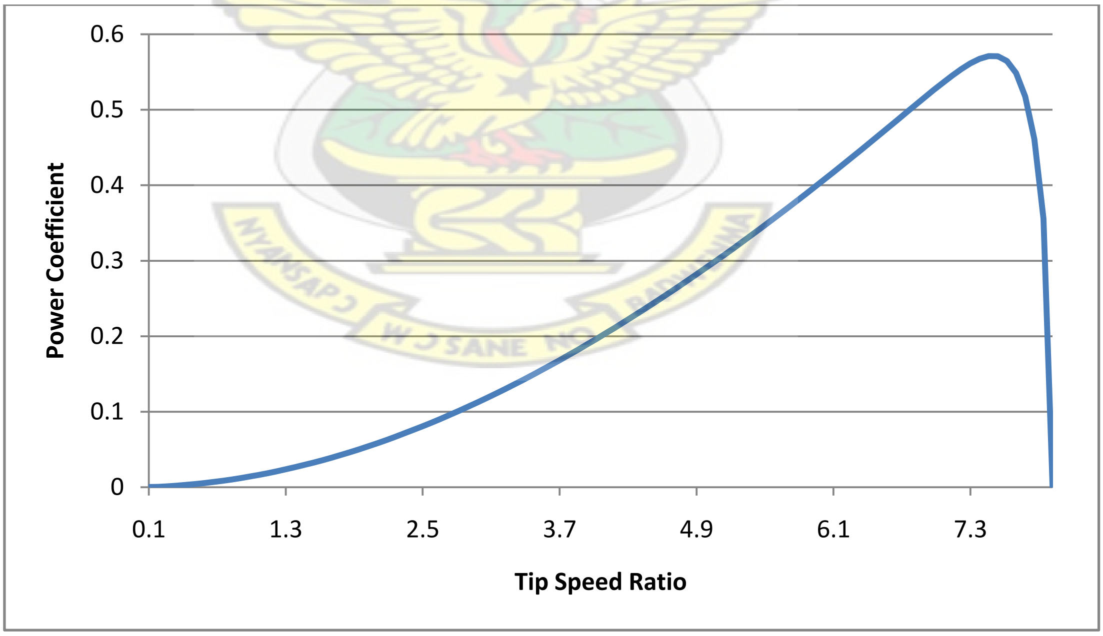

Figure 4.63: Variation of Elemental Power Coefficient with Respect to Elemental Tip Speed Ratio for Selig Donovan 8000

Figure 4.64 also shows how power coefficient relates to torque and thrust distribution along the blade profile. It depicts when the maximum thrust and torque occurred along the blade against the required power coefficient. The maximum thrust and torque were considered in the design of the blade profile.

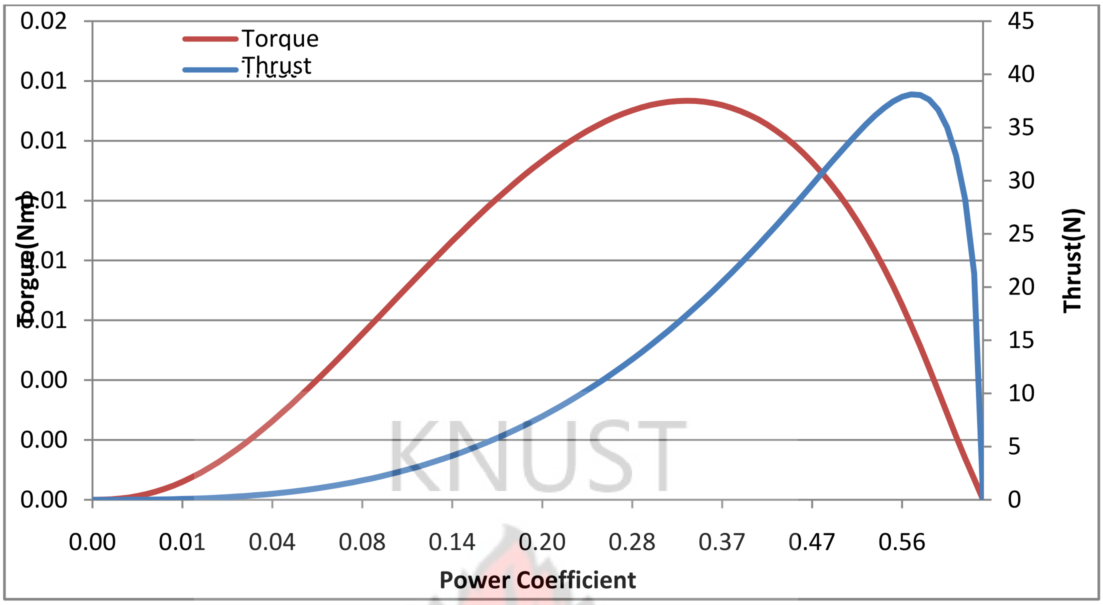

Figure 4.64: Power Coefficient against Torque and Thrust Distribution for Selig Donovan 8000

4.2.9 Blade design Results for Selig 3021

Both Figure 4.65 and Figure 4.66 show an elemental blade section and a set of elemental blade sections up to 50th element to substantiate the pattern of the dimensional views of the blade profile.The plot in Figure 4.67 clearly shows the elemental power coefficient versus relative wind angles for values of local tip speed ratios of λ_1= 4, λ_2=5 ……, λ_5= 8. The highest elemental power coefficient as well as the generalized power coefficient, C_P of 0.5884 occurred at a relative wind angle of 10.03^o as shown in Figures 4.68.

Moreover, when the power coefficient was plotted against various chord length ratios, the optimum power and hence lift occurred at a chord length ratio (c/R) of 0.80 at the same C_P of 0.5884 as shown in Figure 4.69. Similarly, a tip speed ratio of 7.44 occurred at the same power coefficient as indicated in Figure 4.70.

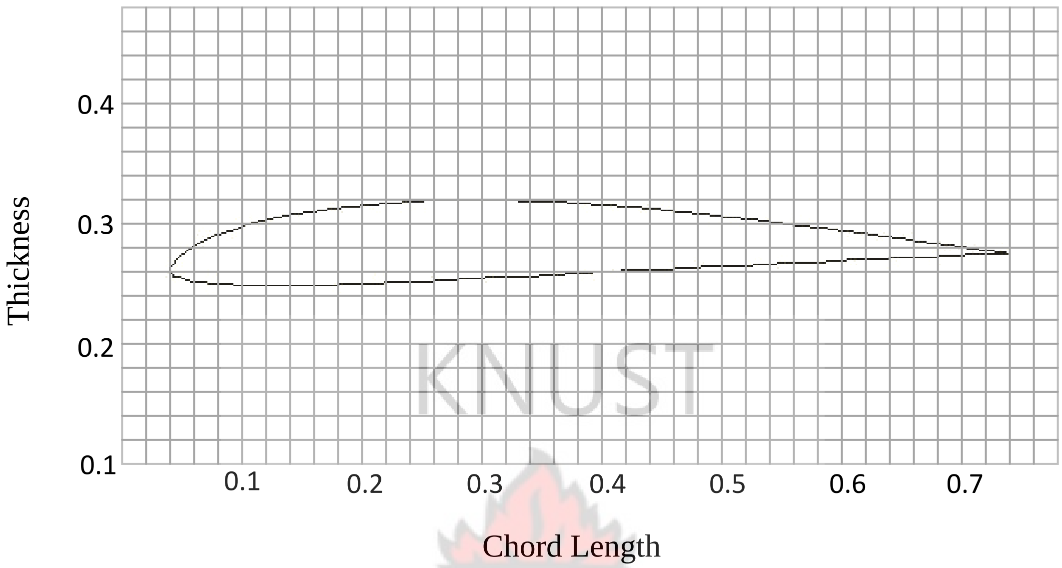

Figure 4.65: 2-D Sectional View of Selig 3021 Designed Blade Profile Element

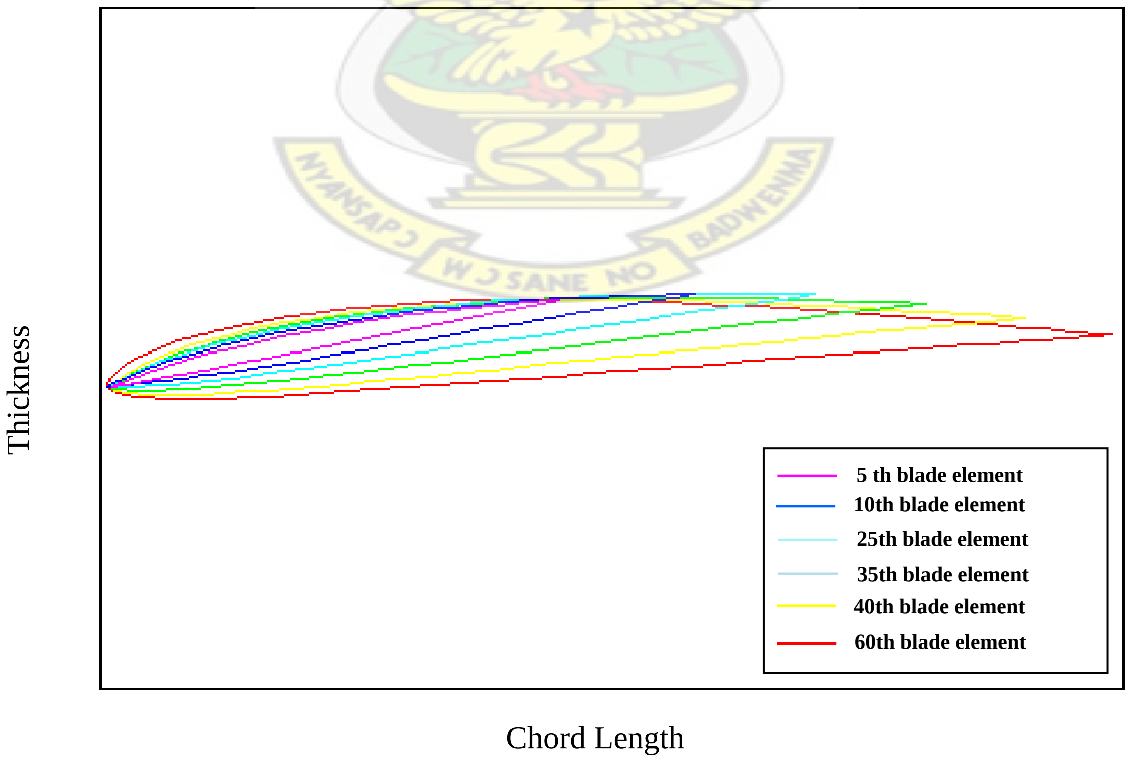

Figure 4.66: 2-D Sectional View of Selig 3021 Designed Blade Profile for a Set of Blade Elements

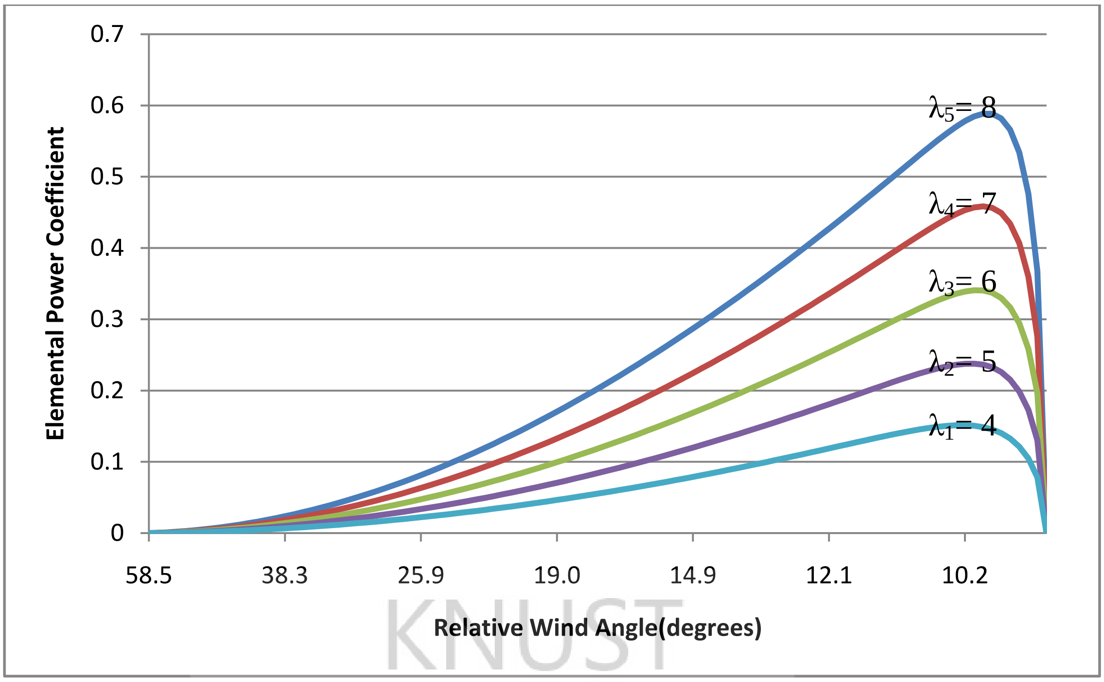

Figure 4.67: A Graph of Power Coefficient against Relative Wind Angle for Selig 3021

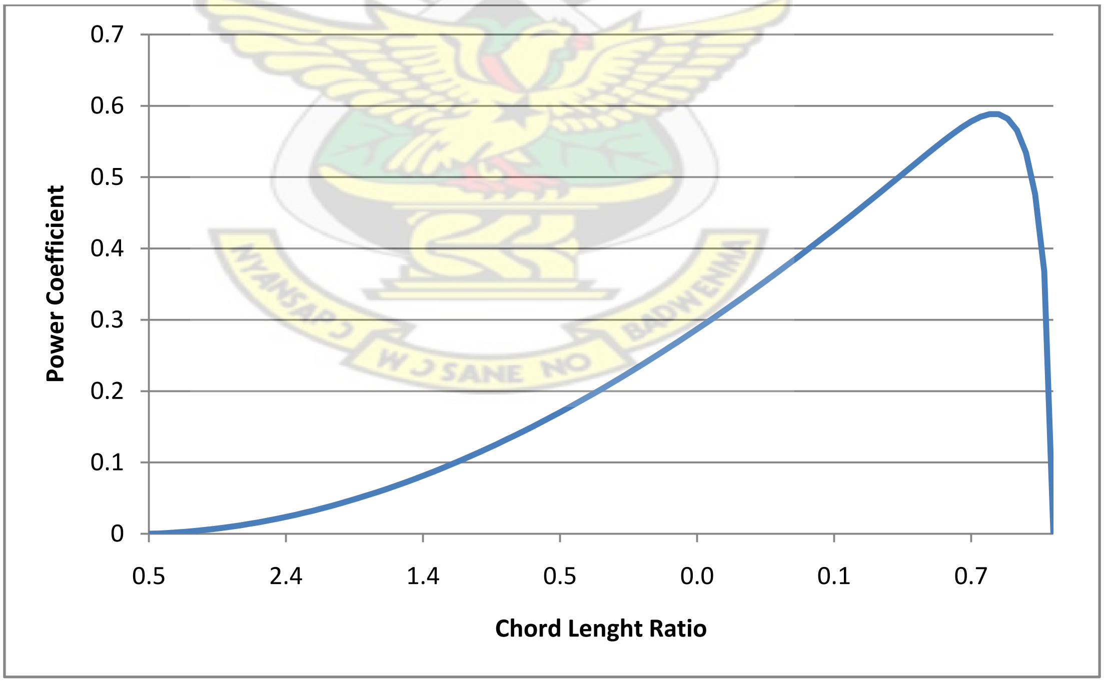

Figure 4.68: Variation of Power Coefficient to Chord Length Ratio for Selig 3021

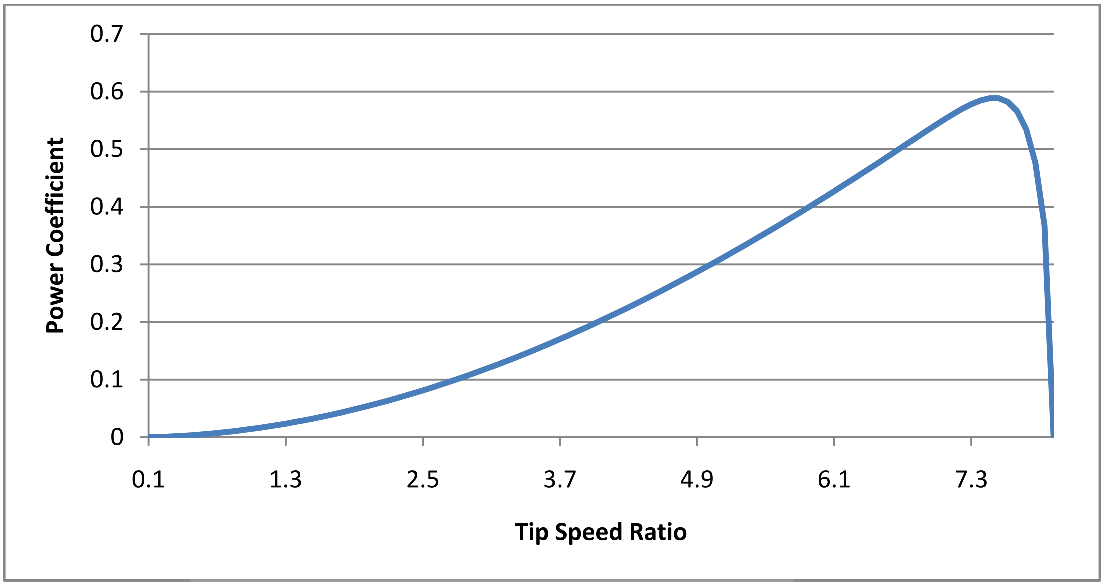

Figure 4.69: Variation of Elemental Power Coefficient to Elemental Tip Speed Ratio for Selig 3021

Figure 4.70 also shows the twist distribution for the designed blade which gives a normalized outline as the various radial locations gave a positive twist angle pattern. This could be observed from the Figure that the twist angle is highest at the root and least at the tip of the blade as radial location increases accordingly.

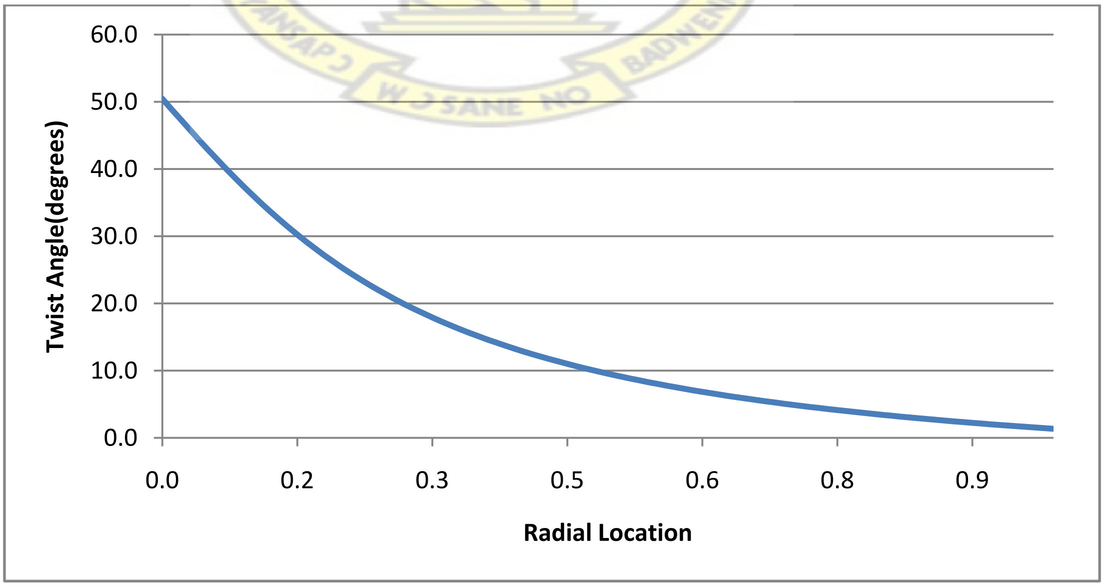

Figure 4.70: Twist Distribution for the Designed Blade for Selig 3021

Figure 4.71 also shows how power coefficient relates to torque and thrust distribution along the blade profile. It depicts when the maximum thrust and torque occurred along the blade against the required power coefficient. The maximum thrust and torque were considered in the design of the blade profile.

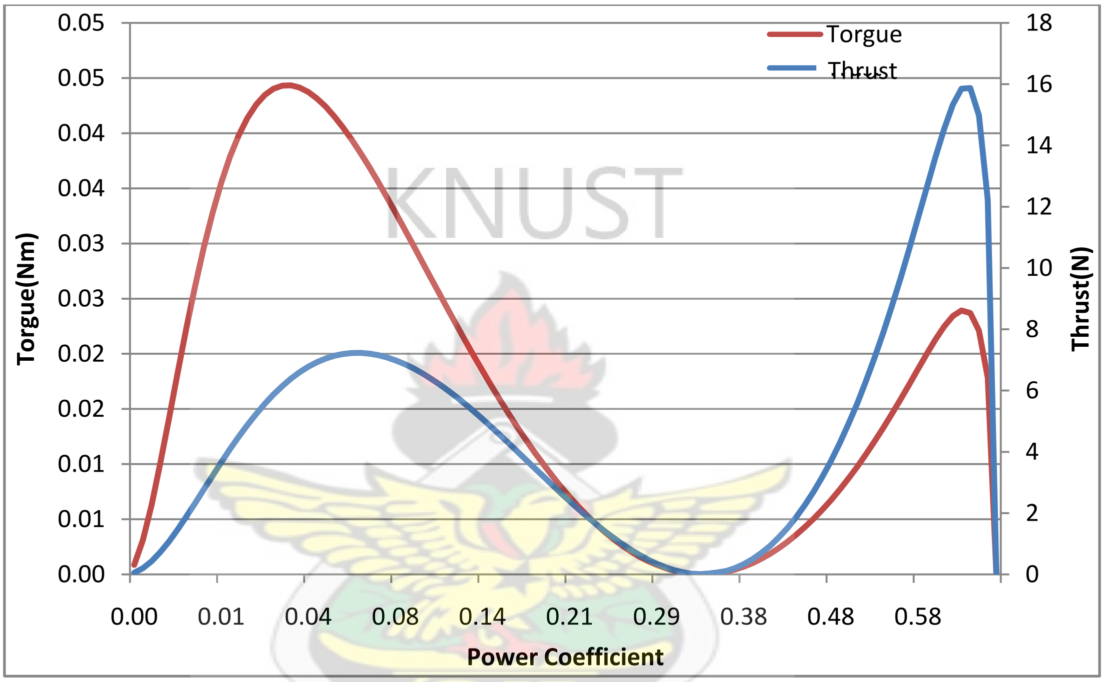

Figure 4.71: Power Coefficient against Torque and Thrust Distribution for Selig 3021

4.2.10 Blade design Results for Ara-D 10%

Both Figure 4.72 and Figure 4.73 show an elemental blade section and a set of elemental blade sections up to 50th element to substantiate the pattern of the dimensional views of the blade profile. The plot in Figure 4.74 clearly shows the elemental power coefficient versus relative wind angles for values of local tip speed ratios of λ_1= 4, λ_2=5 ….., λ_5= 8. The highest elemental power coefficient as well as the generalized power coefficient, C_P of 0.50 occurred at a relative wind angle of 10.03^o as shown in Figures 4.75.

Moreover, when the power coefficient was plotted against various chord length ratios, the optimum power and hence lift occurred at a chord length ratio (c/R) of 0.49 at the same C_P of 0.50 as in Figure 4.76. Similarly, a tip speed ratio of 7.44 occurred at the same power coefficient as indicated in Figure 4.77.

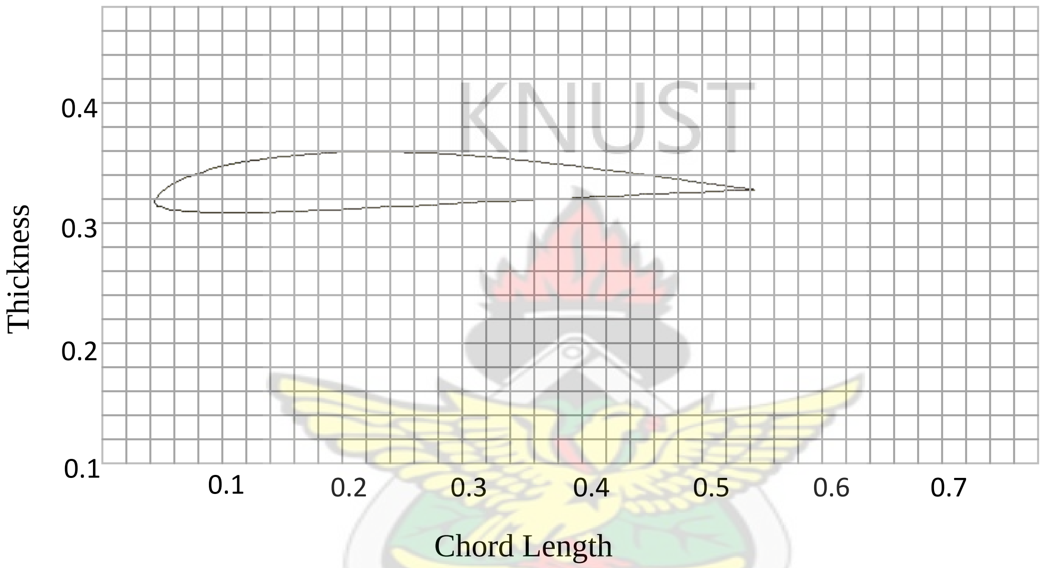

Figure 4.72: 2-D Sectional View of Ara-D 10% Designed Blade Profile Element

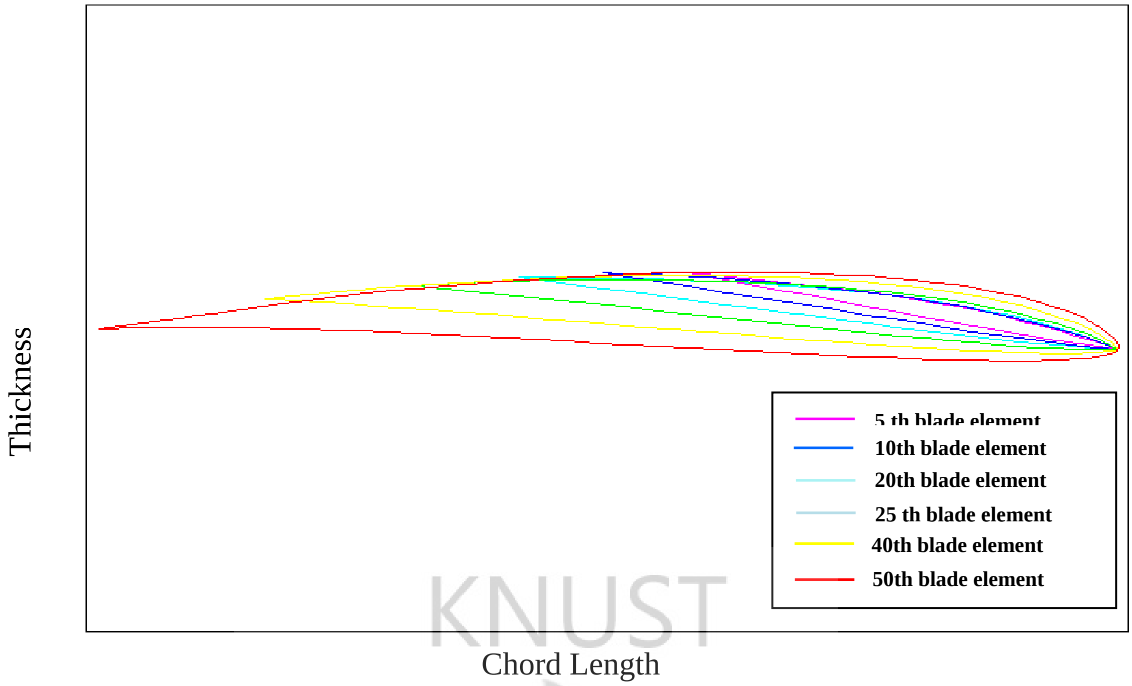

Figure 4.73: 2-D Sectional View of Ara-D 10% Designed Blade Profile for a Set of Blade Elements

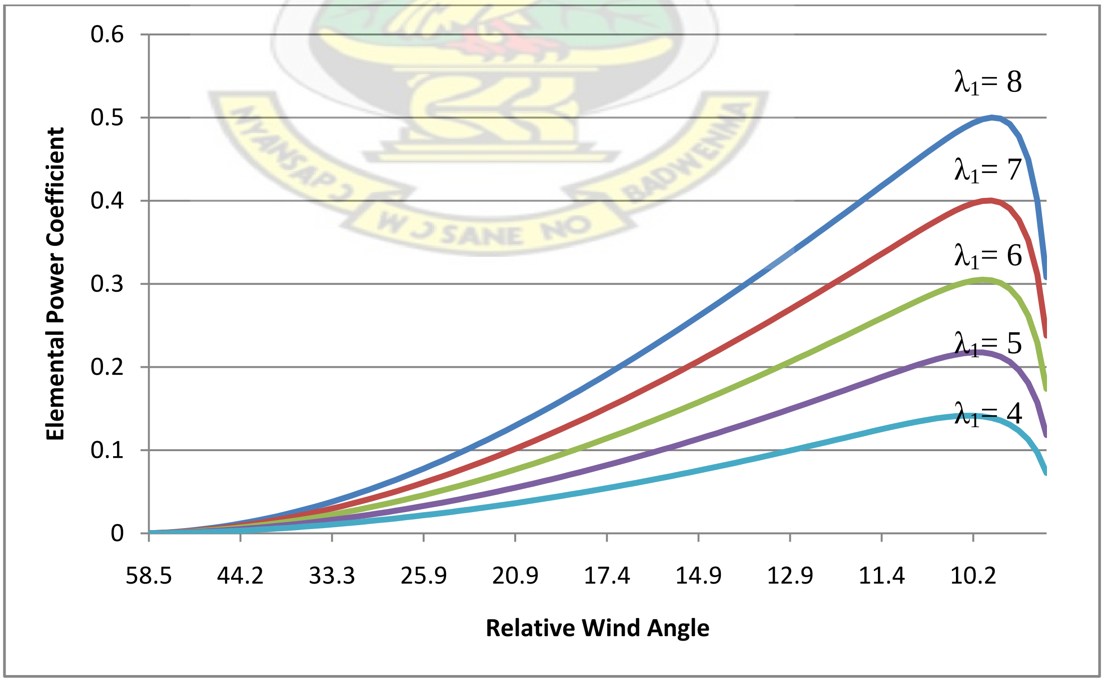

Figure 4.74: Variation of Elemental Power Coefficient with Relative Wind Angles for Values of Local Tip-Speed Ratio for Ara-D 10%

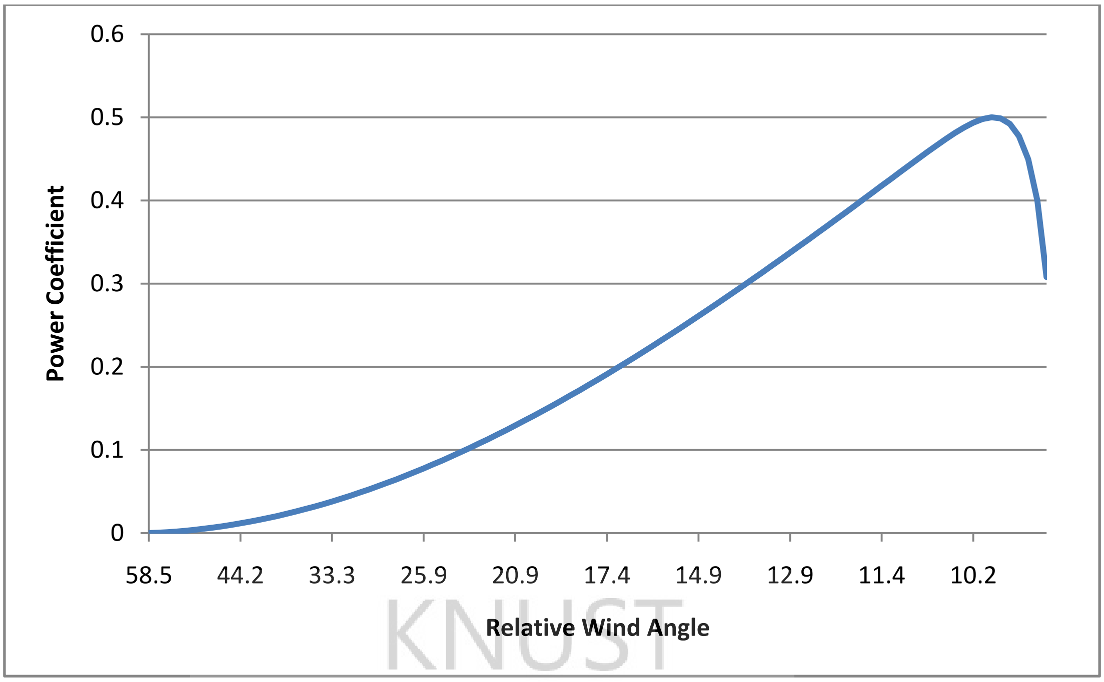

Figure 4.75: A graph of Power Coefficient against Relative Wind Angle for Ara-D 10%

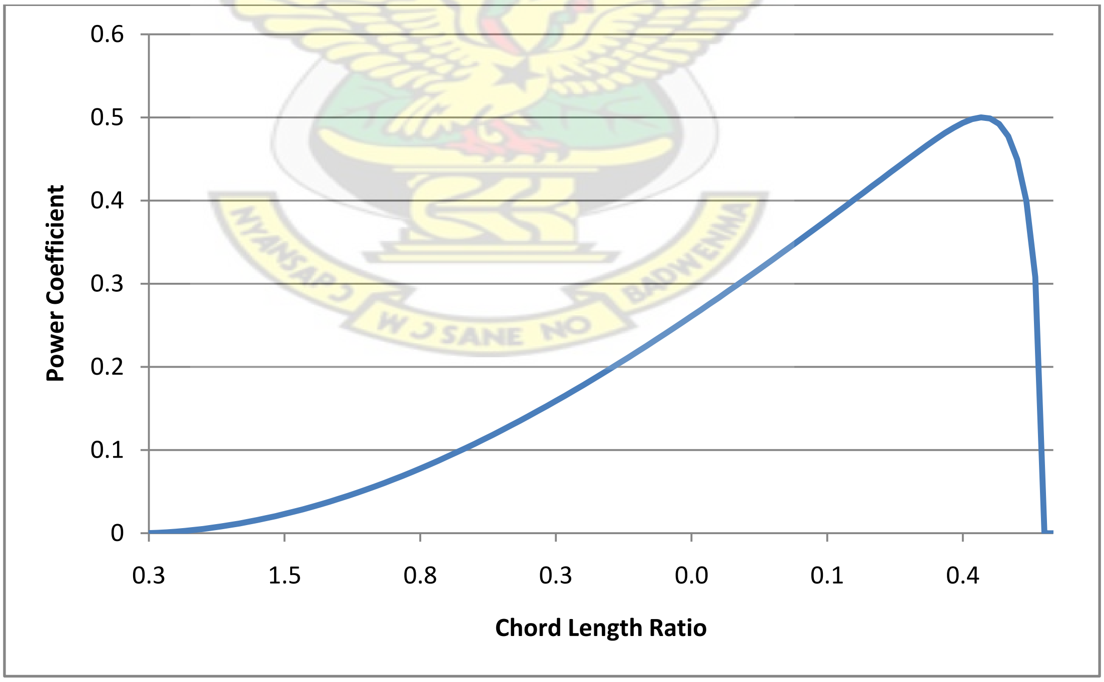

Figure 4.76: Variation of Power Coefficient to Chord Length Ratio for Ara-D 10%

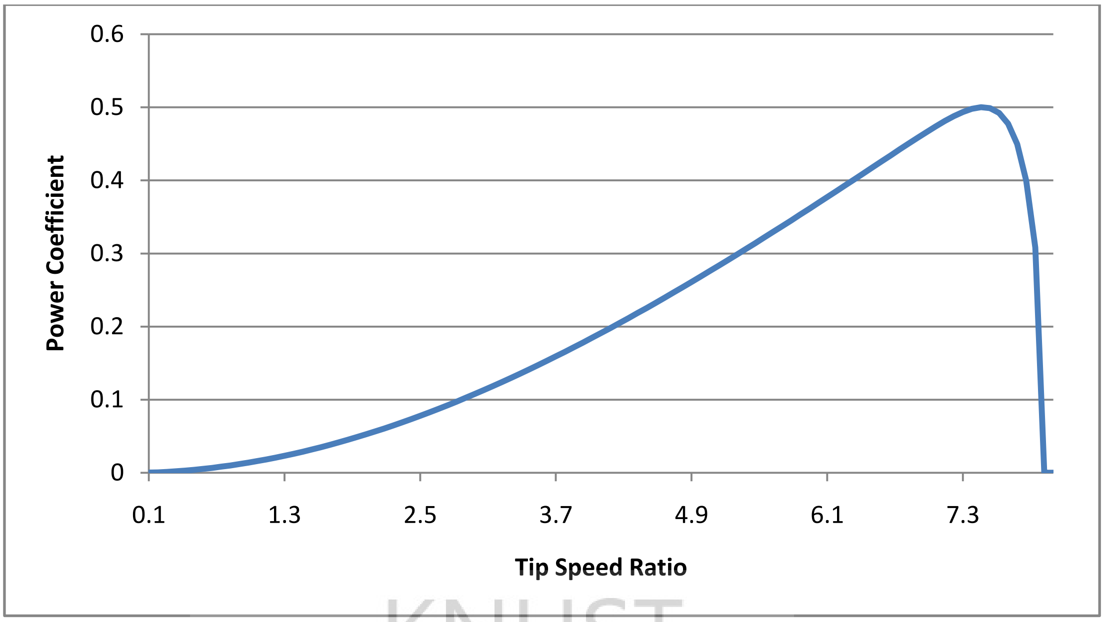

Figure 4.77: Variation of Elemental Power coefficient to Elemental Tip Speed Ratio for Ara-D 10%

Figure 4.78 also shows the twist distribution for the designed blade which gives a normalized outline as the various radial locations gave a positive twist angle pattern. This could be observed from the Figure that the twist angle is highest at the root and least at the tip of the blade as radial location increases accordingly.

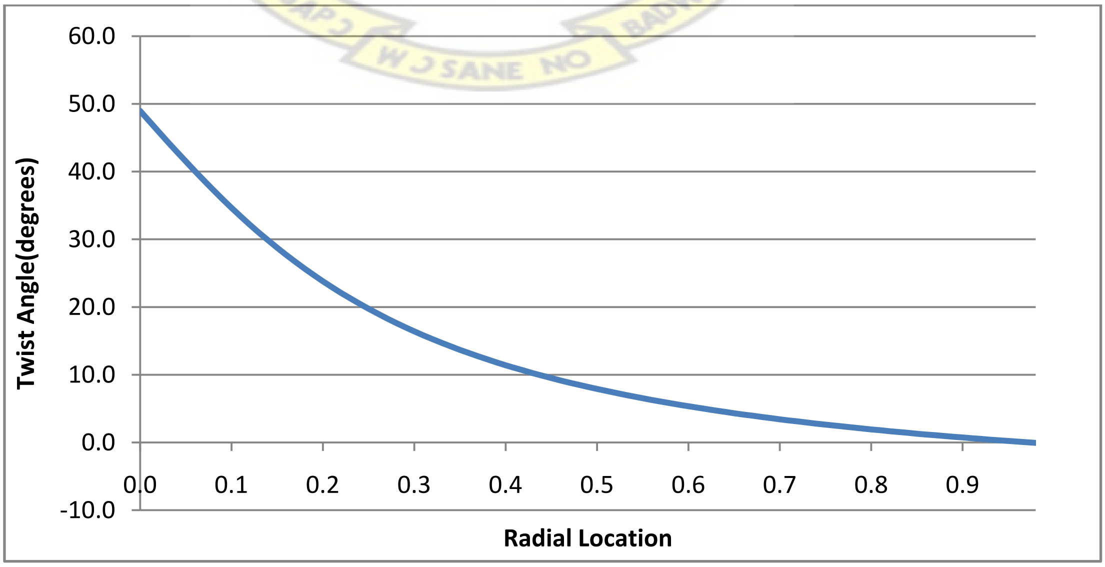

Figure 4.78: Twist Distribution for the Designed Blade for Ara-D 10%

Figure 4.79 also shows how power coefficient relates to torque and thrust distribution along the blade profile. It depicts when the maximum thrust and torque occurred along the blade against the required power coefficient. The maximum thrust and torque were considered in the design of the blade profile.

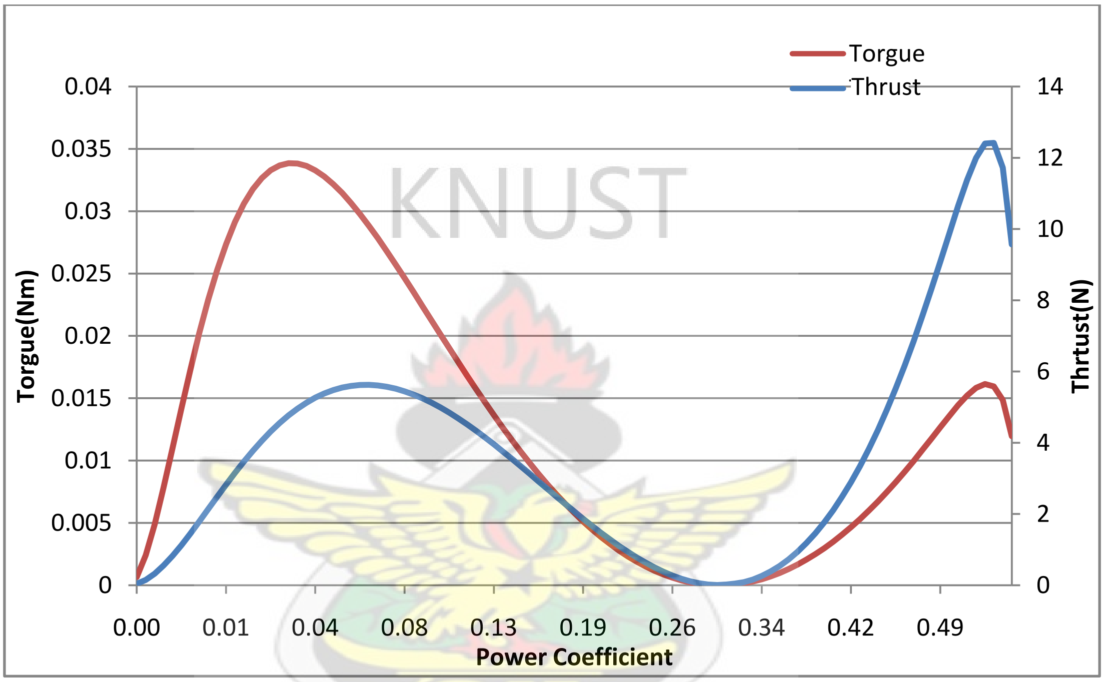

Figure 4.79: Power Coefficient against Torque and Thrust Distribution for Ara D-10%

4.3 Model of the LWS Blade Profile

Figure 4.80 and Figure 4.81 show the elemental blade section and the set of elemental blade sections to substantiate the pattern of the dimensional views.

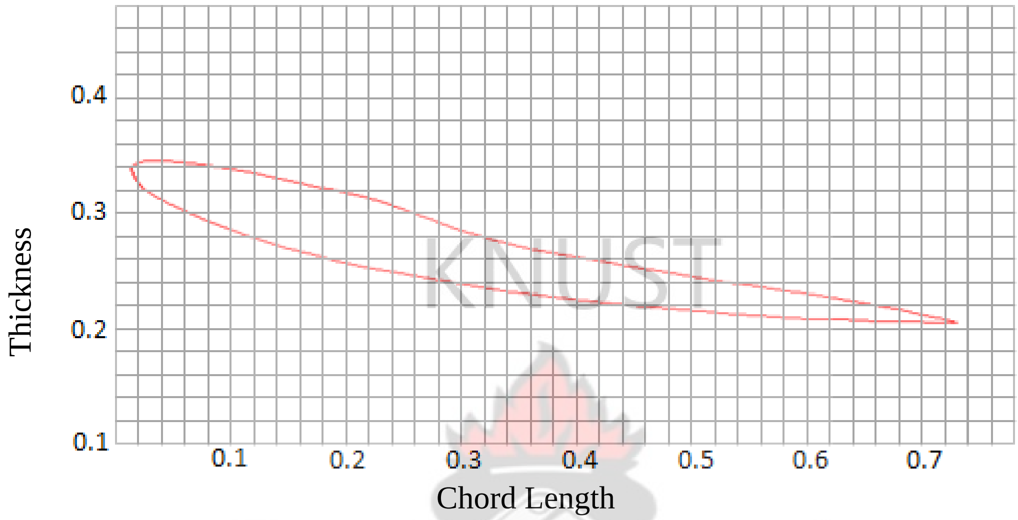

Figure 4.80: 2-D Sectional View of LWS Designed Blade Profile Element

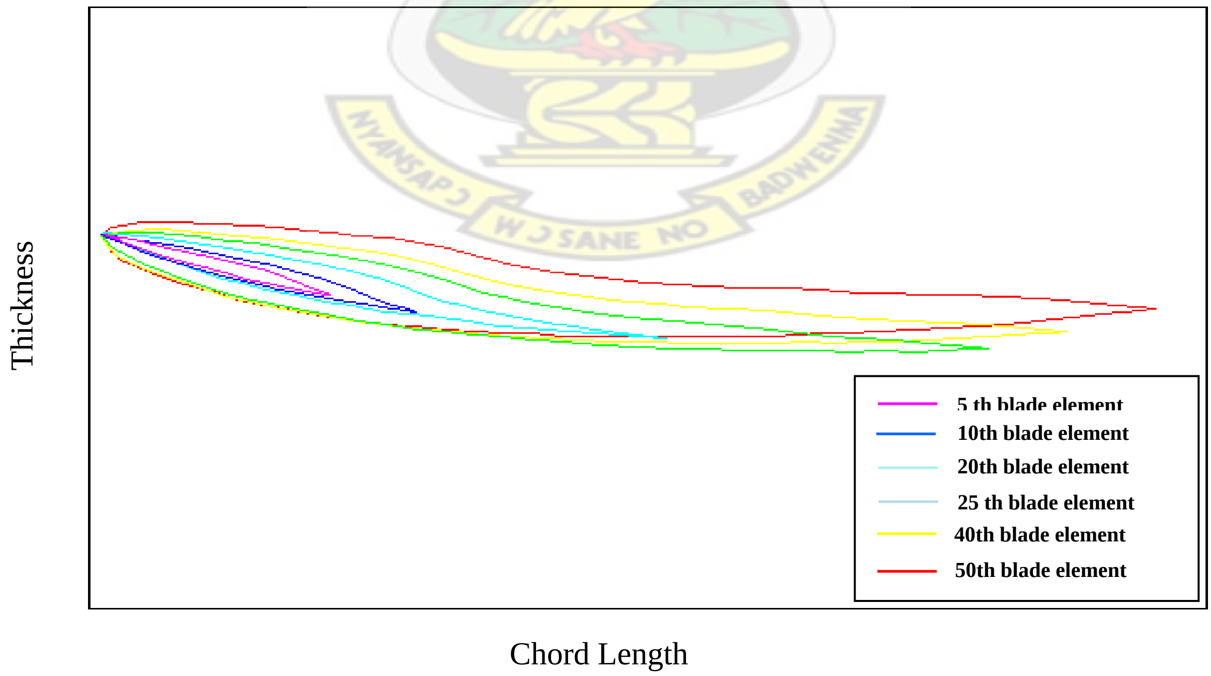

Figure 4.81: 2-D Sectional View of LWS Blade Profile for a Set of Blade Elements

The final LWS blade airfoil is obtained by combining all the optimum sections of the ten blade airfoils discussed in section 4.2 along their respective radial locations to produce the 3D model of the LWS Blade airfoil in Figure 4.82.

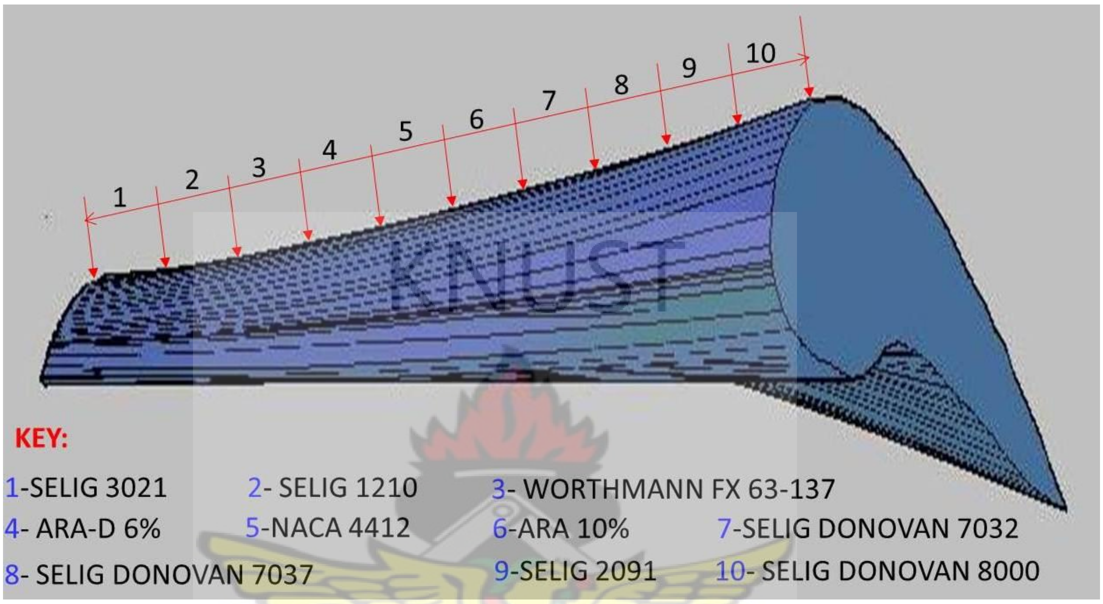

Figure 4.82: 3-D Model of the LWS Blade Profile

4.4 Designed LWS Blade Profile Results versus Existing Profiles

The results of the designed **LWS** blade profile is compared with all the existing ten profiles discussed earlier. It would be seen that most of the designed parameters in this blade profile is comparatively better than the existing profiles. Several plotted graphs are used to attest to the fact that the LWS blade profile is the best alternative when operating in an area of at least 3m/s wind speed.

In Figure 4.83, it could be seen that the power coefficient is least for Selig 2091 and highest for the LWS blade profile. This is also true for the power output of the blade profile as there is a direct proportionality between the power coefficient and the power output of a blade profile. The highest power among the existing profiles is 31.04 W recorded by Selig Donovan 7032 whilst that of the designed LWS Blade profile is 48.23 W which the later is approximately 35.64% greater than Selig Donovan 7032.

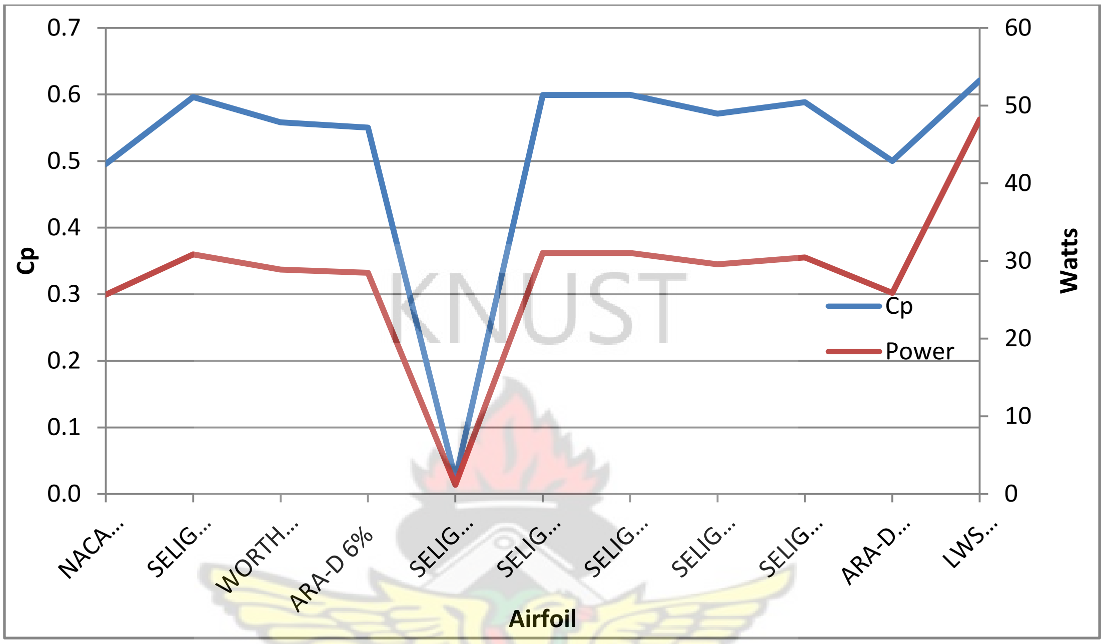

Figure 4.83: Comparison of Airfoils against Power Coefficient and Power

The ratio of the speed at which the tip of the blade would move relative to the undisturbed free wind speed upstream for the ten profiles varies from 7.3 to 8.0 as shown in Figure 4.84. The higher the tip speed ratio, the faster the rotation of the blade. From the aforementioned Figure, it showed that the LWS Blade profile recorded a tip speed ratio of 8.0 which is comparatively a better ratio that will enhance the rotation of the blade.

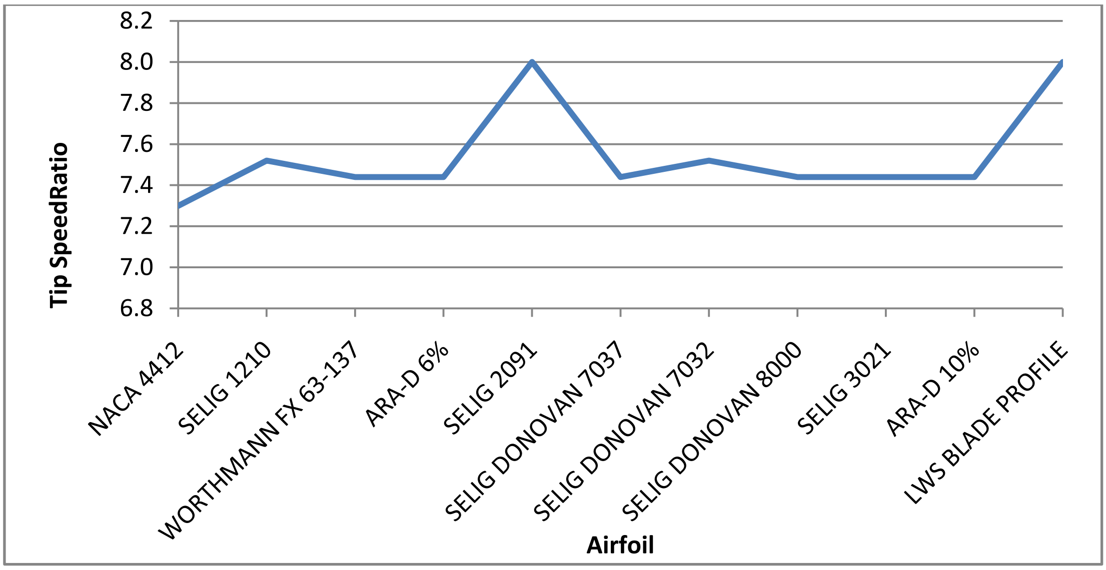

Figure 4.84: Airfoils versus Tip Speed Ratio

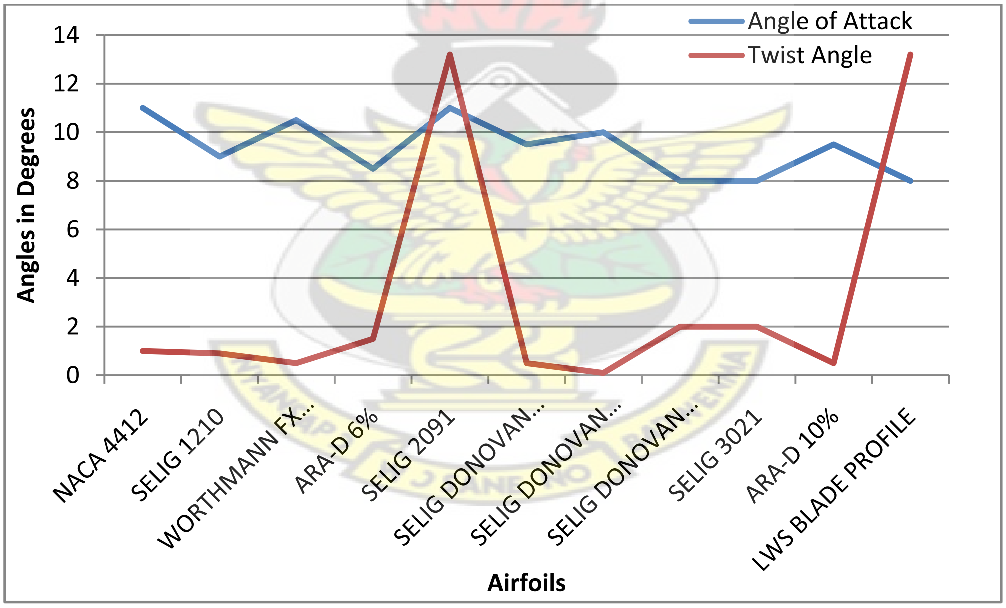

Figure 4.85: Angle of Attack and Twist Angle versus Airfoils

Also, the angle between respective chord line and their local relative airflow direction of all the profiles are plotted as shown in Figure 4.85. Comparing the angle of attack of the LWS blade profile to the ten profiles it is seen that the former recorded 8.0°. The parameters achieved by the LWS blade profile is better compared to the rest of the ten profiles as it helps to prevent the blade from stalling during its operation.

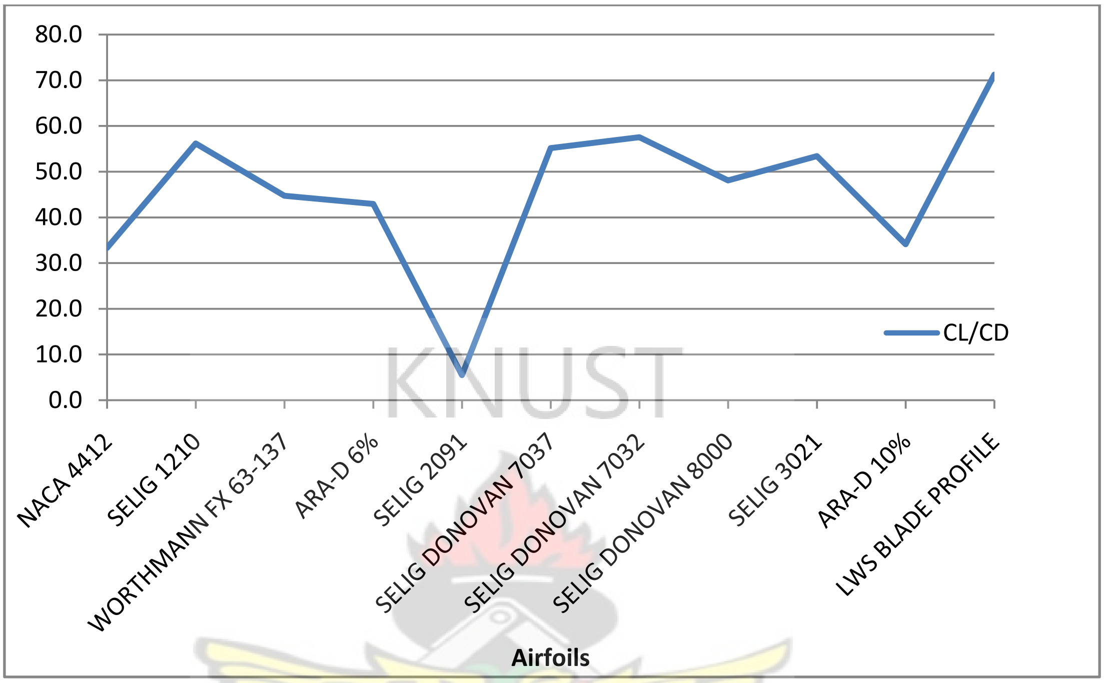

Figure 4.86: Aerodynamic Coefficient against Airfoils

From Figure 4.86 the drag coefficient is very much less than the lift coefficient making the lift to drag ratio C_L/C_D better than 50. The LWS blade profile gives a better ratio compared to all the ten profiles.

Both Figure 4.87 and Figure 4.88 give detailed information as to how the chord and thrust distributions faired along the blade where its maximum power coefficient was recorded. In both cases the LWS blade profile was maximum, recording 0.9 m which attest to the fact that the LWS blade profile has been optimized and can give maximum circulation at low wind speed.

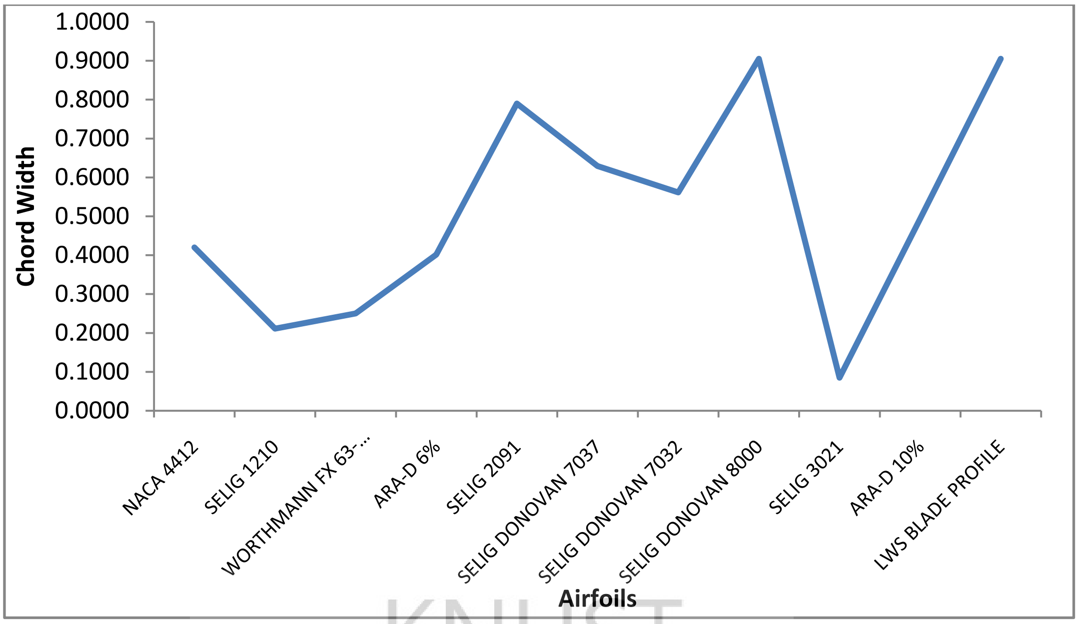

Figure 4.87: Chord Width against Airfoils

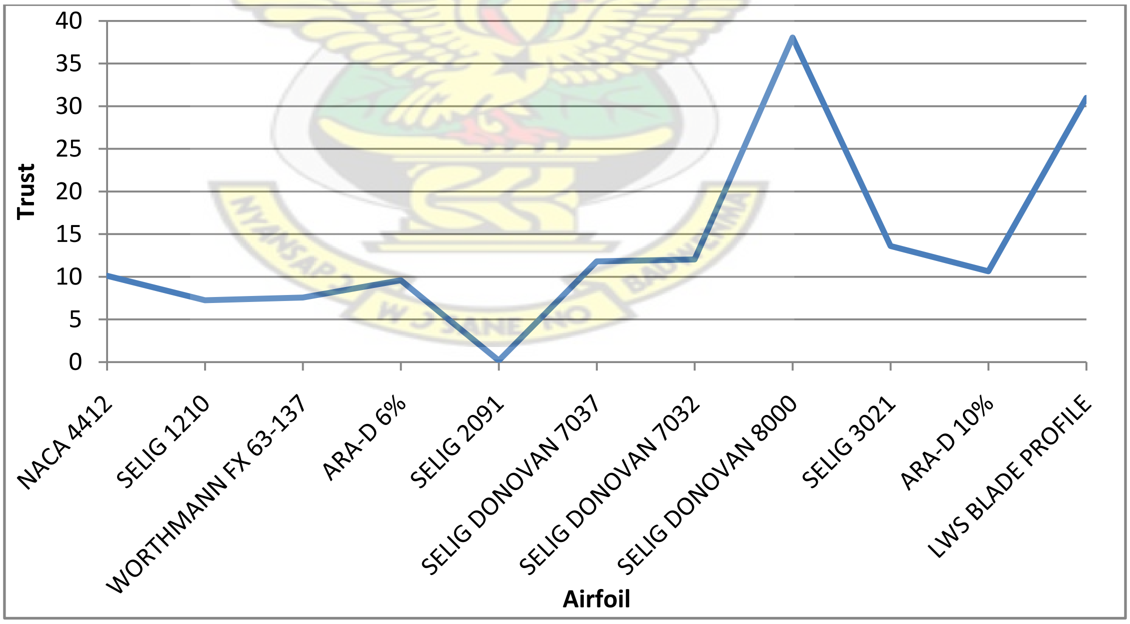

Figure 4.88: Airfoil against the Thrust along various Airfoils

4.5 Validations of Low Wind Speed Blade Profile Results

The power of the modified LWS blade profile is validated with the standard Power/Wind speed data of the Evans R9000 wind turbine performance to verify that the power obtained for the designed LWS blade profile is in conformity with the international standard data of wind turbine companies. The R9000 turbine whose data performance will be used as a real data for validation is specifically designed to capture more energy at lower wind speeds which makes it one of the most efficient turbines available. The LWS blade profile is capable of producing an approximate power output of 50 W (Figure 4.89) at 3 m/s at 12 m above sea level. This power positively correlates with an interpolated power output of nearly 50 W at 3 m/s and 50 m above sea level from the Power versus Wind Speed curve of the Evans R9000 wind turbine chart (Figure 4.90).

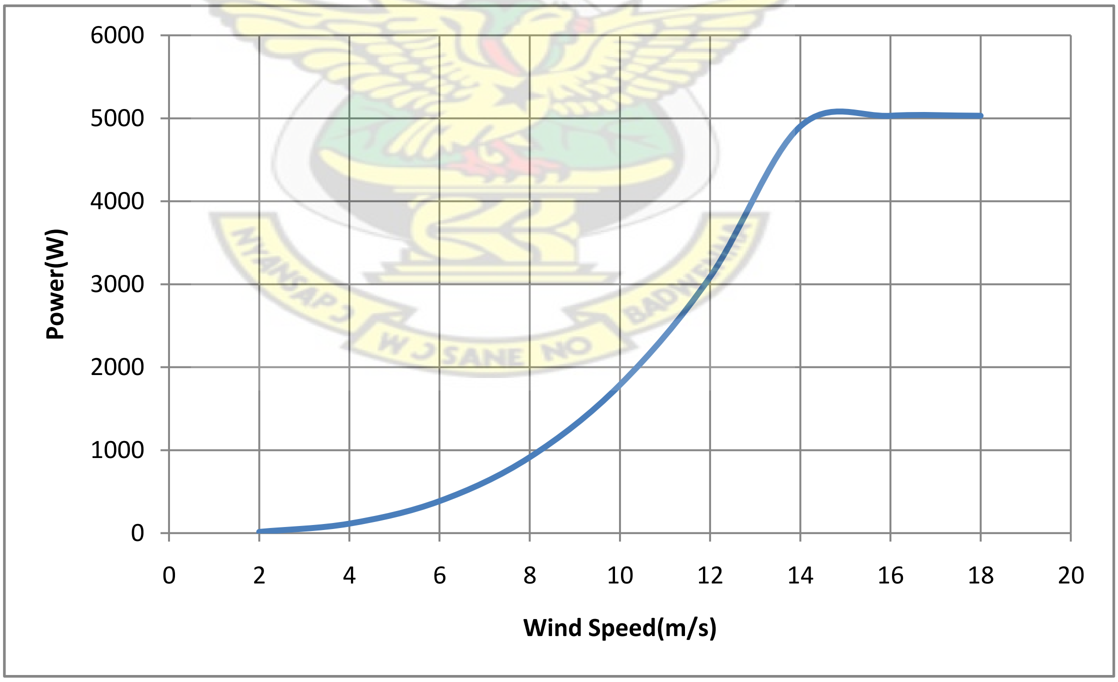

Figure 4.89: Power versus Wind Speed at 12 m above sea level for LWS blade Profile

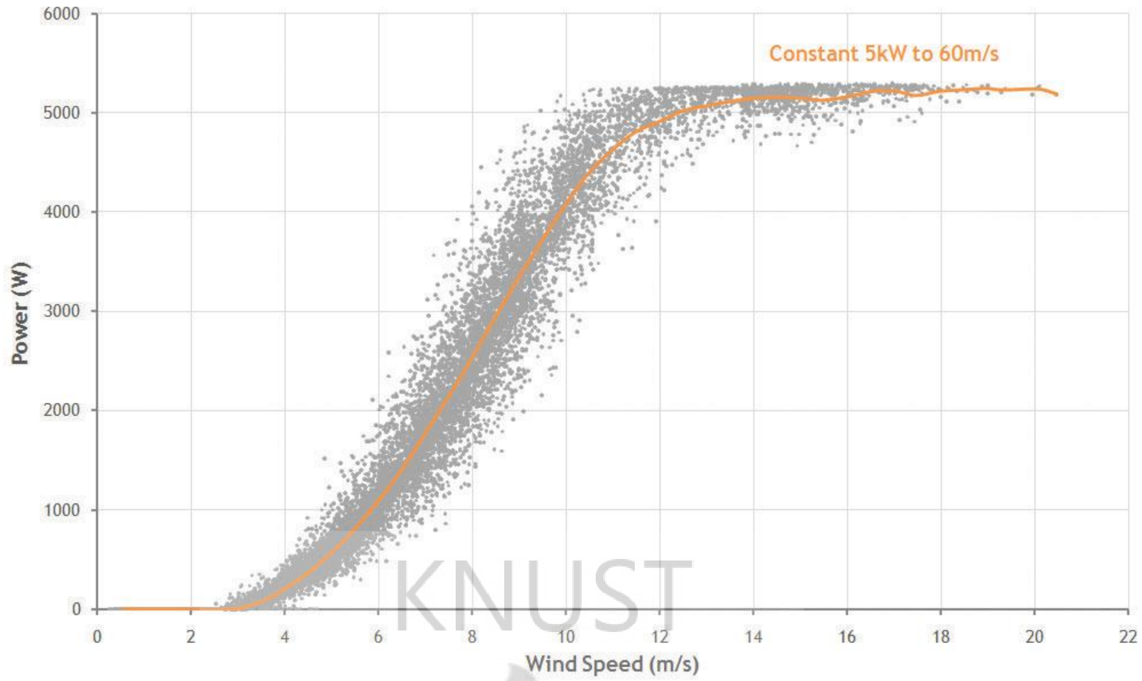

Figure 4.90: Standard Power generated against Variable Wind Speed at 50 m above sea level

It is also evident that, the designed LWS blade profile is in consonance with the existing blade profile power outputs from recognized wind turbine companies. A critical comparison would also reveal that since the LWS blade profile was designed to operate at an altitude of 12 m above sea level, it is expected that a higher power output would be achieved when its operation altitude is increased from 12 m to 50 m above sea level. This is because at high altitude there is high wind circulation which tends to increase the power output of the blade.

CHAPTER FIVE

Conclusions and Recommendations

5.1 Conclusion

A new profile or airfoil capable of producing a high lift at low wind speed has been designed. The profile could deliver a power of approximately 50 W which is about 35.64% greater than the best profile (Selig Donovan 7032) within the existing profiles in terms of power output.

The blade momentum theory was used to critically inspect and analyze all the ten profiles. It revealed that Selig Donovan 7032 is the best profile that could be used to produce electricity at areas of low wind speed. However, the redesigned LWS Blade Profile is more efficient than the Selig Donovan 7032 as it produces extra power of 35.64% more than later. Several graphs were plotted using blade profile parameters to access the performances of the blades. The graphs of Power Coefficient versus Relative wind angle gave a maximum C_p of 0.6 for Selig Donovan 7032 at 5.2^o.

It is found that a standard wind speed of 3 m/s corresponds to 50 W while the redesigned profile gave closely the same power of 48.23 W at 3 m/s. This power is about almost the same as that of the existing standard power for the Evance R9000 blade profile. Comparatively, there is very good correlation between the power output of the redesigned LWS Blade profile and the existing standard profile.

In addition, when the proposed power obtained from the LWS blade profile was validated with the international wind turbine data it yielded good correlation. It is found that, the power for the LWS blade profile is quiet higher than that which existed. The power obtained for the LWS blade profile confirms that it is an improvement upon the existing profiles.

The optimized designed LWS blade profile is professed to be the best profile that could generate an effective, sustainable and high lift and power at average wind speed of at least 3m/s when the necessary structural and electrical components are incorporated. Finally, Club Cycom, a computer software combined with iterative procedures using the BEM has been used to optimized a wind turbine airfoil for low wind speed applications.

5.2 Recommendations

The following recommendations are necessary for future researchers:

1. Future researchers could concentrate on the construction and testing of the proposed LWS blade design. The constructed wind turbine must be expanded and take into accounts the structural and electrical components to ensure a feasible power generation.

2. Moreover, a more challenging but efficient computer program could be written for the two flow charts in this work to ensure flexible and dynamic way of designing new turbine blades at low wind speeds for construction and testing.

3. Future extensions of this thesis could study how the materials properties such as mass distribution would be used in constructing the LWS blades.

References

1. Humpback whales inspire new wind turbine technology (2010) http://www.stle.org/assets/news/document/TechBeat_TLT_1208.pdf (Accessed 2010, August 10).
2. Katzenberger E. F. and Rich M. J. (1956), An investigation of helicopter descent and landing characteristics following power failure. *Journal of Aeron Sci*, 23(4):345–356.
3. Energy Report - Wind Energy, Chapter 11 (2008) http://www.window.state.tx.us/specialrpt/energy/renewable/wind.php (Accessed 2010, April 4).
4. National Aeronuatics and Space Administration (1998), *Scientific and Aerospace Technical Report Volume 36*, Langley Research Center.
5. The Republic of Uganda Ministry of Energy and Mineral Development (2010)http://energyandminerals.go.ug/downloads/EnergyPolicy.pdf (Accessed 2010, May 17).
6. Wind Turbine Blade Design (2010), - MDPI.com http://www.mdpi.com/1996-1073/5/9/3425/pdf (Accessed 2010, August 15)
7. Wind Turbine Design (2010), Wikipedia, http://en.wikipedia.org/wiki/Wind_turbine_design (Accessed 2010, August 6)
8. Mickaël Edon, (2009), 38 Meter Wind Turbine Blade Design Internship Report, http://ns7.freeheberg.com/~mach085/38_meter_wind_turbine_blade_design.pdf (Accessed 2010, August 4)
9. Wind Turbine Aerodynamics (2008), http://www.turbinesinfo.com/wind-turbine-aerodynamics/(Accessed 2010, June 16)

10. Tu Tan and Liang Tao (2008), Saimaa University of Applied Sciences, Lappeenranta Technology, Research and Utilization of Windmill.

11. Solar and Wind Energy Resource Assessment (2005), National Renewable Energy Report.

12. Houghton, E. L.; Carpenter, P.W. (2003), *Aerodynamics for Engineering Students* (5th ed.) Butterworth Heinmann. ed.

13. Manwell, J., McGowan, J., and Rogers, A. (2002), *Wind Energy Explained. Theory, Design and Application.* John Wiley and Sons, Ltd.

14. Hansen, A. and Butterfield, C. (1993), Aerodynamics of horizontal-axis wind turbines. *Annual Review of Fluid Mechanics*.

15. Walker, J. and Jenkins, N. (1997), *Wind Energy Technology*. JohnWiley and Sons, Ltd.

16. "Wind turbine aerodynamics: A state-of-the-art" (2007), from Karman Institute if Fluid Dynamics. Lecture Series.

17. *Det Norske Veritas*. DNV-OS-J101 (2009), Design of Offshore Wind Turbine Structures

18. Emme, Svend (2011), New type of wind turbine tower *Metal Industry,*

19. Bir G. and Migliore P. from NREL (2010), "Preliminary Structural Design of Composite Blades for two and three blade rotors".

20. Johnson, Scott J.; van Dam, C.P. and Berg, Dale E. (2008), "Active Load Control Techniques for Wind Turbines". Sandia National Laboratory.

21. Jamieson, Peter. Innovation in Wind Turbine Design (2011), p155, *John Wiley & Sons*.

22. Det Norske Veritas (2001), *Guidelines for Design of Wind Turbines*. Copenhagen: Det Norske Veritas

APPENDIX I

Sample Iteration Results for a Blade Profile

Profile/Airfoil	N	Cp	Opt-β	Optimum Relative Wind Angle					Elemental Power				
				Opt-β1	Opt-β2	Opt-β3	Opt-β4	Opt-β5	CP1	CP2	CP3	CP4	CP5
SELIG DONOVAN 7037	1st	0.0001	0.3596	0.3491	0.3517	0.3543	0.3569	0.3596	0.0001	0.0001	0.0001	0.0001	0.0000
	2nd	0.0005	0.3491	0.3305	0.3349	0.3395	0.3442	0.3491	0.0005	0.0004	0.0003	0.0002	0.0001
	3rd	0.0011	0.3395	0.3145	0.3202	0.3262	0.3327	0.3395	0.0011	0.0009	0.0007	0.0005	0.0003
	4th	0.0019	0.3305	0.3009	0.3074	0.3145	0.3222	0.3305	0.0019	0.0015	0.0011	0.0008	0.0005
	5th	0.0029	0.3222	0.2893	0.2963	0.3041	0.3127	0.3222	0.0029	0.0023	0.0017	0.0012	0.0008
	6th	0.0040	0.3145	0.2794	0.2866	0.2948	0.3041	0.3145	0.0040	0.0032	0.0024	0.0017	0.0011
	7th	0.0053	0.3074	0.2710	0.2782	0.2866	0.2963	0.3074	0.0053	0.0042	0.0032	0.0023	0.0015
	8th	0.0068	0.3009	0.2638	0.2710	0.2794	0.2893	0.3009	0.0068	0.0053	0.0040	0.0029	0.0019
	9th	0.0083	0.2948	0.2576	0.2646	0.2729	0.2829	0.2948	0.0083	0.0066	0.0050	0.0036	0.0024
	10th	0.0101	0.2893	0.2523	0.2591	0.2672	0.2771	0.2893	0.0101	0.0079	0.0060	0.0043	0.0029
	11th	0.0120	0.2841	0.2477	0.2542	0.2621	0.2719	0.2841	0.0120	0.0094	0.0071	0.0051	0.0034
	12th	0.0140	0.2794	0.2438	0.2500	0.2576	0.2672	0.2794	0.0140	0.0110	0.0083	0.0060	0.0040
	13th	0.0162	0.2750	0.2403	0.2462	0.2536	0.2630	0.2750	0.0162	0.0127	0.0096	0.0069	0.0046
	14th	0.0186	0.2710	0.2372	0.2429	0.2500	0.2591	0.2710	0.0186	0.0146	0.0110	0.0079	0.0053
	15th	0.0211	0.2672	0.2345	0.2399	0.2467	0.2555	0.2672	0.0211	0.0165	0.0125	0.0090	0.0060
	16th	0.0238	0.2638	0.2321	0.2372	0.2438	0.2523	0.2638	0.0238	0.0186	0.0140	0.0101	0.0068
	17th	0.0266	0.2606	0.2299	0.2348	0.2411	0.2494	0.2606	0.0266	0.0208	0.0157	0.0113	0.0075
	18th	0.0295	0.2576	0.2280	0.2327	0.2387	0.2467	0.2576	0.0295	0.0231	0.0174	0.0125	0.0083
	19th	0.0327	0.2549	0.2262	0.2307	0.2365	0.2442	0.2549	0.0327	0.0255	0.0192	0.0138	0.0092
	20th	0.0359	0.2523	0.2245	0.2289	0.2345	0.2420	0.2523	0.0359	0.0280	0.0211	0.0151	0.0101
	21st	0.0393	0.2500	0.2230	0.2273	0.2327	0.2399	0.2500	0.0393	0.0307	0.0231	0.0165	0.0110
	22nd	0.0429	0.2477	0.2217	0.2258	0.2310	0.2380	0.2477	0.0429	0.0335	0.0252	0.0180	0.0120
	23rd	0.0466	0.2457	0.2204	0.2244	0.2294	0.2362	0.2457	0.0466	0.0363	0.0273	0.0195	0.0130
	24th	0.0505	0.2438	0.2192	0.2230	0.2280	0.2345	0.2438	0.0505	0.0393	0.0295	0.0211	0.0140
	25th	0.0545	0.2420	0.2180	0.2218	0.2266	0.2330	0.2420	0.0545	0.0425	0.0319	0.0228	0.0151
	26th	0.0587	0.2403	0.2170	0.2207	0.2253	0.2315	0.2403	0.0587	0.0457	0.0343	0.0245	0.0162
	27th	0.0630	0.2387	0.2160	0.2196	0.2242	0.2302	0.2387	0.0630	0.0490	0.0368	0.0262	0.0174
	28th	0.0674	0.2372	0.2150	0.2186	0.2230	0.2289	0.2372	0.0674	0.0525	0.0393	0.0280	0.0186
	29th	0.0720	0.2358	0.2141	0.2176	0.2220	0.2277	0.2358	0.0720	0.0561	0.0420	0.0299	0.0198
	30th	0.0768	0.2345	0.2132	0.2167	0.2210	0.2266	0.2345	0.0768	0.0597	0.0448	0.0319	0.0211
	31st	0.0816	0.2333	0.2124	0.2159	0.2201	0.2255	0.2333	0.0816	0.0635	0.0476	0.0339	0.0224
	32nd	0.0867	0.2321	0.2116	0.2150	0.2192	0.2245	0.2321	0.0867	0.0674	0.0505	0.0359	0.0238
	33rd	0.0918	0.2310	0.2108	0.2142	0.2183	0.2236	0.2310	0.0918	0.0714	0.0535	0.0380	0.0252
	34th	0.0971	0.2299	0.2100	0.2134	0.2175	0.2227	0.2299	0.0971	0.0756	0.0566	0.0402	0.0266
	35th	0.1026	0.2289	0.2093	0.2127	0.2167	0.2218	0.2289	0.1026	0.0798	0.0597	0.0425	0.0280
	36th	0.1081	0.2280	0.2086	0.2120	0.2160	0.2210	0.2280	0.1081	0.0841	0.0630	0.0448	0.0295
	37th	0.1138	0.2270	0.2079	0.2113	0.2153	0.2202	0.2270	0.1138	0.0886	0.0663	0.0471	0.0311
	38th	0.1197	0.2262	0.2072	0.2106	0.2146	0.2195	0.2262	0.1197	0.0931	0.0697	0.0495	0.0327
	39th	0.1257	0.2253	0.2065	0.2099	0.2139	0.2187	0.2253	0.1257	0.0978	0.0732	0.0520	0.0343
	40th	0.1318	0.2245	0.2059	0.2093	0.2132	0.2180	0.2245	0.1318	0.1026	0.0768	0.0545	0.0359
	41st	0.1380	0.2238	0.2052	0.2087	0.2126	0.2174	0.2238	0.1380	0.1074	0.0804	0.0571	0.0376
	42nd	0.1444	0.2230	0.2046	0.2081	0.2120	0.2167	0.2230	0.1444	0.1124	0.0841	0.0597	0.0393
	43rd	0.1509	0.2223	0.2040	0.2075	0.2114	0.2161	0.2223	0.1509	0.1175	0.0879	0.0624	0.0411
	44th	0.1575	0.2217	0.2034	0.2069	0.2108	0.2155	0.2217	0.1575	0.1226	0.0918	0.0652	0.0429
	45th	0.1642	0.2210	0.2028	0.2063	0.2102	0.2149	0.2210	0.1642	0.1279	0.0958	0.0680	0.0448
	46th	0.1711	0.2204	0.2022	0.2057	0.2097	0.2143	0.2204	0.1711	0.1333	0.0998	0.0709	0.0466
	47th	0.1781	0.2198	0.2016	0.2052	0.2091	0.2138	0.2198	0.1781	0.1388	0.1039	0.0738	0.0485
	48th	0.1852	0.2192	0.2010	0.2046	0.2086	0.2132	0.2192	0.1852	0.1444	0.1081	0.0768	0.0505
	49th	0.1925	0.2186	0.2004	0.2041	0.2081	0.2127	0.2186	0.1925	0.1500	0.1124	0.0798	0.0525
	50th	0.1998	0.2180	0.1998	0.2035	0.2075	0.2122	0.2180	0.1998	0.1558	0.1167	0.0829	0.0545

N	Elemental Chord Length Distribution						α	γ	Twist Angles						Elemental Relative Wind Angles				
	CMAX	C1	C2	C3	C4	C5			1	2	3	4	5	β	β1	β2	β3	β4	β5
1st	0.4295	0.4295	0.3240	0.2327	0.1560	0.0941	9.5	49.0	47.45	47.83	48.21	48.59	48.97	58.47	56.95	57.33	57.71	58.09	58.47
2nd	0.7904	0.7904	0.6009	0.4350	0.2937	0.1785	9.5	47.5	44.44	45.19	45.94	46.69	47.45	56.95	53.94	54.69	55.44	56.19	56.95
3rd	1.0893	1.0893	0.8347	0.6089	0.4143	0.2536	9.5	45.9	41.50	42.59	43.70	44.81	45.94	55.44	51.00	52.09	53.20	54.31	55.44
4th	1.3328	1.3328	1.0294	0.7568	0.5190	0.3201	9.5	44.4	38.67	40.07	41.50	42.96	44.44	53.94	48.17	49.57	51.00	52.46	53.94
5th	1.5276	1.5276	1.1890	0.8810	0.6088	0.3784	9.5	43.0	35.97	37.64	39.37	41.14	42.96	52.46	45.47	47.14	48.87	50.64	52.46
6th	1.6799	1.6799	1.3174	0.9837	0.6850	0.4290	9.5	41.5	33.41	35.31	37.30	39.37	41.50	51.00	42.91	44.81	46.80	48.87	51.00
7th	1.7956	1.7956	1.4183	1.0669	0.7487	0.4724	9.5	40.1	31.00	33.10	35.31	37.64	40.07	49.57	40.50	42.60	44.81	47.14	49.57
8th	1.8801	1.8801	1.4952	1.1329	0.8010	0.5092	9.5	38.7	28.75	31.00	33.41	35.97	38.67	48.17	38.25	40.50	42.91	45.47	48.17
9th	1.9381	1.9381	1.5513	1.1835	0.8429	0.5398	9.5	37.3	26.66	29.03	31.59	34.35	37.30	46.80	36.16	38.53	41.09	43.85	46.80
10th	1.9740	1.9740	1.5894	1.2206	0.8754	0.5648	9.5	36.0	24.73	27.17	29.86	32.79	35.97	45.47	34.23	36.67	39.36	42.29	45.47
11th	1.9913	1.9913	1.6123	1.2458	0.8995	0.5845	9.5	34.7	22.93	25.44	28.22	31.29	34.67	44.17	32.43	34.94	37.72	40.79	44.17
12th	1.9932	1.9932	1.6221	1.2607	0.9161	0.5994	9.5	33.4	21.28	23.81	26.66	29.86	33.41	42.91	30.78	33.31	36.16	39.36	42.91
13th	1.9825	1.9825	1.6209	1.2666	0.9260	0.6099	9.5	32.2	19.75	22.30	25.20	28.48	32.18	41.68	29.25	31.80	34.70	37.98	41.68
14th	1.9614	1.9614	1.6105	1.2647	0.9301	0.6165	9.5	31.0	18.34	20.89	23.81	27.17	31.00	40.50	27.84	30.39	33.31	36.67	40.50
15th	1.9317	1.9317	1.5923	1.2562	0.9289	0.6196	9.5	29.9	17.04	19.57	22.51	25.92	29.86	39.36	26.54	29.07	32.01	35.42	39.36
16th	1.8950	1.8950	1.5676	1.2421	0.9231	0.6194	9.5	28.8	15.83	18.34	21.28	24.73	28.75	38.25	25.33	27.84	30.78	34.23	38.25
17th	1.8528	1.8528	1.5376	1.2231	0.9134	0.6163	9.5	27.7	14.72	17.19	20.12	23.59	27.69	37.19	24.22	26.69	29.62	33.09	37.19
18th	1.8060	1.8060	1.5032	1.2001	0.9003	0.6107	9.5	26.7	13.69	16.12	19.03	22.51	26.66	36.16	23.19	25.62	28.53	32.01	36.16
19th	1.7556	1.7556	1.4651	1.1737	0.8841	0.6028	9.5	25.7	12.73	15.13	18.00	21.48	25.68	35.18	22.23	24.63	27.50	30.98	35.18
20th	1.7025	1.7025	1.4242	1.1444	0.8654	0.5929	9.5	24.7	11.84	14.19	17.04	20.50	24.73	34.23	21.34	23.69	26.54	30.00	34.23
21st	1.6472	1.6472	1.3810	1.1128	0.8446	0.5812	9.5	23.8	11.01	13.32	16.12	19.57	23.81	33.31	20.51	22.82	25.62	29.07	33.31
22nd	1.5903	1.5903	1.3359	1.0793	0.8219	0.5680	9.5	22.9	10.24	12.50	15.26	18.68	22.93	32.43	19.74	22.00	24.76	28.18	32.43
23rd	1.5323	1.5323	1.2895	1.0443	0.7977	0.5534	9.5	22.1	9.52	11.73	14.45	17.84	22.09	31.59	19.02	21.23	23.95	27.34	31.59
24th	1.4736	1.4736	1.2422	1.0081	0.7723	0.5378	9.5	21.3	8.84	11.01	13.69	17.04	21.28	30.78	18.34	20.51	23.19	26.54	30.78
25th	1.4145	1.4145	1.1941	0.9710	0.7458	0.5211	9.5	20.5	8.21	10.33	12.96	16.27	20.50	30.00	17.71	19.83	22.46	25.77	30.00
26th	1.3552	1.3552	1.1456	0.9333	0.7186	0.5037	9.5	19.8	7.62	9.69	12.27	15.55	19.75	29.25	17.12	19.19	21.77	25.05	29.25
27th	1.2961	1.2961	1.0970	0.8952	0.6908	0.4857	9.5	19.0	7.06	9.09	11.62	14.85	19.03	28.53	16.56	18.59	21.12	24.35	28.53
28th	1.2374	1.2374	1.0485	0.8568	0.6626	0.4671	9.5	18.3	6.54	8.52	11.01	14.19	18.34	27.84	16.04	18.02	20.51	23.69	27.84
29th	1.1792	1.1792	1.0001	0.8185	0.6341	0.4481	9.5	17.7	6.05	7.98	10.42	13.56	17.68	27.18	15.55	17.48	19.92	23.06	27.18
30th	1.1216	1.1216	0.9522	0.7802	0.6055	0.4288	9.5	17.0	5.58	7.48	9.87	12.96	17.04	26.54	15.08	16.98	19.37	22.46	26.54
31st	1.0648	1.0648	0.9047	0.7422	0.5768	0.4094	9.5	16.4	5.14	6.99	9.34	12.39	16.42	25.92	14.64	16.49	18.84	21.89	25.92
32nd	1.0090	1.0090	0.8579	0.7045	0.5483	0.3898	9.5	15.8	4.72	6.54	8.84	11.84	15.83	25.33	14.22	16.04	18.34	21.34	25.33
33rd	0.9542	0.9542	0.8119	0.6673	0.5200	0.3703	9.5	15.3	4.33	6.11	8.36	11.31	15.26	24.76	13.83	15.61	17.86	20.81	24.76
34th	0.9005	0.9005	0.7667	0.6306	0.4919	0.3508	9.5	14.7	3.96	5.69	7.91	10.81	14.72	24.22	13.46	15.19	17.41	20.31	24.22
35th	0.8481	0.8481	0.7224	0.5946	0.4643	0.3315	9.5	14.2	3.60	5.30	7.48	10.33	14.19	23.69	13.10	14.80	16.98	19.83	23.69
36th	0.7968	0.7968	0.6790	0.5592	0.4370	0.3123	9.5	13.7	3.27	4.93	7.06	9.87	13.69	23.19	12.77	14.43	16.56	19.37	23.19
37th	0.7469	0.7469	0.6367	0.5247	0.4103	0.2935	9.5	13.2	2.94	4.57	6.67	9.43	13.20	22.70	12.44	14.07	16.17	18.93	22.70
38th	0.6984	0.6984	0.5955	0.4909	0.3841	0.2749	9.5	12.7	2.64	4.24	6.29	9.01	12.73	22.23	12.14	13.74	15.79	18.51	22.23
39th	0.6513	0.6513	0.5555	0.4581	0.3586	0.2567	9.5	12.3	2.35	3.91	5.93	8.60	12.27	21.77	11.85	13.41	15.43	18.10	21.77
40th	0.6056	0.6056	0.5167	0.4262	0.3337	0.2389	9.5	11.8	2.07	3.60	5.58	8.21	11.84	21.34	11.57	13.10	15.08	17.71	21.34
41st	0.5615	0.5615	0.4791	0.3952	0.3094	0.2215	9.5	11.4	1.80	3.31	5.25	7.84	11.42	20.92	11.30	12.81	14.75	17.34	20.92
42nd	0.5188	0.5188	0.4427	0.3652	0.2860	0.2046	9.5	11.0	1.55	3.02	4.93	7.48	11.01	20.51	11.05	12.52	14.43	16.98	20.51
43rd	0.4777	0.4777	0.4077	0.3363	0.2633	0.1882	9.5	10.6	1.31	2.75	4.62	7.13	10.62	20.12	10.81	12.25	14.12	16.63	20.12
44th	0.4383	0.4383	0.3739	0.3084	0.2414	0.1724	9.5	10.2	1.07	2.49	4.33	6.80	10.24	19.74	10.57	11.99	13.83	16.30	19.74
45th	0.4004	0.4004	0.3416	0.2817	0.2203	0.1571	9.5	9.9	0.85	2.24	4.05	6.47	9.87	19.37	10.35	11.74	13.55	15.97	19.37
46th	0.3641	0.3641	0.3106	0.2560	0.2001	0.1425	9.5	9.5	0.63	2.00	3.78	6.17	9.52	19.02	10.13	11.50	13.28	15.67	19.02
47th	0.3295	0.3295	0.2810	0.2315	0.1807	0.1284	9.5	9.2	0.43	1.77	3.52	5.87	9.17	18.67	9.93	11.27	13.02	15.37	18.67
48th	0.2965	0.2965	0.2528	0.2081	0.1623	0.1150	9.5	8.8	0.23	1.55	3.27	5.58	8.84	18.34	9.73	11.05	12.77	15.08	18.34
49th	0.2653	0.2653	0.2260	0.1859	0.1448	0.1023	9.5	8.5	0.04	1.34	3.02	5.30	8.52	18.02	9.54	10.84	12.52	14.80	18.02
50th	0.2357	0.2357	0.2007	0.1649	0.1282	0.0903	9.5	8.2	-0.14	1.13	2.79	5.03	8.21	17.71	9.36	10.63	12.29	14.53	17.71

N	rMax	Tip Speed/Local Tip Speed Ratio										Tip Loss Correction Factor					Ω1	Ω2	Ω3	Ω4	Ω5	V	B	B/2	R	r	r/R	c/R	CD/CL			Trust	Torque
		r1	r2	r3	r4	r5	1	2	3	4	5	Q1	Q2	Q3	Q4	Q5													C_D	C_L	C_D/C_L		
1st	0.08	0.080	0.07	0.06	0.05	0.04	8.00	7.00	6.00	5.00	4.00	1.00	1.00	1.00	1.00	1.00	24.00	21.00	18.00	15.00	12.00	3.00	3.00	1.50	1.00	0.01	0.01	0.43	0.02	1.27	0.02	0.0454	0.0008
2nd	0.16	0.160	0.14	0.12	0.10	0.08	8.00	7.00	6.00	5.00	4.00	1.00	1.00	1.00	1.00	1.00	24.00	21.00	18.00	15.00	12.00	3.00	3.00	1.50	1.00	0.02	0.02	0.79	0.02	1.27	0.02	0.1747	0.0027
3rd	0.24	0.240	0.21	0.18	0.15	0.12	8.00	7.00	6.00	5.00	4.00	1.00	1.00	1.00	1.00	1.00	24.00	21.00	18.00	15.00	12.00	3.00	3.00	1.50	1.00	0.03	0.03	1.09	0.02	1.27	0.02	0.3765	0.0056
4th	0.32	0.320	0.28	0.24	0.20	0.16	8.00	7.00	6.00	5.00	4.00	1.00	1.00	1.00	1.00	1.00	24.00	21.00	18.00	15.00	12.00	3.00	3.00	1.50	1.00	0.04	0.04	1.33	0.02	1.27	0.02	0.6387	0.0089
5th	0.40	0.400	0.35	0.30	0.25	0.20	8.00	7.00	6.00	5.00	4.00	1.00	1.00	1.00	1.00	1.00	24.00	21.00	18.00	15.00	12.00	3.00	3.00	1.50	1.00	0.05	0.05	1.53	0.02	1.27	0.02	0.9490	0.0125
6th	0.48	0.480	0.42	0.36	0.30	0.24	8.00	7.00	6.00	5.00	4.00	1.00	1.00	1.00	1.00	1.00	24.00	21.00	18.00	15.00	12.00	3.00	3.00	1.50	1.00	0.06	0.06	1.68	0.02	1.27	0.02	1.2956	0.0162
7th	0.56	0.560	0.49	0.42	0.35	0.28	8.00	7.00	6.00	5.00	4.00	1.00	1.00	1.00	1.00	1.00	24.00	21.00	18.00	15.00	12.00	3.00	3.00	1.50	1.00	0.07	0.07	1.80	0.02	1.27	0.02	1.6677	0.0197
8th	0.64	0.640	0.56	0.48	0.40	0.32	8.00	7.00	6.00	5.00	4.00	1.00	1.00	1.00	1.00	1.00	24.00	21.00	18.00	15.00	12.00	3.00	3.00	1.50	1.00	0.08	0.08	1.88	0.02	1.27	0.02	2.0552	0.0231
9th	0.72	0.720	0.63	0.54	0.45	0.36	8.00	7.00	6.00	5.00	4.00	1.00	1.00	1.00	1.00	1.00	24.00	21.00	18.00	15.00	12.00	3.00	3.00	1.50	1.00	0.09	0.09	1.94	0.02	1.27	0.02	2.4498	0.0262
10th	0.80	0.800	0.70	0.60	0.50	0.40	8.00	7.00	6.00	5.00	4.00	1.00	1.00	1.00	1.00	1.00	24.00	21.00	18.00	15.00	12.00	3.00	3.00	1.50	1.00	0.10	0.10	1.97	0.02	1.27	0.02	2.8439	0.0289
11th	0.88	0.880	0.77	0.66	0.55	0.44	8.00	7.00	6.00	5.00	4.00	1.00	1.00	1.00	1.00	1.00	24.00	21.00	18.00	15.00	12.00	3.00	3.00	1.50	1.00	0.11	0.11	1.99	0.02	1.27	0.02	3.2313	0.0314
12th	0.96	0.960	0.84	0.72	0.60	0.48	8.00	7.00	6.00	5.00	4.00	1.00	1.00	1.00	1.00	1.00	24.00	21.00	18.00	15.00	12.00	3.00	3.00	1.50	1.00	0.12	0.12	1.99	0.02	1.27	0.02	3.6069	0.0334
13th	1.04	1.040	0.91	0.78	0.65	0.52	8.00	7.00	6.00	5.00	4.00	1.00	1.00	1.00	1.00	1.00	24.00	21.00	18.00	15.00	12.00	3.00	3.00	1.50	1.00	0.13	0.13	1.98	0.02	1.27	0.02	3.9665	0.0351
14th	1.12	1.120	0.98	0.84	0.70	0.56	8.00	7.00	6.00	5.00	4.00	1.00	1.00	1.00	1.00	1.00	24.00	21.00	18.00	15.00	12.00	3.00	3.00	1.50	1.00	0.14	0.14	1.96	0.02	1.27	0.02	4.3067	0.0365
15th	1.20	1.200	1.05	0.90	0.75	0.60	8.00	7.00	6.00	5.00	4.00	1.00	1.00	1.00	1.00	1.00	24.00	21.00	18.00	15.00	12.00	3.00	3.00	1.50	1.00	0.15	0.15	1.93	0.02	1.27	0.02	4.6248	0.0376
16th	1.28	1.280	1.12	0.96	0.80	0.64	8.00	7.00	6.00	5.00	4.00	1.00	1.00	1.00	1.00	1.00	24.00	21.00	18.00	15.00	12.00	3.00	3.00	1.50	1.00	0.16	0.16	1.90	0.02	1.27	0.02	4.9189	0.0383
17th	1.36	1.360	1.19	1.02	0.85	0.68	8.00	7.00	6.00	5.00	4.00	1.00	1.00	1.00	1.00	1.00	24.00	21.00	18.00	15.00	12.00	3.00	3.00	1.50	1.00	0.17	0.17	1.85	0.02	1.27	0.02	5.1874	0.0388
18th	1.44	1.440	1.26	1.08	0.90	0.72	8.00	7.00	6.00	5.00	4.00	1.00	1.00	1.00	1.00	1.00	24.00	21.00	18.00	15.00	12.00	3.00	3.00	1.50	1.00	0.18	0.18	1.81	0.02	1.27	0.02	5.4292	0.0391
19th	1.52	1.520	1.33	1.14	0.95	0.76	8.00	7.00	6.00	5.00	4.00	1.00	1.00	1.00	1.00	1.00	24.00	21.00	18.00	15.00	12.00	3.00	3.00	1.50	1.00	0.19	0.19	1.76	0.02	1.27	0.02	5.6438	0.0391
20th	1.60	1.600	1.40	1.20	1.00	0.80	8.00	7.00	6.00	5.00	4.00	1.00	1.00	1.00	1.00	1.00	24.00	21.00	18.00	15.00	12.00	3.00	3.00	1.50	1.00	0.20	0.20	1.70	0.02	1.27	0.02	5.8308	0.0389
21st	1.68	1.680	1.47	1.26	1.05	0.84	8.00	7.00	6.00	5.00	4.00	1.00	1.00	1.00	1.00	1.00	24.00	21.00	18.00	15.00	12.00	3.00	3.00	1.50	1.00	0.21	0.21	1.65	0.02	1.27	0.02	5.9902	0.0386
22nd	1.76	1.760	1.54	1.32	1.10	0.88	8.00	7.00	6.00	5.00	4.00	1.00	1.00	1.00	1.00	1.00	24.00	21.00	18.00	15.00	12.00	3.00	3.00	1.50	1.00	0.22	0.22	1.59	0.02	1.27	0.02	6.1220	0.0380
23rd	1.84	1.840	1.61	1.38	1.15	0.92	8.00	7.00	6.00	5.00	4.00	1.00	1.00	1.00	1.00	1.00	24.00	21.00	18.00	15.00	12.00	3.00	3.00	1.50	1.00	0.23	0.23	1.53	0.02	1.27	0.02	6.2267	0.0374
24th	1.92	1.920	1.68	1.44	1.20	0.96	8.00	7.00	6.00	5.00	4.00	1.00	1.00	1.00	1.00	1.00	24.00	21.00	18.00	15.00	12.00	3.00	3.00	1.50	1.00	0.24	0.24	1.47	0.02	1.27	0.02	6.3048	0.0366
25th	2.00	2.000	1.75	1.50	1.25	1.00	8.00	7.00	6.00	5.00	4.00	1.00	1.00	1.00	1.00	1.00	24.00	21.00	18.00	15.00	12.00	3.00	3.00	1.50	1.00	0.25	0.25	1.41	0.02	1.27	0.02	6.3569	0.0357
26th	2.08	2.080	1.82	1.56	1.30	1.04	8.00	7.00	6.00	5.00	4.00	1.00	1.00	1.00	1.00	1.00	24.00	21.00	18.00	15.00	12.00	3.00	3.00	1.50	1.00	0.26	0.26	1.36	0.02	1.27	0.02	6.3839	0.0347
27th	2.16	2.160	1.89	1.62	1.35	1.08	8.00	7.00	6.00	5.00	4.00	1.00	1.00	1.00	1.00	1.00	24.00	21.00	18.00	15.00	12.00	3.00	3.00	1.50	1.00	0.27	0.27	1.30	0.02	1.27	0.02	6.3865	0.0336
28th	2.24	2.240	1.96	1.68	1.40	1.12	8.00	7.00	6.00	5.00	4.00	1.00	1.00	1.00	1.00	1.00	24.00	21.00	18.00	15.00	12.00	3.00	3.00	1.50	1.00	0.28	0.28	1.24	0.02	1.27	0.02	6.3658	0.0325
29th	2.32	2.320	2.03	1.74	1.45	1.16	8.00	7.00	6.00	5.00	4.00	1.00	1.00	1.00	1.00	1.00	24.00	21.00	18.00	15.00	12.00	3.00	3.00	1.50	1.00	0.29	0.29	1.18	0.02	1.27	0.02	6.3227	0.0313
30th	2.40	2.400	2.10	1.80	1.50	1.20	8.00	7.00	6.00	5.00	4.00	1.00	1.00	1.00	1.00	1.00	24.00	21.00	18.00	15.00	12.00	3.00	3.00	1.50	1.00	0.30	0.30	1.12	0.02	1.27	0.02	6.2584	0.0301
31st	2.48	2.480	2.17	1.86	1.55	1.24	8.00	7.00	6.00	5.00	4.00	1.00	1.00	1.00	1.00	1.00	24.00	21.00	18.00	15.00	12.00	3.00	3.00	1.50	1.00	0.31	0.31	1.06	0.02	1.27	0.02	6.1739	0.0289
32nd	2.56	2.560	2.24	1.92	1.60	1.28	8.00	7.00	6.00	5.00	4.00	1.00	1.00	1.00	1.00	1.00	24.00	21.00	18.00	15.00	12.00	3.00	3.00	1.50	1.00	0.32	0.32	1.01	0.02	1.27	0.02	6.0703	0.0276
33rd	2.64	2.640	2.31	1.98	1.65	1.32	8.00	7.00	6.00	5.00	4.00	1.00	1.00	1.00	1.00	1.00	24.00	21.00	18.00	15.00	12.00	3.00	3.00	1.50	1.00	0.33	0.33	0.95	0.02	1.27	0.02	5.9488	0.0263
34th	2.72	2.720	2.38	2.04	1.70	1.36	8.00	7.00	6.00	5.00	4.00	1.00	1.00	1.00	1.00	1.00	24.00	21.00	18.00	15.00	12.00	3.00	3.00	1.50	1.00	0.34	0.34	0.90	0.02	1.27	0.02	5.8107	0.0250
35th	2.80	2.800	2.45	2.10	1.75	1.40	8.00	7.00	6.00	5.00	4.00	1.00	1.00	1.00	1.00	1.00	24.00	21.00	18.00	15.00	12.00	3.00	3.00	1.50	1.00	0.35	0.35	0.85	0.02	1.27	0.02	5.6571	0.0237
36th	2.88	2.880	2.52	2.16	1.80	1.44	8.00	7.00	6.00	5.00	4.00	1.00	1.00	1.00	1.00	1.00	24.00	21.00	18.00	15.00	12.00	3.00	3.00	1.50	1.00	0.36	0.36	0.80	0.02	1.27	0.02	5.4893	0.0224
37th	2.96	2.960	2.59	2.22	1.85	1.48	8.00	7.00	6.00	5.00	4.00	1.00	1.00	1.00	1.00	1.00	24.00	21.00	18.00	15.00	12.00	3.00	3.00	1.50	1.00	0.37	0.37	0.75	0.02	1.27	0.02	5.3084	0.0212
38th	3.04	3.040	2.66	2.28	1.90	1.52	8.00	7.00	6.00	5.00	4.00	1.00	1.00	1.00	1.00	1.00	24.00	21.00	18.00	15.00	12.00	3.00	3.00	1.50	1.00	0.38	0.38	0.70	0.02	1.27	0.02	5.1157	0.0199
39th	3.12	3.120	2.73	2.34	1.95	1.56	8.00	7.00	6.00	5.00	4.00	1.00	1.00	1.00	1.00	1.00	24.00	21.00	18.00	15.00	12.00	3.00	3.00	1.50	1.00	0.39	0.39	0.65	0.02	1.27	0.02	4.9126	0.0186
40th	3.20	3.200	2.80	2.40	2.00	1.60	8.00	7.00	6.00	5.00	4.00	1.00	1.00	1.00	1.00	1.00	24.00	21.00	18.00	15.00	12.00	3.00	3.00	1.50	1.00	0.40	0.40	0.61	0.02	1.27	0.02	4.7001	0.0174
41st	3.28	3.280	2.87	2.46	2.05	1.64	8.00	7.00	6.00	5.00	4.00	1.00	1.00	1.00	1.00	1.00	24.00	21.00	18.00	15.00	12.00	3.00	3.00	1.50	1.00	0.41	0.41	0.56	0.02	1.27	0.02	4.4796	0.0162
42nd	3.36	3.360	2.94	2.52	2.10	1.68	8.00	7.00	6.00	5.00	4.00	1.00	1.00	1.00	1.00	1.00	24.00	21.00	18.00	15.00	12.00	3.00	3.00	1.50	1.00	0.42	0.42	0.52	0.02	1.27	0.02	4.2524	0.0150
43rd	3.44	3.440	3.01	2.58	2.15	1.72	8.00	7.00	6.00	5.00	4.00	1.00	1.00	1.00	1.00	1.00	24.00	21.00	18.00	15.00	12.00	3.00	3.00	1.50	1.00	0.43	0.43	0.48	0.02	1.27	0.02	4.0196	0.0139
44th	3.52	3.520	3.08	2.64	2.20	1.76	8.00	7.00	6.00	5.00	4.00	1.00	1.00	1.00	1.00	1.00	24.00	21.00	18.00	15.00	12.00	3.00	3.00	1.50	1.00	0.44	0.44	0.44	0.02	1.27	0.02	3.7826	0.0128
45th	3.60	3.600	3.15	2.70	2.25	1.80	8.00	7.00	6.00	5.00	4.00	1.00	1.00	1.00	1.00	1.00	24.00	21.00	18.00	15.00	12.00	3.00	3.00	1.50	1.00	0.45	0.45	0.40	0.02	1.27	0.02	3.5426	0.0117
46th	3.68	3.680	3.22	2.76	2.30	1.84	8.00	7.00	6.00	5.00	4.00	1.00	1.00	1.00	1.00	1.00	24.00	21.00	18.00	15.00	12.00	3.00	3.00	1.50	1.00	0.46	0.46	0.36	0.02	1.27	0.02	3.3008	0.0107
47th	3.76	3.760	3.29	2.82	2.35	1.88	8.00	7.00	6.00	5.00	4.00	1.00	1.00	1.00	1.00	1.00	24.00	21.00	18.00	15.00	12.00	3.00	3.00	1.50	1.00	0.47	0.47	0.33	0.02	1.27	0.02	3.0585	0.0097
48th	3.84	3.840	3.36	2.88	2.40	1.92	8.00	7.00	6.00	5.00	4.00	1.00	1.00	1.00	1.00	1.00	24.00	21.00	18.00	15.00	12.00	3.00	3.00	1.50	1.00	0.48	0.48	0.30	0.02	1.27	0.02	2.8169	0.0087
49th	3.92	3.920	3.43	2.94	2.45	1.96	8.00	7.00	6.00	5.00	4.00	1.00	1.00	1.00	1.00	1.00	24.00	21.00	18.00	15.00	12.00	3.00	3.00	1.50	1.00	0.49	0.49	0.27	0.02	1.27	0.02	2.5774	0.0078
50th	4.00	4.000	3.50	3.00	2.50	2.00	8.00	7.00	6.00	5.00	4.00	1.00	1.00	1.00	1.00	1.00	24.00	21.00	18.00	15.00	12.00	3.00	3.00	1.50	1.00	0.50	0.50	0.24	0.02	1.27	0.02	2.3410	0.0070

Profile/Airfoil	N	Cp	Opt-β	Opt-β1	Opt-β2	Opt-β3	Opt-β4	Opt-β5	C_{P1}	C_{P2}	C_{P3}	C_{P4}	C_{P5}	C_{MAX}	C_1	C_2	C_3	C_4	C_5			1	2	3	4	5	β	β1	β2	β3	β4	β5	rMax	r1	r2	r3	r4	r5	1	2	3	4	5	Q1	Q2	Q3	Q4	Q5	Ω1	Ω2	Ω3	Ω4	Ω5	V	B	B/2	R	r	r/R	c/R	C_D	C_L	C_D/C_L	Trust	Torque
				Optimum Relative Wind Angle					Elemental Power					Elemental Chord Length Distribution								Twist Angles						Elemental Relative Wind Angles						Tip Speed/Local Tip Speed Ratio										Tip Loss Correction Factor																	CD/CL				
SELIG DONOVAN 7037	51st	0.2073	0.2175	0.1993	0.2030	0.2070	0.2117	0.2175	0.2073	0.1617	0.1212	0.0860	0.0566	0.2078	0.2078	0.1768	0.1451	0.1126	0.0789	9.5	7.9	-0.32	0.93	2.56	4.78	7.91	17.41	9.18	10.43	12.06	14.28	17.41	4.08	4.080	3.57	3.06	2.55	2.04	8.00	7.00	6.00	5.00	4.00	1.00	1.00	1.00	1.00	1.00	24.00	21.00	18.00	15.00	12.00	3.00	3.00	1.50	1.00	0.51	0.51	0.21	0.02	1.27	0.02	2.1091	0.0062
	52nd	0.2149	0.2170	0.1987	0.2025	0.2065	0.2112	0.2170	0.2149	0.1677	0.1257	0.0892	0.0587	0.1817	0.1817	0.1544	0.1266	0.0979	0.0682	9.5	7.6	-0.49	0.74	2.35	4.53	7.62	17.12	9.01	10.24	11.85	14.03	17.12	4.16	4.160	3.64	3.12	2.60	2.08	8.00	7.00	6.00	5.00	4.00	1.00	1.00	1.00	1.00	1.00	24.00	21.00	18.00	15.00	12.00	3.00	3.00	1.50	1.00	0.52	0.52	0.18	0.02	1.27	0.02	1.8829	0.0054
	53rd	0.2227	0.2165	0.1982	0.2019	0.2060	0.2107	0.2165	0.2227	0.1737	0.1302	0.0925	0.0608	0.1572	0.1572	0.1335	0.1092	0.0842	0.0583	9.5	7.3	-0.65	0.56	2.14	4.28	7.34	16.84	8.85	10.06	11.64	13.78	16.84	4.24	4.240	3.71	3.18	2.65	2.12	8.00	7.00	6.00	5.00	4.00	1.00	1.00	1.00	1.00	1.00	24.00	21.00	18.00	15.00	12.00	3.00	3.00	1.50	1.00	0.53	0.53	0.16	0.02	1.27	0.02	1.6637	0.0047
	54th	0.2305	0.2160	0.1976	0.2014	0.2056	0.2102	0.2160	0.2305	0.1799	0.1349	0.0958	0.0630	0.1345	0.1345	0.1141	0.0931	0.0715	0.0492	9.5	7.1	-0.81	0.38	1.93	4.05	7.06	16.56	8.69	9.88	11.43	13.55	16.56	4.32	4.320	3.78	3.24	2.70	2.16	8.00	7.00	6.00	5.00	4.00	1.00	1.00	1.00	1.00	1.00	24.00	21.00	18.00	15.00	12.00	3.00	3.00	1.50	1.00	0.54	0.54	0.13	0.02	1.27	0.02	1.4526	0.0040
	55th	0.2384	0.2155	0.1971	0.2009	0.2051	0.2098	0.2155	0.2384	0.1861	0.1396	0.0991	0.0652	0.1136	0.1136	0.0961	0.0783	0.0598	0.0407	9.5	6.8	-0.96	0.21	1.74	3.82	6.80	16.30	8.54	9.71	11.24	13.32	16.30	4.40	4.400	3.85	3.30	2.75	2.20	8.00	7.00	6.00	5.00	4.00	1.00	1.00	1.00	1.00	1.00	24.00	21.00	18.00	15.00	12.00	3.00	3.00	1.50	1.00	0.55	0.55	0.11	0.02	1.27	0.02	1.2509	0.0034
	56th	0.2465	0.2150	0.1965	0.2004	0.2046	0.2093	0.2150	0.2465	0.1925	0.1444	0.1026	0.0674	0.0944	0.0944	0.0797	0.0647	0.0492	0.0331	9.5	6.5	-1.11	0.04	1.55	3.60	6.54	16.04	8.39	9.54	11.05	13.10	16.04	4.48	4.480	3.92	3.36	2.80	2.24	8.00	7.00	6.00	5.00	4.00	1.00	1.00	1.00	1.00	1.00	24.00	21.00	18.00	15.00	12.00	3.00	3.00	1.50	1.00	0.56	0.56	0.09	0.02	1.27	0.02	1.0598	0.0028
	57th	0.2547	0.2145	0.1960	0.1999	0.2041	0.2088	0.2145	0.2547	0.1989	0.1492	0.1060	0.0697	0.0770	0.0770	0.0648	0.0524	0.0395	0.0262	9.5	6.3	-1.25	-0.12	1.37	3.39	6.29	15.79	8.25	9.38	10.87	12.89	15.79	4.56	4.560	3.99	3.42	2.85	2.28	8.00	7.00	6.00	5.00	4.00	1.00	1.00	1.00	1.00	1.00	24.00	21.00	18.00	15.00	12.00	3.00	3.00	1.50	1.00	0.57	0.57	0.08	0.02	1.27	0.02	0.8806	0.0023
	58th	0.2630	0.2141	0.1954	0.1994	0.2037	0.2084	0.2141	0.2630	0.2054	0.1542	0.1095	0.0720	0.0613	0.0613	0.0515	0.0414	0.0309	0.0201	9.5	6.0	-1.39	-0.28	1.19	3.18	6.05	15.55	8.11	9.22	10.69	12.68	15.55	4.64	4.640	4.06	3.48	2.90	2.32	8.00	7.00	6.00	5.00	4.00	1.00	1.00	1.00	1.00	1.00	24.00	21.00	18.00	15.00	12.00	3.00	3.00	1.50	1.00	0.58	0.58	0.06	0.02	1.27	0.02	0.7144	0.0018
	59th	0.2714	0.2136	0.1949	0.1989	0.2032	0.2080	0.2136	0.2714	0.2121	0.1592	0.1131	0.0744	0.0474	0.0474	0.0396	0.0316	0.0233	0.0148	9.5	5.8	-1.53	-0.43	1.02	2.98	5.81	15.31	7.97	9.07	10.52	12.48	15.31	4.72	4.720	4.13	3.54	2.95	2.36	8.00	7.00	6.00	5.00	4.00	1.00	1.00	1.00	1.00	1.00	24.00	21.00	18.00	15.00	12.00	3.00	3.00	1.50	1.00	0.59	0.59	0.05	0.02	1.27	0.02	0.5625	0.0014
	60th	0.2799	0.2132	0.1944	0.1984	0.2028	0.2075	0.2132	0.2799	0.2188	0.1642	0.1167	0.0768	0.0353	0.0353	0.0293	0.0232	0.0168	0.0103	9.5	5.6	-1.65	-0.57	0.85	2.79	5.58	15.08	7.85	8.93	10.35	12.29	15.08	4.80	4.800	4.20	3.60	3.00	2.40	8.00	7.00	6.00	5.00	4.00	1.00	1.00	1.00	1.00	1.00	24.00	21.00	18.00	15.00	12.00	3.00	3.00	1.50	1.00	0.60	0.60	0.04	0.02	1.27	0.02	0.4261	0.0011
	61st	0.2885	0.2128	0.1938	0.1980	0.2023	0.2071	0.2128	0.2885	0.2256	0.1694	0.1204	0.0792	0.0249	0.0249	0.0205	0.0160	0.0114	0.0066	9.5	5.4	-1.78	-0.71	0.69	2.60	5.36	14.86	7.72	8.79	10.19	12.10	14.86	4.88	4.880	4.27	3.66	3.05	2.44	8.00	7.00	6.00	5.00	4.00	1.00	1.00	1.00	1.00	1.00	24.00	21.00	18.00	15.00	12.00	3.00	3.00	1.50	1.00	0.61	0.61	0.02	0.02	1.27	0.02	0.3064	0.0007
	62nd	0.2972	0.2124	0.1933	0.1975	0.2019	0.2067	0.2124	0.2972	0.2325	0.1746	0.1241	0.0816	0.0163	0.0163	0.0133	0.0102	0.0070	0.0037	9.5	5.1	-1.90	-0.85	0.53	2.42	5.14	14.64	7.60	8.65	10.03	11.92	14.64	4.96	4.960	4.34	3.72	3.10	2.48	8.00	7.00	6.00	5.00	4.00	1.00	1.00	1.00	1.00	1.00	24.00	21.00	18.00	15.00	12.00	3.00	3.00	1.50	1.00	0.62	0.62	0.02	0.02	1.27	0.02	0.2046	0.0005
	63rd	0.3061	0.2119	0.1928	0.1970	0.2014	0.2063	0.2119	0.3061	0.2394	0.1799	0.1279	0.0841	0.0096	0.0096	0.0077	0.0057	0.0036	0.0016	9.5	4.9	-2.02	-0.98	0.38	2.24	4.93	14.43	7.48	8.52	9.88	11.74	14.43	5.04	5.040	4.41	3.78	3.15	2.52	8.00	7.00	6.00	5.00	4.00	1.00	1.00	1.00	1.00	1.00	24.00	21.00	18.00	15.00	12.00	3.00	3.00	1.50	1.00	0.63	0.63	0.01	0.02	1.27	0.02	0.1220	0.0003
	64th	0.3150	0.2115	0.1923	0.1965	0.2010	0.2059	0.2115	0.3150	0.2465	0.1852	0.1318	0.0866	0.0046	0.0046	0.0035	0.0025	0.0014	0.0004	9.5	4.7	-2.13	-1.11	0.23	2.07	4.72	14.22	7.37	8.39	9.73	11.57	14.22	5.12	5.120	4.48	3.84	3.20	2.56	8.00	7.00	6.00	5.00	4.00	1.00	1.00	1.00	1.00	1.00	24.00	21.00	18.00	15.00	12.00	3.00	3.00	1.50	1.00	0.64	0.64	0.00	0.02	1.27	0.02	0.0597	0.0001
	65th	0.3240	0.2111	0.1917	0.1960	0.2006	0.2055	0.2111	0.3240	0.2537	0.1907	0.1356	0.0892	0.0014	0.0014	0.0010	0.0006	0.0002	0.0000	9.5	4.5	-2.24	-1.24	0.09	1.90	4.53	14.03	7.26	8.26	9.59	11.40	14.03	5.20	5.200	4.55	3.90	3.25	2.60	8.00	7.00	6.00	5.00	4.00	1.00	1.00	1.00	1.00	1.00	24.00	21.00	18.00	15.00	12.00	3.00	3.00	1.50	1.00	0.65	0.65	0.00	0.02	1.27	0.02	0.0189	0.0000
	66th	0.3332	0.2107	0.1912	0.1956	0.2001	0.2051	0.2107	0.3332	0.2609	0.1961	0.1396	0.0918	0.0004	0.0001	0.0000	0.0000	0.0001	0.0004	9.5	4.3	-2.35	-1.36	-0.05	1.74	4.33	13.83	7.15	8.14	9.45	11.24	13.83	5.28	5.280	4.62	3.96	3.30	2.64	8.00	7.00	6.00	5.00	4.00	1.00	1.00	1.00	1.00	1.00	24.00	21.00	18.00	15.00	12.00	3.00	3.00	1.50	1.00	0.66	0.66	0.00	0.02	1.27	0.02	0.0060	0.0000
	67th	0.3424	0.2103	0.1907	0.1951	0.1997	0.2047	0.2103	0.3424	0.2682	0.2017	0.1436	0.0944	0.0017	0.0005	0.0006	0.0008	0.0011	0.0017	9.5	4.1	-2.45	-1.48	-0.19	1.58	4.14	13.64	7.05	8.02	9.31	11.08	13.64	5.36	5.360	4.69	4.02	3.35	2.68	8.00	7.00	6.00	5.00	4.00	1.00	1.00	1.00	1.00	1.00	24.00	21.00	18.00	15.00	12.00	3.00	3.00	1.50	1.00	0.67	0.67	0.00	0.02	1.27	0.02	0.0236	0.0001
	68th	0.3517	0.2099	0.1902	0.1946	0.1993	0.2043	0.2099	0.3517	0.2756	0.2073	0.1476	0.0971	0.0039	0.0027	0.0027	0.0029	0.0032	0.0039	9.5	4.0	-2.56	-1.59	-0.32	1.43	3.96	13.46	6.94	7.91	9.18	10.93	13.46	5.44	5.440	4.76	4.08	3.40	2.72	8.00	7.00	6.00	5.00	4.00	1.00	1.00	1.00	1.00	1.00	24.00	21.00	18.00	15.00	12.00	3.00	3.00	1.50	1.00	0.68	0.68	0.00	0.02	1.27	0.02	0.0535	0.0001
	69th	0.3612	0.2095	0.1897	0.1942	0.1989	0.2039	0.2095	0.3612	0.2831	0.2130	0.1517	0.0997	0.0069	0.0068	0.0065	0.0063	0.0063	0.0069	9.5	3.8	-2.65	-1.70	-0.45	1.28	3.78	13.28	6.85	7.80	9.05	10.78	13.28	5.52	5.520	4.83	4.14	3.45	2.76	8.00	7.00	6.00	5.00	4.00	1.00	1.00	1.00	1.00	1.00	24.00	21.00	18.00	15.00	12.00	3.00	3.00	1.50	1.00	0.69	0.69	0.01	0.02	1.27	0.02	0.0962	0.0002
	70th	0.3707	0.2091	0.1891	0.1937	0.1984	0.2035	0.2091	0.3707	0.2907	0.2188	0.1558	0.1025	0.0126	0.0126	0.0118	0.0111	0.0106	0.0107	9.5	3.6	-2.75	-1.81	-0.57	1.13	3.60	13.10	6.75	7.69	8.93	10.63	13.10	5.60	5.600	4.90	4.20	3.50	2.80	8.00	7.00	6.00	5.00	4.00	1.00	1.00	1.00	1.00	1.00	24.00	21.00	18.00	15.00	12.00	3.00	3.00	1.50	1.00	0.70	0.70	0.01	0.02	1.27	0.02	0.1800	0.0004
	71st	0.3804	0.2087	0.1886	0.1932	0.1980	0.2031	0.2087	0.3804	0.2983	0.2246	0.1600	0.1052	0.0203	0.0203	0.0187	0.0172	0.0160	0.0154	9.5	3.4	-2.84	-1.92	-0.69	0.99	3.43	12.93	6.66	7.58	8.81	10.49	12.93	5.68	5.680	4.97	4.26	3.55	2.84	8.00	7.00	6.00	5.00	4.00	1.00	1.00	1.00	1.00	1.00	24.00	21.00	18.00	15.00	12.00	3.00	3.00	1.50	1.00	0.71	0.71	0.02	0.02	1.27	0.02	0.2936	0.0006
	72nd	0.3901	0.2083	0.1881	0.1928	0.1976	0.2027	0.2083	0.3901	0.3060	0.2305	0.1642	0.1080	0.0298	0.0298	0.0271	0.0246	0.0225	0.0210	9.5	3.3	-2.93	-2.02	-0.81	0.85	3.27	12.77	6.57	7.48	8.69	10.35	12.77	5.76	5.760	5.04	4.32	3.60	2.88	8.00	7.00	6.00	5.00	4.00	1.00	1.00	1.00	1.00	1.00	24.00	21.00	18.00	15.00	12.00	3.00	3.00	1.50	1.00	0.72	0.72	0.03	0.02	1.27	0.02	0.4371	0.0009
	73rd	0.3999	0.2078	0.1876	0.1923	0.1972	0.2023	0.2078	0.3999	0.3139	0.2364	0.1684	0.1108	0.0411	0.0411	0.0372	0.0334	0.0301	0.0274	9.5	3.1	-3.02	-2.12	-0.93	0.71	3.10	12.60	6.48	7.38	8.57	10.21	12.60	5.84	5.840	5.11	4.38	3.65	2.92	8.00	7.00	6.00	5.00	4.00	1.00	1.00	1.00	1.00	1.00	24.00	21.00	18.00	15.00	12.00	3.00	3.00	1.50	1.00	0.73	0.73	0.04	0.02	1.27	0.02	0.6118	0.0012
	74th	0.4098	0.2074	0.1871	0.1919	0.1968	0.2019	0.2074	0.4098	0.3217	0.2424	0.1727	0.1136	0.0543	0.0543	0.0488	0.0436	0.0388	0.0347	9.5	2.9	-3.11	-2.22	-1.04	0.58	2.94	12.44	6.39	7.28	8.46	10.08	12.44	5.92	5.920	5.18	4.44	3.70	2.96	8.00	7.00	6.00	5.00	4.00	1.00	1.00	1.00	1.00	1.00	24.00	21.00	18.00	15.00	12.00	3.00	3.00	1.50	1.00	0.74	0.74	0.05	0.02	1.27	0.02	0.8187	0.0016
	75th	0.4198	0.2069	0.1866	0.1914	0.1963	0.2015	0.2069	0.4198	0.3297	0.2485	0.1771	0.1164	0.0692	0.0692	0.0620	0.0551	0.0486	0.0429	9.5	2.8	-3.19	-2.31	-1.15	0.45	2.79	12.29	6.31	7.19	8.35	9.95	12.29	6.00	6.000	5.25	4.50	3.75	3.00	8.00	7.00	6.00	5.00	4.00	1.00	1.00	1.00	1.00	1.00	24.00	21.00	18.00	15.00	12.00	3.00	3.00	1.50	1.00	0.75	0.75	0.07	0.02	1.27	0.02	1.0591	0.0021
	76th	0.4299	0.2065	0.1861	0.1909	0.1959	0.2011	0.2065	0.4299	0.3377	0.2546	0.1815	0.1193	0.0860	0.0860	0.0768	0.0680	0.0595	0.0519	9.5	2.6	-3.27	-2.40	-1.25	0.33	2.64	12.14	6.23	7.10	8.25	9.83	12.14	6.08	6.080	5.32	4.56	3.80	3.04	8.00	7.00	6.00	5.00	4.00	1.00	1.00	1.00	1.00	1.00	24.00	21.00	18.00	15.00	12.00	3.00	3.00	1.50	1.00	0.76	0.76	0.09	0.02	1.27	0.02	1.3342	0.0026
	77th	0.4401	0.2059	0.1856	0.1905	0.1955	0.2006	0.2059	0.4401	0.3459	0.2608	0.1859	0.1221	0.1046	0.1046	0.0932	0.0822	0.0715	0.0617	9.5	2.5	-3.35	-2.49	-1.36	0.21	2.49	11.99	6.15	7.01	8.14	9.71	11.99	6.16	6.160	5.39	4.62	3.85	3.08	8.00	7.00	6.00	5.00	4.00	1.00	1.00	1.00	1.00	1.00	24.00	21.00	18.00	15.00	12.00	3.00	3.00	1.50	1.00	0.77	0.77	0.10	0.02	1.27	0.02	1.6451	0.0031
	78th	0.4504	0.2054	0.1851	0.1900	0.1950	0.2002	0.2054	0.4504	0.3540	0.2670	0.1903	0.1250	0.1250	0.1250	0.1112	0.0977	0.0847	0.0724	9.5	2.3	-3.43	-2.58	-1.46	0.09	2.35	11.85	6.07	6.92	8.04	9.59	11.85	6.24	6.240	5.46	4.68	3.90	3.12	8.00	7.00	6.00	5.00	4.00	1.00	1.00	1.00	1.00	0.99	24.00	21.00	18.00	15.00	12.00	3.00	3.00	1.50	1.00	0.78	0.78	0.13	0.02	1.27	0.02	1.9930	0.0037
	79th	0.4607	0.2048	0.1846	0.1895	0.1946	0.1997	0.2048	0.4607	0.3623	0.2733	0.1948	0.1278	0.1473	0.1473	0.1308	0.1146	0.0989	0.0840	9.5	2.2	-3.51	-2.67	-1.56	-0.03	2.21	11.71	5.99	6.83	7.94	9.47	11.71	6.32	6.320	5.53	4.74	3.95	3.16	8.00	7.00	6.00	5.00	4.00	1.00	1.00	1.00	1.00	0.99	24.00	21.00	18.00	15.00	12.00	3.00	3.00	1.50	1.00	0.79	0.79	0.15	0.02	1.27	0.02	2.3791	0.0044
	80th	0.4711	0.2041	0.1840	0.1891	0.1941	0.1992	0.2041	0.4711	0.3706	0.2796	0.1992	0.1306	0.1714	0.1714	0.1520	0.1328	0.1142	0.0963	9.5	2.1	-3.58	-2.75	-1.65	-0.14	2.07	11.57	5.92	6.75	7.85	9.36	11.57	6.40	6.400	5.60	4.80	4.00	3.20	8.00	7.00	6.00	5.00	4.00	1.00	1.00	1.00	1.00	0.99	24.00	21.00	18.00	15.00	12.00	3.00	3.00	1.50	1.00	0.80	0.80	0.17	0.02	1.27	0.02	2.8046	0.0051
	81st	0.4816	0.2034	0.1835	0.1886	0.1937	0.1987	0.2034	0.4816	0.3789	0.2859	0.2037	0.1334	0.1973	0.1973	0.1747	0.1524	0.1306	0.1095	9.5	1.9	-3.65	-2.83	-1.75	-0.25	1.93	11.43	5.85	6.67	7.75	9.25	11.43	6.48	6.480	5.67	4.86	4.05	3.24	8.00	7.00	6.00	5.00	4.00	1.00	1.00	1.00	1.00	0.99	24.00	21.00	18.00	15.00	12.00	3.00	3.00	1.50	1.00	0.81	0.81	0.20	0.02	1.27	0.02	3.2705	0.0059
	82nd	0.4922	0.2025	0.1830	0.1881	0.1932	0.1981	0.2025	0.4922	0.3873	0.2922	0.2081	0.1362	0.2250	0.2250	0.1990	0.1733	0.1480	0.1234	9.5	1.8	-3.72	-2.91	-1.84	-0.36	1.80	11.30	5.78	6.59	7.66	9.14	11.30	6.56	6.560	5.74	4.92	4.10	3.28	8.00	7.00	6.00	5.00	4.00	1.00	1.00	1.00	0.99	0.99	24.00	21.00	18.00	15.00	12.00	3.00	3.00	1.50	1.00	0.82	0.82	0.23	0.02	1.27	0.02	3.7780	0.0067
	83rd	0.5028	0.2015	0.1825	0.1876	0.1926	0.1974	0.2015	0.5028	0.3957	0.2985	0.2125	0.1388	0.2545	0.2545	0.2249	0.1955	0.1664	0.1380	9.5	1.7	-3.79	-2.99	-1.93	-0.47	1.68	11.18	5.71	6.51	7.57	9.03	11.18	6.64	6.640	5.81	4.98	4.15	3.32	8.00	7.00	6.00	5.00	4.00	1.00	1.00	1.00	0.99	0.98	24.00	21.00	18.00	15.00	12.00	3.00	3.00	1.50	1.00	0.83	0.83	0.25	0.02	1.27	0.02	4.3280	0.0076
	84th	0.5134	0.2004	0.1819	0.1870	0.1920	0.1966	0.2004	0.5134	0.4041	0.3048	0.2168	0.1414	0.2859	0.2859	0.2523	0.2189	0.1858	0.1533	9.5	1.5	-3.86	-3.07	-2.02	-0.57	1.55	11.05	5.64	6.43	7.48	8.93	11.05	6.72	6.720	5.88	5.04	4.20	3.36	8.00	7.00	6.00	5.00	4.00	1.00	1.00	1.00	0.99	0.98	24.00	21.00	18.00	15.00	12.00	3.00	3.00	1.50	1.00	0.84	0.84	0.29	0.02	1.27	0.02	4.9214	0.0085
	85th	0.5241	0.1991	0.1813	0.1864	0.1913	0.1957	0.1991	0.5241	0.4125	0.3110	0.2209	0.1438	0.3190	0.3190	0.2812	0.2436	0.2061	0.1691	9.5	1.4	-3.92	-3.14	-2.10	-0.67	1.43	10.93	5.58	6.36	7.40	8.83	10.93	6.80	6.800	5.95	5.10	4.25	3.40	8.00	7.00	6.00	5.00	4.00	1.00	1.00	0.99	0.99	0.97	24.00	21.00	18.00	15.00	12.00	3.00	3.00	1.50	1.00	0.85	0.85	0.32	0.02	1.27	0.02	5.5590	0.0095
	86th	0.5347	0.1975	0.1807	0.1858	0.1905	0.1946	0.1975	0.5347	0.4208	0.3170	0.2249	0.1461	0.3538	0.3538	0.3115	0.2693	0.2272	0.1854	9.5	1.3	-3.99	-3.21	-2.19	-0.77	1.31	10.81	5.51	6.29	7.31	8.73	10.81	6.88	6.880	6.02	5.16	4.30	3.44	8.00	7.00	6.00	5.00	4.00	1.00	1.00	0.99	0.98	0.97	24.00	21.00	18.00	15.00	12.00	3.00	3.00	1.50	1.00	0.86	0.86	0.35	0.02	1.27	0.02	6.2412	0.0105
	87th	0.5452	0.1956	0.1801	0.1850	0.1896	0.1934	0.1956	0.5452	0.4289	0.3229	0.2287	0.1481	0.3903	0.3903	0.3432	0.2961	0.2490	0.2021	9.5	1.2	-4.05	-3.28	-2.27	-0.87	1.19	10.69	5.45	6.22	7.23	8.63	10.69	6.96	6.960	6.09	5.22	4.35	3.48	8.00	7.00	6.00	5.00	4.00	1.00	0.99	0.99	0.98	0.96	24.00	21.00	18.00	15.00	12.00	3.00	3.00	1.50	1.00	0.87	0.87	0.39	0.02	1.27	0.02	6.9677	0.0116
	88th	0.5554	0.1934	0.1793	0.1841	0.1884	0.1918	0.1934	0.5554	0.4367	0.3283	0.2321	0.1498	0.4283	0.4283	0.3761	0.3237	0.2712	0.2189	9.5	1.1	-4.11	-3.35	-2.35	-0.96	1.07	10.57	5.39	6.15	7.15	8.54	10.57	7.04	7.040	6.16	5.28	4.40	3.52	8.00	7.00	6.00	5.00	4.00	1.00	0.99	0.99	0.97	0.95	24.00	21.00	18.00	15.00	12.00	3.00	3.00	1.50	1.00	0.88	0.88	0.43	0.02	1.27	0.02	7.7377	0.0127
	89th	0.5653	0.1907	0.1784	0.1830	0.1870	0.1899	0.1907	0.5653	0.4440	0.3333	0.2350	0.1511	0.4677	0.4677	0.4100	0.3519	0.2937	0.2356	9.5	1.0	-4.17	-3.42	-2.43	-1.06	0.96	10.46	5.33	6.08	7.07	8.44	10.46	7.12	7.120	6.23	5.34	4.45	3.56	8.00	7.00	6.00	5.00	4.00	0.99	0.99	0.98	0.96	0.94	24.00	21.00	18.00	15.00	12.00	3.00	3.00	1.50	1.00	0.89	0.89	0.47	0.02	1.27	0.02	8.5487	0.0139
	90th	0.5745	0.1875	0.1773	0.1817	0.1852	0.1875	0.1875	0.5745	0.4507	0.3376	0.2373	0.1519	0.5082	0.5082	0.4445	0.3804	0.3160	0.2518	9.5	0.8	-4.23	-3.49	-2.51	-1.15	0.85	10.35	5.27	6.01	6.99	8.35	10.35	7.20	7.200	6.30	5.40	4.50	3.60	8.00	7.00	6.00	5.00	4.00	0.99	0.98	0.97	0.95	0.92	24.00	21.00	18.00	15.00	12.00	3.00	3.00	1.50	1.00	0.90	0.90	0.51	0.02	1.27	0.02	9.3959	0.0150
	91st	0.5827	0.1844	0.1759	0.1799	0.1829	0.1844	0.1835	0.5827	0.4563	0.3408	0.2386	0.1520	0.5492	0.5492	0.4791	0.4085	0.3377	0.2673	9.5	0.7	-4.29	-3.55	-2.58	-1.24	0.74	10.24	5.21	5.95	6.92	8.26	10.24	7.28	7.280	6.37	5.46	4.55	3.64	8.00	7.00	6.00	5.00	4.00	0.98	0.98	0.96	0.94	0.91	24.00	21.00	18.00	15.00	12.00	3.00	3.00	1.50	1.00	0.91	0.91	0.55	0.02	1.27	0.02	10.2708	0.0162
	92nd	0.5893	0.1806	0.1741	0.1776	0.1799	0.1806	0.1787	0.5893	0.4602	0.3426	0.2388	0.1512	0.5900	0.5900	0.5130	0.4355	0.3580	0.2812	9.5	0.6	-4.34	-3.62	-2.65	-1.32	0.63	10.13	5.16	5.88	6.85	8.18	10.13	7.36	7.360	6.44	5.52	4.60	3.68	8.00	7.00	6.00	5.00	4.00	0.98	0.97	0.95	0.92	0.88	24.00	21.00	18.00	15.00	12.00	3.00	3.00	1.50	1.00	0.92	0.92	0.59	0.02	1.27	0.02	11.1585	0.0174
	93rd	0.5933	0.1759	0.1715	0.1744	0.1759	0.1757	0.1727	0.5933	0.4618	0.3424	0.2374	0.1494	0.6292	0.6292	0.5449	0.4603	0.3759	0.2930	9.5	0.5	-4.40	-3.68	-2.73	-1.41	0.53	10.03	5.10	5.82	6.77	8.09	10.03	7.44	7.440	6.51	5.58	4.65	3.72	8.00	7.00	6.00	5.00	4.00	0.97	0.95	0.93	0.90	0.86	24.00	21.00	18.00	15.00	12.00	3.00	3.00	1.50	1.00	0.93	0.93	0.63	0.02	1.27	0.02	12.0341	0.0186
	94th	0.5933	0.1706	0.1679	0.1699	0.1706	0.1693	0.1653	0.5933	0.4599	0.3392	0.2338	0.1461	0.6648	0.6648	0.5729	0.4811	0.3902	0.3016	9.5	0.4	-4.45	-3.74	-2.80	-1.49	0.43	9.93	5.05	5.76	6.70	8.01	9.93	7.52	7.520	6.58	5.64	4.70	3.76	8.00	7.00	6.00	5.00	4.00	0.95	0.93	0.90	0.87	0.82	24.00	21.00	18.00	15.00	12.00	3.00	3.00	1.50	1.00	0.94	0.94	0.66	0.02	1.27	0.02	12.8558	0.0196
	95th	0.5870	0.1638	0.1626	0.1638	0.1634	0.1611	0.1562	0.5870	0.4526	0.3319	0.2272	0.1409	0.6933	0.6933	0.5940	0.4955	0.3988	0.3055	9.5	0.3	-4.50	-3.80	-2.87	-1.57	0.33	9.83	5.00	5.70	6.63	7.93	9.83	7.60	7.600	6.65	5.70	4.75	3.80	8.00	7.00	6.00	5.00	4.00	0.92	0.90	0.87	0.83	0.78	24.00	21.00	18.00	15.00	12.00	3.00	3.00	1.50	1.00	0.95	0.95	0.69	0.02	1.27	0.02	13.5543	0.0204
	96th	0.5708	0.1550	0.1548	0.1550	0.1536	0.1503	0.1446	0.5708	0.4374	0.3185	0.2164	0.1332	0.7091	0.7091	0.6034	0.4995	0.3986	0.3026	9.5	0.2	-4.55	-3.86	-2.93	-1.65	0.23	9.73	4.95	5.64	6.57	7.85	9.73	7.68	7.680	6.72	5.76	4.80	3.84	8.00	7.00	6.00	5.00	4.00	0.88	0.85	0.82	0.77	0.72	24.00	21.00	18.00	15.00	12.00	3.00	3.00	1.50	1.00	0.96	0.96	0.71	0.02	1.27	0.02	14.0133	0.0209
	97th	0.5388	0.1432	0.1432	0.1423	0.1399	0.1359	0.1296	0.5388	0.4100	0.2963	0.1997	0.1219	0.7026	0.7026	0.5932	0.4870	0.3852	0.2897	9.5	0.1	-4.60	-3.91	-3.00	-1.73	0.13	9.63	4.90	5.59	6.50	7.77	9.63	7.76	7.760	6.79	5.82	4.85	3.88	8.00	7.00	6.00	5.00	4.00	0.81	0.78	0.75	0.70	0.65	24.00	21.00	18.00	15.00	12.00	3.00	3.00	1.50	1.00	0.97	0.97	0.70	0.02	1.27	0.02	14.0333	0.0207
	98th	0.4803	0.1250	0.1250	0.1233	0.1203	0.1158	0.1095	0.4803	0.3626	0.2599	0.1738	0.1052	0.6561	0.6561	0.5493	0.4470	0.3504	0.2609	9.5	0.0	-4.65	-3.97	-3.07	-1.81	0.04	9.54	4.85	5.53	6.43	7.69	9.54	7.84	7.840	6.86	5.88	4.90	3.92	8.00	7.00	6.00	5.00	4.00	0.71	0.68	0.64	0.60	0.55	24.00	21.00	18.00	15.00	12.00	3.00	3.00	1.50	1.00	0.98	0.98	0.66	0.02	1.27	0.02	13.2447	0.0193
	99th	0.3710	0.0946	0.0946	0.0925	0.0895	0.0855	0.0801	0.3710	0.2777	0.1974	0.1309	0.0785	0.5300	0.5300	0.4397	0.3546	0.2754	0.2031	9.5	0.1	-4.70	-4.03	-3.13	-1.89	-0.05	9.45	4.80	5.47	6.37	7.61	9.45	7.92	7.920	6.93	5.94	4.95	3.96	8.00	7.00	6.00	5.00	4.00	0.54	0.51	0.48	0.44	0.40	24.00	21.00	18.00	15.00	12.00	3.00	3.00	1.50	1.00	0.99	0.99	0.53	0.02	1.27	0.02	10.8105	0.0156
	100th	0.0000	0.0000	0.0000	0.0000	0.0000	0.0000	0.0000	0.0000	0.0000	0.0000	0.0000	0.0000	0.0000	0.0000	0.0000	0.0000	0.0000	0.0000	9.5	0.1	-4.75	-4.08	-3.19	-1.96	-0.14	9.36	4.75	5.42	6.31	7.54	9.36	8.00	8.000	7.00	6.00	5.00	4.00	8.00	7.00	6.00	5.00	4.00	0.00	0.00	0.00	0.00	0.00	24.00	21.00	18.00	15.00	12.00	3.00	3.00	1.50	1.00	1.00	1.00	0.00	0.02	1.27	0.02	0.0000	0.0000

APPENDIX II

Tables for Aerodynamic Parameters of Profiles

Table A: NACA 4412

Aerodynamic properties	Value
Thickness	12.0%
Camber	4.0%
Trailing edge angle	14.4^{o}
Stall angle	6.0
Max C_L	1.507
Max L/D	57.209
Max L/D C_L	1.188
Zero-lift angle	-4.0

Table B: Selig 1210

Aerodynamic properties	Value
Thickness	12.0%
Camber	7.2%
Trailing edge angle	6.9^{o}
Stall angle	9.0^{o}
Max C_L	2.248
Max L/D	73.283
Max L/D C_L	1.961
Zero-lift angle	-10.5

Table C: Worthmann FX 63-137

Aerodynamic properties	Value
Thickness	12.0%
Camber	7.2%
Trailing edge angle	6.9^{o}
Stall angle	9.0^{o}
Max C_L	2.248
Max L/D	73.283
Max L/D C_L	1.961
Zero-lift angle	-10.5

Table D: Ara-D 6%

Aerodynamic properties	Value
Thickness	6.0%
Camber	5.0%
Trailing edge angle	7.0^{o}
Stall angle	8.5^{o}
Max C_L	1.589
Max L/D	42.431
Max L/D C_L	1.545
Zero-lift angle	-5.5

Table E: Selig 2091

Aerodynamic properties	Value
Thickness	10.1%
Camber	3.9%
Trailing edge angle	6.3^o
Stall angle	11.0^o
Max C_L	1.348
Max L/D	54.826
Max L/D C_L	0.965
Zero-lift angle	-3.5

Table F: Selig Donovan7032

Aerodynamic properties	Value
Thickness	10.0%
Camber	3.7%
Trailing edge angle	7.4^o
Stall angle	10.0^o
Max C_L	1.381
Max L/D	56.369
Max L/D C_L	1.081
Zero-lift angle	-4.0

Table G: Selig Donovan 7037

Aerodynamic properties	Value
Thickness	9.2%
Camber	3.0%
Trailing edge angle	8.2^{o}
Stall angle	9.5^{o}
Max C_L	1.269
Max L/D	54.221
Max L/D C_L	0.899
Zero-lift angle	-3.0

Table H: Selig Donovan 8000

Aerodynamic properties	Value
Thickness	8.9%
Camber	1.7%
Trailing edge angle	7.7^{o}
Stall angle	8.0^{o}
Max C_L	1.058
Max L/D	47.616
Max L/D C_L	0.908
Zero-lift angle	-1.5

Table H: Selig 3021

Aerodynamic properties	**Value**
Thickness	9.5%
Camber	3.0%
Trailing edge angle	10.3^o
Stall angle	8.0
Max C_L	1.122
Max L/D	54.002
Max L/D C_L	0.877
Zero-lift angle	-2.5

Table J: Ara-D 10%

Aerodynamic properties	**Value**
Thickness	10.0%
Camber	4.0%
Trailing edge angle	10.3^o
Stall angle	9.5
Max C_L	1.433
Max L/D	34.006
Max L/D C_L	1.178
Zero-lift angle	-3.5

APPENDIX III

Lift and Drag Polar Graphs of Profiles

Graph A: NACA 4412

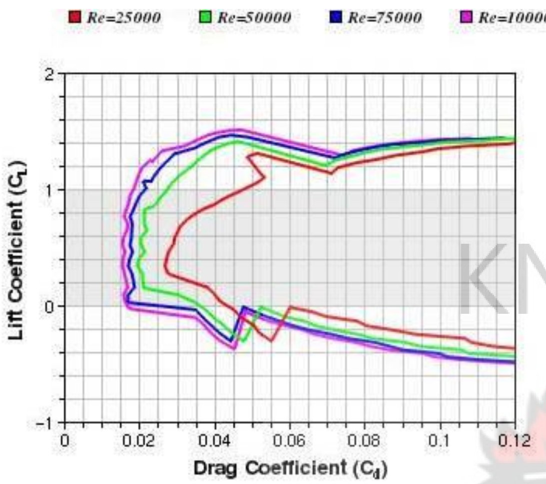

Drag Polar for NACA 4412

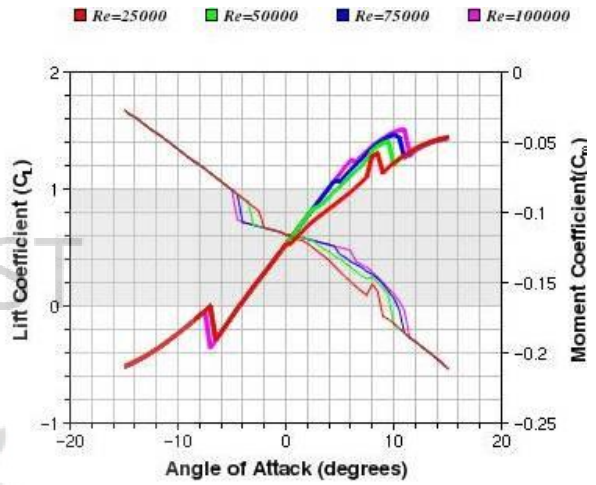

Lift for NACA 4412

Graph B: Selig 1210

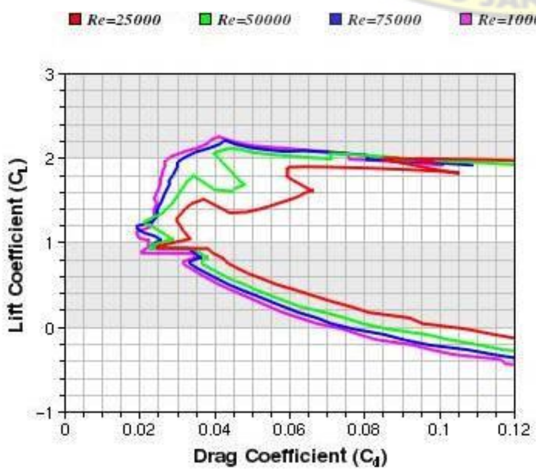

Drag Polar for Selig1210

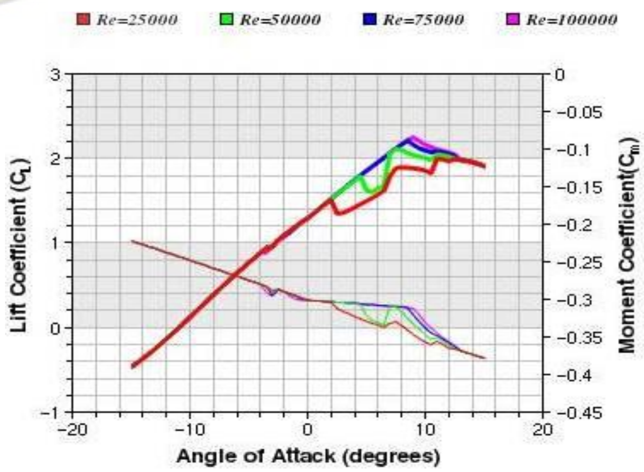

Lift for Selig 1210

Graph C: Worthmann FX 63-137

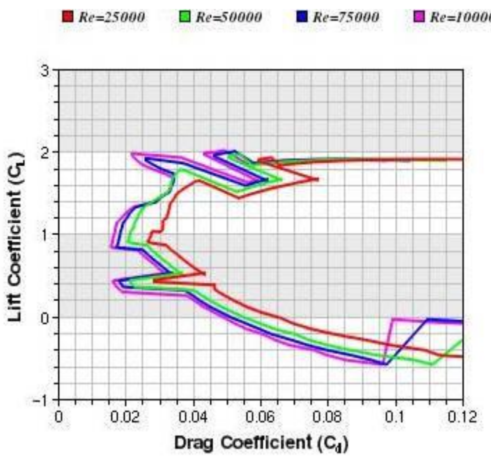

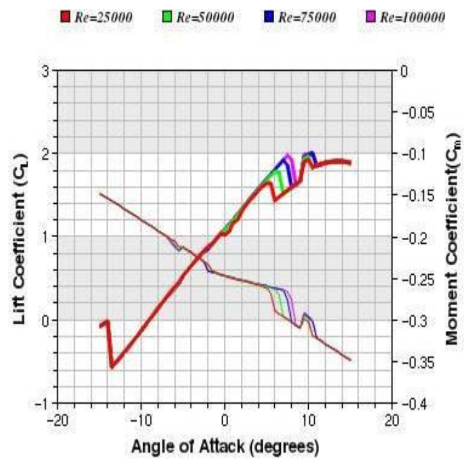

Drag Polar for Worthmann FX 63-137 Lift for Worthmann FX 63-137

Graph D: Ara-D 6%

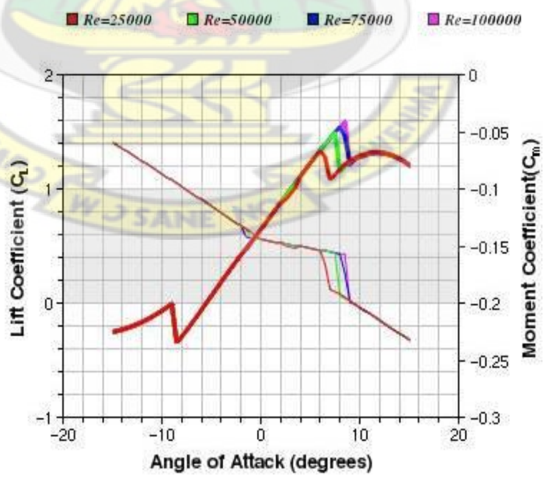

Drag Polar for Ara-D 6%

Graph E: SELIG2091

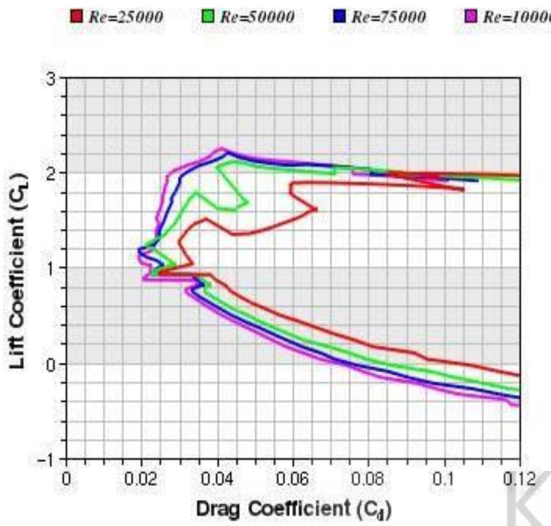

Drag Polar for Selig 2091

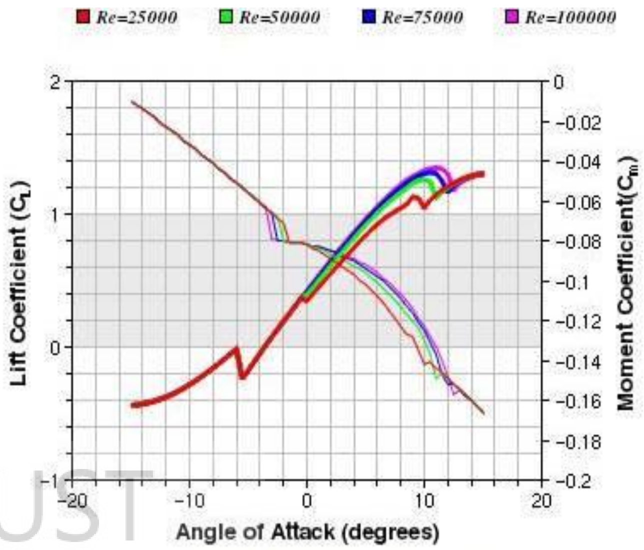

Lift for Selig 2091

Graph F: Selig Donovan7032

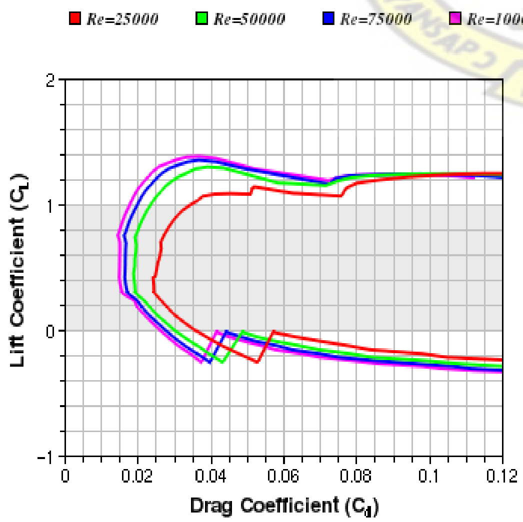

Drag Polar for Selig Donovan 7032

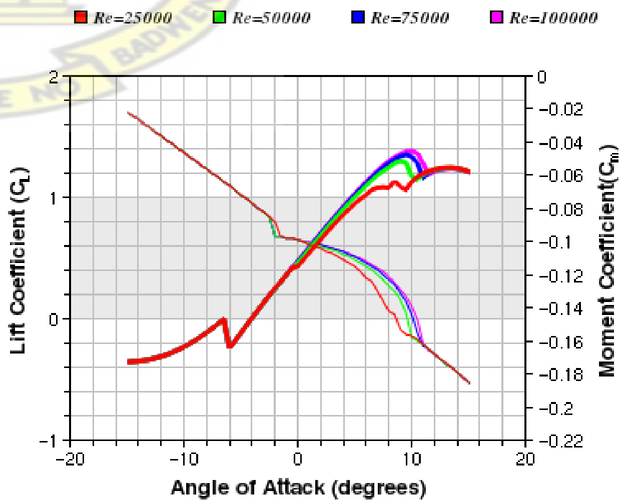

Lift for Selig Donovan 7032

Graph G: Selig Donovan7037

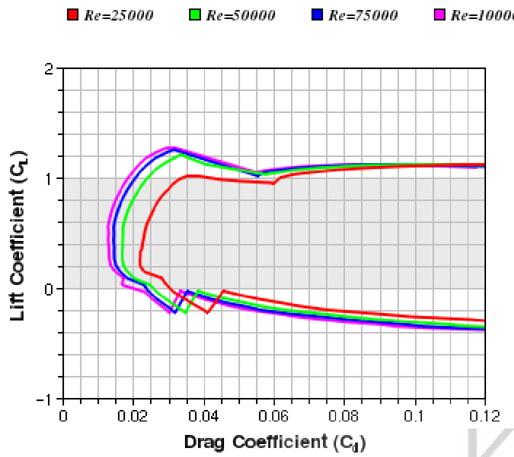

Drag Polar for Selig Donovan 7037

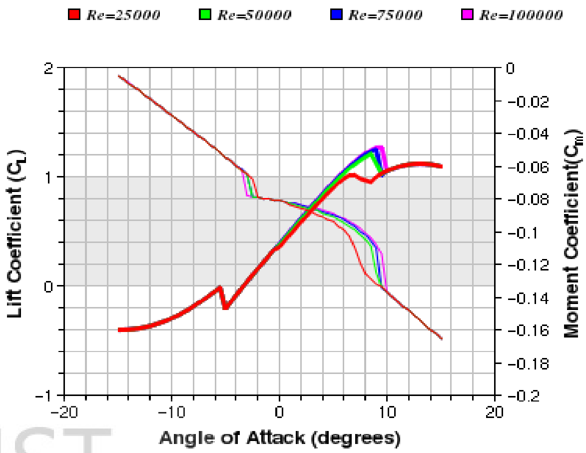

Lift for Selig Donovan7037

Graph H: Selig Donovan8000

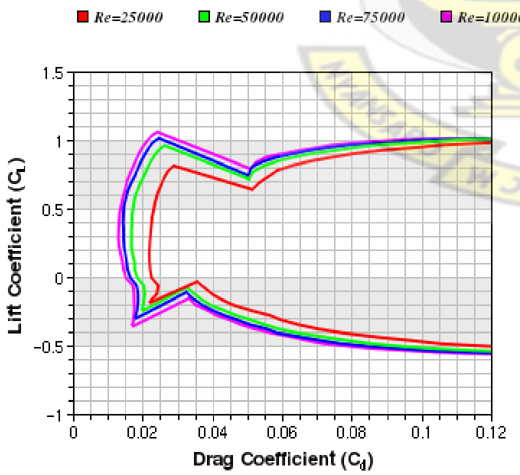

Drag Polar for Selig Donovan 8000

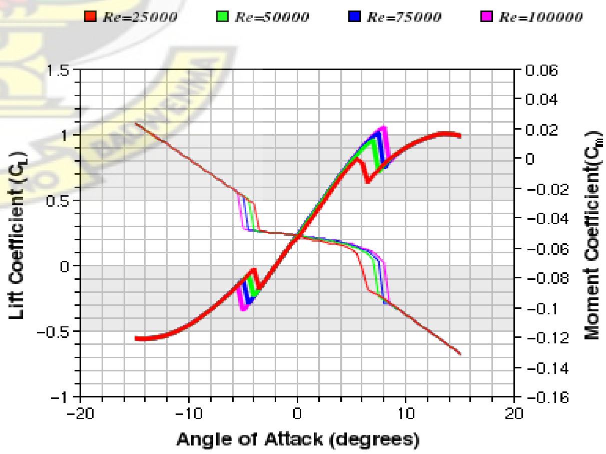

Lift for Selig Donovan8000

Graph I: Selig3021

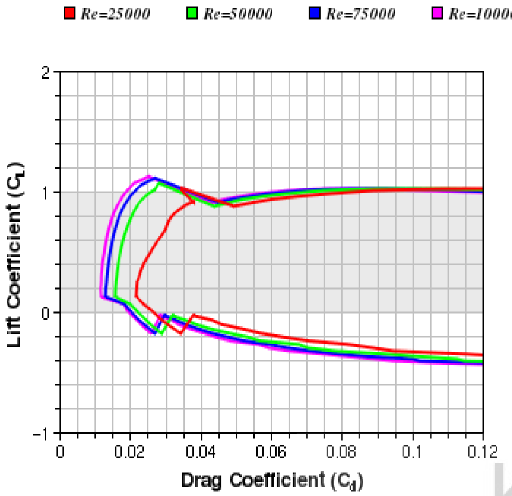

Drag Polar for Selig3021

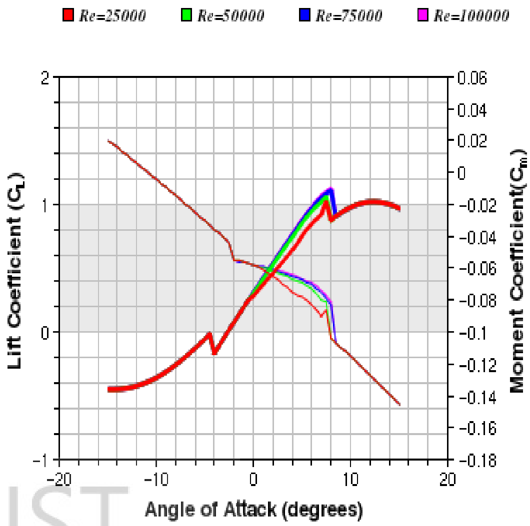

Lift for Selig3021

Graph J: Ara-D 10%

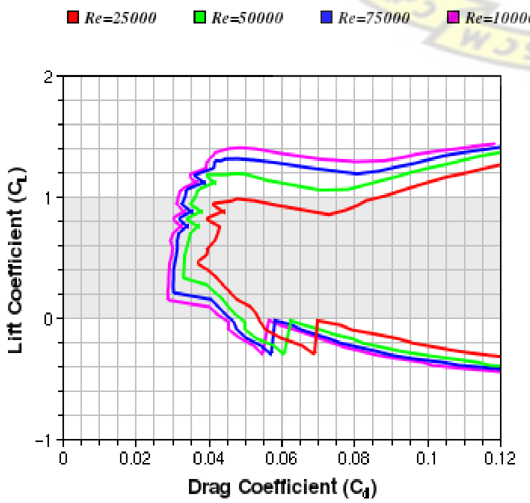

Drag Polar for Ara-D 10%

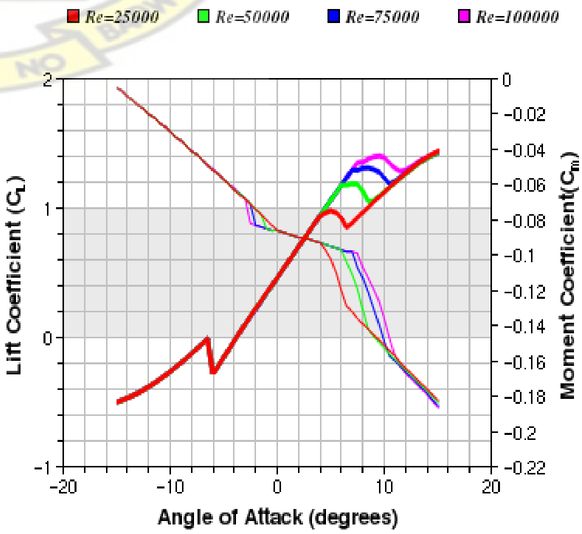

Lift for Ara-D 10%